2016-01-01

Label-Free Quantitative Proteomics Reveals a Novel SGTA/Peroxiredoxin I Complex That Regulates Androgen Receptor Activity

Yenni Alejandra Garcia
University of Texas at El Paso, yagarcia3@utep.edu

LABEL-FREE QUANTITATIVE PROTEOMICS REVEALS A NOVEL SGTA/PEROXIREDOXIN 1 COMPLEX THAT REGULATES ANDROGEN RECEPTOR ACTIVITY

YENNI ALEJANDRA GARCIA

Doctoral Program in Biological Sciences

APPROVED:

Marc B. Cox, MSPH, Ph.D., Chair

Igor C. Almeida, Ph.D.

Siddhartha Das, Ph.D.

Arshad Khan, Ph.D.

Laura O'Dell, Ph.D.

Charles Ambler, Ph.D.
Dean of the Graduate School

Dedication

This dissertation is dedicated to my mother Blanca E. Garcia, my father Lorenzo Garcia and my two sisters Blanca Ileana and Ana Palmira Garcia from whom I've received tremendous support and who, with their faith in God, have pushed me to keep going.

LABEL-FREE QUANTITATIVE PROTEOMICS REVEALS A NOVEL SGTA/PEROXIREDOXIN 1 COMPLEX THAT REGULATES ANDROGEN RECEPTOR ACTIVITY

by

YENNI ALEJANDRA GARCIA, B.S.

DISSERTATION

Presented to the Faculty of the Graduate School of

The University of Texas at El Paso

in Partial Fulfillment

of the Requirements

for the Degree of

Doctor of Philosophy

Department of Biological Sciences

THE UNIVERSITY OF TEXAS AT EL PASO

May 2016

Acknowledgements

Primarily, I would like to thank my mentor Dr. Marc B. Cox whom I call my "Science Dad" for his immense support in my project and professional development. I am grateful for all the direction he has provided me with, and the encouragement to continue when science becomes challenging. I also would like to thank him for allowing me to mentor undergraduate students, whom I have learned a great extent from. A special thanks goes to my committee members who have inspired me and shaped me to become a better scientist. I am indebted to Dr. Igor C. Almeida for providing me scientific training in proteomics and for his enthusiasm in asking me stimulating questions about methodology. He has been a great mentor as well. I am delighted Dr. Siddhartha Das was part of my committee because his sprit for science is contagious. I was always excited to show him new data and discuss possible mechanisms of SGTA action. I appreciate all the encouragement he provided for my professional development. I am grateful for Dr. Arshad Khan's capacity to bring stimulating questions to my project and teaching me to become a complete scientist; he is a very talented scientist. I am immensely grateful to Dr. Laura O'Dell for sharing her knowledge in neuroendocrinology, grant writing, and providing me with advise that has helped foster my success throughout graduate school and I will carry in my future endeavors.

I would like to thank the DNA Core facilities at UTEP especially Ana Betancourt for helping with all the sequencing and the friendship created. I thank UTEP's Biomolecule Analysis Core Facility, in particular Dr. Emma Arigi, Dr. Nathan VerBerkmoes, Brian Grajeda, and Gloria Polanco, for helping me with LC-MS/MS and all proteomic techniques. A special thanks goes to the collaborators who have contributed to the SGTA story:

- Dr. Jill Johnson's laboratory from the Department of Biological Sciences, University of Idaho, Moscow, Idaho
- Dr. Johannes Buchner's laboratory from the Center for Integrated Protein Science at the Department Chemie, Technishce Universität München, Germany

- Dr. Ahmed Chadli's laboratory from the Cancer Research Center, Georgia Regents University, Augusta, Georgia
- Dr. Hyungwon Choi's laboratory from the National University of Singapore

A huge thanks goes to my "lab family" whom I have experienced many stories with. Special thanks to Dr. Johanny Kugelman-Meneses de Leon for introducing and inspiring me to the lab life and sharing her passion for science. I am grateful for Drs. Cheryl Storer-Samaniego, and Diondra C. Harris for the bond we created and for always having the patience to teach me and help me with my professional development. Huge thanks to my lab neighbor, Naihsuan C. Guy, with whom I generated many ideas, shared resources, and troubleshooted experiments. A special acknowledgment to Dr. Jeffrey Sivils for providing me with insightful ideas and all the past members of the Cox Lab. I would like to give a special thanks to the undergraduate students that worked closely with me: Jacaranda Solis, Omar Gutierrez Ruiz, and Luis Prieto. I am very proud of their accomplishments and they have now become great friends. I know they will achieve great work in science and the labs they step on will be lucky to have them. Jacaranda Solis helped with the initial aspect of truncation mutants and with the urine experiments in yeast. She is working as a researcher at Texas Tech Lubbock. Omar Gutierrez helped tremendously in the cloning of the truncations aspect of the project. He is now working as a researcher at Sloan Kettering Memorial Center. Luis Prieto helped impressively with the proteomics aspect of the project and "saw the light" and will be starting his PhD degree in Mayo Clinic this summer. I am very proud of them and grateful to have had them as mentees.

I would also like to thank Nina Ortiz and Ashley Payan for their support and wish them the best of luck in the Cox lab, I know they will create meaningful work and contribute vastly to the field of molecular chaperones in prostate cancer. I would like to thank my fellow graduate friends Gloria Polanco, Zack Martinez, Angelica Lopez, and Steven Martinez for providing with their joyful spirit and many adventures while working late in lab. I would like to acknowledge my family for all the economic and emotional support. Words cannot describe how valuable they

were throughout this journey. Last but not least, I would like to thank Oscar Tapia for helping me edit my dissertation and providing much-needed emotional support.

This work was supported by the Dodson Research Grant and Travel Grant Support from The University of Texas at El Paso (YAG), The UTEP Department of Biological Sciences Teaching Assistantships (YAG), UTEP Grant Number 5G12RR008124 of the Border Biomedical Research Center (BBRC)/ University of Texas at El Paso from the National Center for Research Resources (NCRR), a component of the National Institutes of Health (NIH), an ARRA supplement to SCORE Grant 1SC1GM084863-02S1 (MBC), and the Cancer Prevention and Research Institution of Texas (CPRIT) Grant RP110444-P2 (MBC).

Abstract

The dynamic Hsp70-90 chaperone machinery along with its cochaperone partners are well-characterized for their ability to fold, assemble, and regulate steroid hormone receptors (SHRs). Human small glutamine rich tetratricopeptide repeat (TPR) containing protein alpha (SGTA) is a recently identified protein that has a characteristic Hsp90-binding TPR domain and is a key participant in the androgen, glucocorticoid, and progesterone receptor signaling pathway. In addition, SGTA plays a role in cellular processes such as cell cycle progression and apoptosis. We have demonstrated that SGTA binds directly to both Hsp70 (kd = 6 μM) and Hsp90 (kd = 11 μM). In a cell-free system, SGTA is unable to affect chaperone complex formation and receptor hormone binding. In addition, deletion of the Q-rich region at the C-terminus of SGTA failed to abrogate AR function in yeast reporter assays. To better understand the functional role of SGTA in SHR regulation, we undertook a label-free quantitative proteomics approach to determine unknown interacting proteins with SGTA in LNCaP human prostate cancer cells. Tandem affinity purification followed by Liquid Chromatography Mass Spectrometry (LC-MS/MS) was performed to identify unknown protein interactions. To determine if interactions were transient or strong, a comparison of a 3-hour versus an overnight incubation was used. Our quantitative data suggest that SGTA interacts with proteins involved in a diverse range of pathways. Peroxiredoxin 1 (PRDX1) was present in both conditions and in the three biological replicates. PRDX1 is involved in redox regulation of the cell and has antioxidant properties. In addition, it has been linked to the androgen receptor (AR) pathway where it can bind to AR and enhance its transactivation. Utilizing SGTA and PRDX1 purified, recombinant proteins, we performed an *in vitro* FLAG pull-down assay using proteins alone or in combination. The *in vitro* FLAG pull-down assays demonstrated that SGTA directly interacts with PRDX1. In addition, PRDX1 co-immunoprecipitated with SGTA in LNCaP cells. Thus, we sought to determine the functional relevance of the SGTA-PRDX1 interaction. We generated CRISPR/Cas9 SGTAKO HeLa and 22RV1 cell lines and assessed the functional relevance of

SGTA and PRDX1. Using luciferase reporter assays we demonstrated that SGTA can antagonize PRDX1 potentiation of AR activity suggesting the mechanism for the negative regulation of AR by SGTA is through competition with PRDX1.

The yeast-based steroid hormone receptor-mediated reporter assay has historically provided much of the evidence regarding the importance of chaperones and cochaperones in steroid hormone receptor signaling pathways and was critical for the characterization of SGTA functional domains in this study. Given our expertise with this system our group modified this assay previously to a short 4-hour assay for use in screening environmental samples for estrogenic activity. Because of the short assay time, sterility is not an issue and samples can be measured directly without extraction or sterilization. As a result, we hypothesized that the assay could be used for the direct measure of estrogenic activity in urine as a novel research tool as well. Thus, we sought to validate its application in human urine samples. The ability and sensitivity of the yeast bioassay to detect estrogenic activity in urine samples from pregnant females in all trimesters was assessed. No toxicity was observed in yeast grown in the presence of human pregnant female urine for 2 hours and the assay was able to accurately detect the increasing estrogenic activity expected with increasing trimester. Upon the addition of β-glucoronidase and sulfatase to deconjugate estrogenic metabolites we demonstrated that the assay sensitivity can be increased significantly (i.e. significantly more estrogenic activity was detected). Thus, these assays represent a novel research tool to detect estrogenic activity in animal and human urine samples in a rapid and sensitive manner.

Table of Contents

List of Tables

List of Figures

Chapter 1: Introduction

1.1 Androgen Receptor Structure, Function, and Physiological Regulation

Steroid Hormone Receptors (SHRs) are an evolutionary conserved group that belongs to the nuclear receptor superfamily. The glucocorticoid (GR), androgen (AR), progesterone (PR), mineralocorticoid (MR), and estrogen (ER) receptors comprise the main SHRs in the nuclear receptor subfamily 3 category (*1-4*). Upon hormone binding, SHRs act as transcription factors in eukaryotes to maintain an array of physiological processes in homeostasis (*5*). These genomic actions constitute processes such as development, reproduction, sexual differentiation, energy metabolism, and electrolyte balance (*6*).

Steroid hormones utilize cholesterol as the precursor and undergo multiple enzymatic conversions to adapt an agonist structure that will bind to its respective receptor. Steroid hormones have tissue specificity and are synthesized in the adrenal cortex (GR and PR), testes (AR), ovaries (ER), and corpus luteum (PR) (*7*). Biosynthesis initiates upon desmolase converting cholesterol to pregnenolone (*8*). Moreover, 3β-hydroxysteroid dehydrogenase modifies it to progesterone where 17-hydroxylase converts it to 17-αhydroxyprogesterone and based on necessity, the enzymatic conversions along with protein interactors will proceed until they reach their target receptor (*8-10*). These ligands will bind to the Ligand Binding Domain (LBD) of the SHR. For instance, testosterone and 5α-DHT are the main ligands for AR; they enter the cell by passive diffusion and upon binding to AR, a conformational change occurs allowing AR to hyperphosphorylate, dimerize, recruit coactivators, translocate to the nucleus and bind to target DNA (*11, 12*).

The AR gene locus is on the X chromosome at Xq11-12, containing 8 exons and coding for a 919 amino acid protein with a 110 kDa mass (*13*). To unravel the receptor itself, a compilation of studies have elucidated four functional domains within the structures of SHRs

(*14, 15*). Clinical, biochemical, and cellular experiments have also highlighted the important role of AR, such as in male sexual differentiation and development in response to physiological processes. The amino terminal transactivation domain (NTD) is the site of the major regulatory domain, activation function-1 (AF-1) (*16*). The DNA-binding domain (DBD) is the hallmark of nuclear receptors due to the high conservation of this domain in nuclear receptors. The DBD is located next to the NTD where the zinc fingers in this area bind to the hormone response element (*17*). Moreover, the hinge region (H) is poorly conserved, provides structural flexibility, and may be a key site of receptor posttranslational modifications (*18*). Finally, the carboxy-terminus, the ligand-binding domain (LBD), which contains the activation factor 2 (AF-2), is the site of hormone binding (*19*).

The NTD is 556 amino acids long and has an important role in AR transactivation; although it can interact with the LBD, transactivation can occur independently (*13, 20*). Its structure remains unknown, however, predictive modeling suggests this region is a globular, disordered, low complexity state upstream of the AF-1 region (*21*). Although the structure is undefined, mutagenesis studies performed in androgen independent cells demonstrated that the WxxLF motif is necessary for AR transactivation (*22*). In addition, GFP deletion mutant transfections in PC-3 LAPC-4 and COS-1 cells revealed a critical region for cytoplasmic localization. Δ50-250AR exhibited higher nuclear localization compared to full length AR, which suggests this region promotes cytoplasmic localization mediated by exportin 1. This was determined using Leptomycin B, which possesses nuclear export inhibitory functions in humans, and led to inhibition of Δ50-250AR cytoplasmic localization. Additionally, at a high dose of the synthetic androgen R1881, these constructs could continue to translocate, thereby proposing a putative mechanism for progression towards castration resistant prostate cancer (CRPC) (*23*).

Much efforts have been made to therapeutically target the LBD of AR, a more modern approach is to utilize antagonists for the NTD and block its transcriptional activity. One challenging aspect of prostate cancer is the cross-talk that occurs with other signaling molecules such as interleukin-6 (IL-6). IL-6 can activate NTD transactivation and increase proliferation through the MAPK and STAT3 signal transduction pathways in LNCaP cells (*24*). For these reasons, small molecule inhibitors EPI-001 and analogs have been designed to target this region and disrupt NTD transactivation by binding the AF-1 region. *In vivo*, EPI-001 has an anti-proliferative profile where the tumors of mice decreased after treatment and apoptosis increased (*25, 26*). The NTD seems to be a plausible method to target with reduced detrimental side effects; however, this does not eliminate drug resistance concerns.

The DBD is located in the middle region of AR and is responsible for binding DNA through its two zinc fingers forming an alpha helix core in a manner that AR can hetero or homo-dimerize and interact with the major groove on the DNA. Upon folding of the first zinc finger, the alpha helix forms allowing it to interact with the major groove in the DNA termed the P-box, and further interacts with transcriptional enhancers (*17, 27*). The second zinc finger interacts with the D-box and is retained by hydrogen bonding (*28*). The flexibility of the DBD is based upon its interaction with the FxxLF motif in the NTD and the LBD. Interestingly, the binding of an antagonist or an agonist has a major influence on where the DBD will bind to and initiate the transcription machinery (*29*). The requirements for DNA binding are not exclusive to its structure; they bind to proteins that facilitate this process such as the AP-1 heterodimer constituents Fos and Jun (*30*).

Receptor recycling and shuttling between cellular compartments are critical for activity and post-translational modifications have a role in these processes. The hinge region is

responsible for carrying two synergy control motifs that have inhibitory functions. Within the AR motifs, acceptor lysines at positions K386 and K520 serve as post-translational modification sites by small ubiquitin-like modifier (SUMO) proteins. This region is responsible for suppressing AR activity and if mutated at these key residues, AR activity increases *in vivo*. A mutation in this region has been found, in AIS and prostate cancer patients, and it can increase AR transcriptional activity (*31*). Whole-cell and cell-free studies have demonstrated that SUMOylation provides a mechanistic role for AR suppression, gene expression, and regulation of nuclear localization (*32-34*). Collectively, these studies provide insight into the mechanistic regulation by SUMO proteins and how they possess inhibitory functions. However, a role for receptor-associated cochaperones in this process is not well understood.

The flexibility of the hinge region in AR promotes signaling pathways to partake a crucial role in AR translocation. This mobility was demonstrated by Tanner and colleagues, where mutagenesis studies performed in the (629)RKLKK(633) motif disturbed various aspects of receptor function (*35*). Moreover, amino acid substitutions performed in Serine 650 to an Alanine led to a decrease in transcriptional activity (*36*). In a similar fashion, Chen and colleagues mutated S650A and sought to determine in a more detailed manner the regulation of AR and Protein Phosphatase 1 (PP1). Co-immunoprecipitation studies showed that AR can bind to PP1α in LNCaP cells and has a time-dependent nuclear entry. The interaction was proven to be functional as these two proteins augmented transcriptional activity based on reporter assays in LNCaP cells. PP1 inhibitors promoted dephosphorylation and nuclear withholding, suggesting the functional interaction could provide clues to future drug targets in the hinge region (*37*). Albeit the detailed mechanism between PP1 and AR is not well understood, the hinge region is a plausible target for combinatorial drugs where much of the chemotherapeutic drugs are designed.

The hinge region possesses a characteristic acetylation motif for modification at the ε-amino lysine residues, which allows proteins to bind and enhance or repress DNA transcription (*38, 39*). AR acetylation mutant L630A in comparison to wild type was unable to stimulate transactivation upon ligand binding (*40*). On the other hand, mimicking this site potentiated transactivation in a PSA promoter even in the presence of minimal hormone levels. Interestingly, this somatic mutation is present in PCA patients providing another mechanistic aspect of progression.

The LBD's 12 alpha helices posed by the androgen receptor is very selective, dynamic, and complex (*41*). The AF-2 region located in the LBD is a crucial player in recruiting coactivators, which are responsible for regulating the transcription of AR-regulated genes. The AF-2 region has promising therapeutic potential due to its binding function 2 (BF2) surface, a hydrophobic cleft that binds alpha-helical peptides. Based on x-ray screens, this surface could potentially serve as a target for small molecules that can regulate AR activity (*42*). Another binding partner of AR is β- catenin, a protein that augments activation of transcription by the initiation of the coactivator p160. Moreover, upon ligand binding, nuclear translocation occurs because the nuclear localization signal (NLS) is able to respond to the zinc fingers, an event mediated by importin. The two zinc fingers located in the hinge region mediate DNA binding (*43*). Mutations in the androgen receptor regulatory sites discussed above are the cause of androgen insensitivity syndrome (AIS) and likely contribute to prostate cancer progression. Apart from the many functional domains within the receptors that could serve as therapeutic targets, the receptors undergo a dynamic chaperone-mediated folding process involving a variety of chaperone and associated cochaperone proteins, all of which also represent potential therapeutic targets.

1.2 Molecular Chaperone-Mediated Steroid Hormone Receptor Maturation

Molecular chaperones and cochaperones have a critical role in SHR assembly and stability (*44*). Based on their ability to serve as transcription factors, SHRs execute and regulate a diverse set of developmental and physiological events in eukaryotes (*2, 45, 46*). Moreover, the dynamic and complex molecular chaperone machinery is paramount for the folding, assembly, and prevention of aggregation of these receptors (*47, 48*). In addition, the chaperone complex plays a key role in monitoring and altering hormonal potency (*49*).

1.2.1 Early Complex

The dynamic chaperoning of SHRs is illustrated in Figure 1.1.1. The primary key steps to initiate the molecular chaperone machinery consist of Heat shock protein 40 (Hsp40) binding to the nascent SHR polypeptide synthesized by the ribosome in the cytosol. The existing model for the chaperone machinery is based on evidence from several model systems such as baker's yeast *Saccharomyces cerevisiae* and rabbit reticulocyte lysate. The typical pathway involves a series of steps: early, intermediate, asymmetrical, and mature to achieve a high affinity state for hormone binding in a sequential time-dependent manner. There are five main proteins required for receptor maturation: Hsp40, Hsp70, Hsp90, HOP, and p23 (*46, 50-52*). Initially, Hsp40 binds to the LBD of the receptor, Hsp40 binds to the ATPase domain of Hsp70 through an HPD motif and transfers the client protein to Hsp70 by hydrolysis (*53-55*). *In vitro* experiments using chicken PR and rabbit reticulocyte lysate demonstrated that when Hsp40 was not present in the complex, PR was unable to bind hormone with high affinity. However, the Pratt laboratory proposed that Hsp40 was not essential for GR based on their stoichiometric studies with the yeast homologue YDJ1 (*52, 56*). The mechanistic aspect of how this regulation occurs is not fully understood; nonetheless, Hsp40 primes the client protein for the following steps in the

chaperoning pathway. There is still a lack of knowledge regarding the role Hsp40 has in disease and the mechanism by which it influences SHRs.

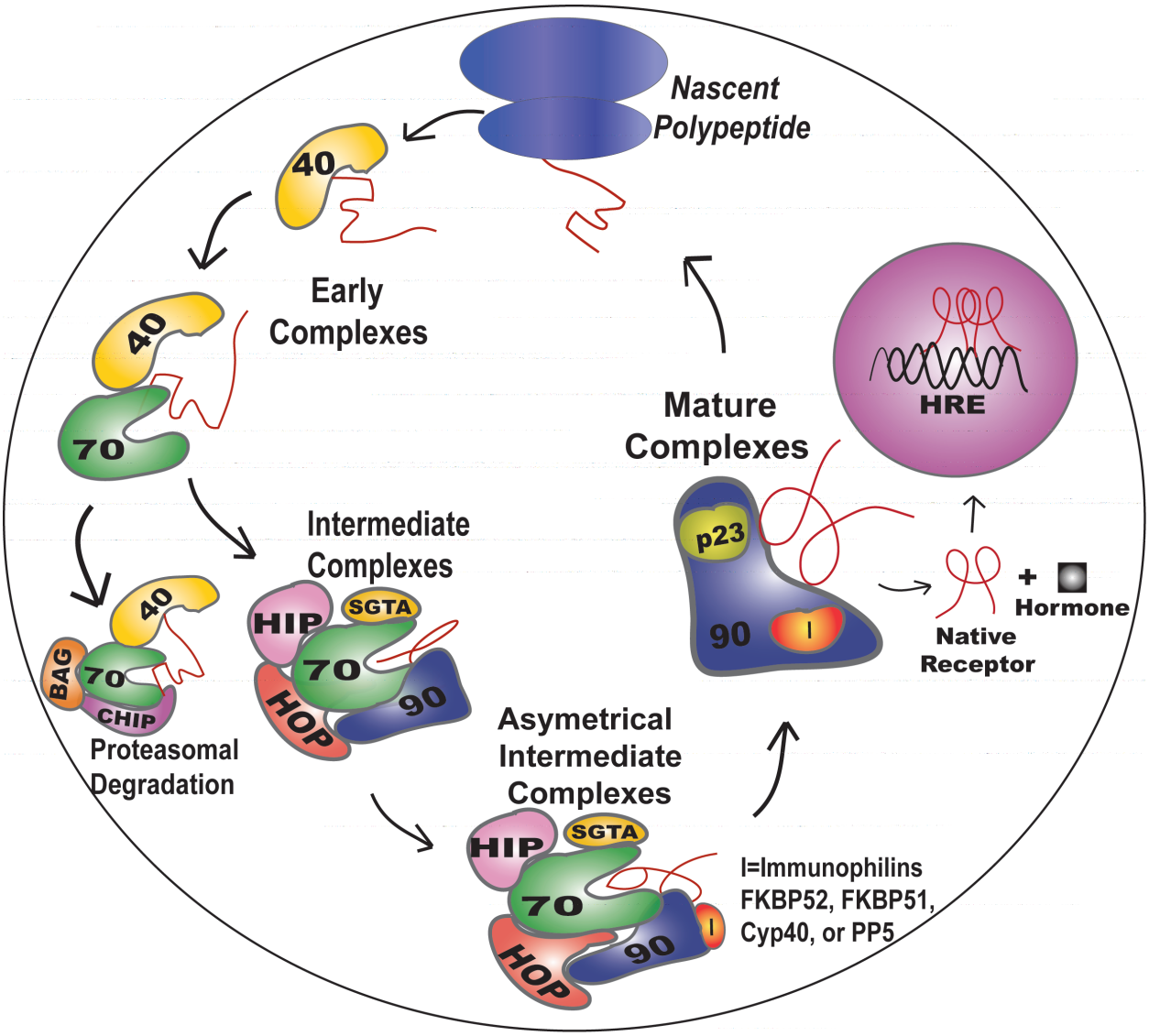

Figure 1.1.1 Steroid Hormone Receptor Chaperone Complex Assembly.

Figure 1.1.1 Steroid Hormone Receptor Chaperone Complex Assembly.

Early complex assembly is initiated upon Heat Shock protein 40 kDa (40) binding to the nascent steroid hormone receptor polypeptide residing in the cytosol. Hsp40 recruits Hsp70 (70) where the fate of the nascent polypeptide is determined to proceed with the intermediate complexes or towards proteasomal degradation. Carboxyl Terminus of Hsp70 Interacting Protein (CHIP) is an E3 Ubiquitin Ligase that along with Bcl-2 associated athanogene (BAG) proteins directs misfolded receptors towards the ubiquitin and proteasomal degradation pathways. In the intermediate complex, Small Glutamine Rich TRP-containing Protein alpha (SGTA) binds to Hsp70. Hsp70 (70) recruits Hsp70 Interacting Protein (HIP) and Hsp70-90 Organizing Protein (HOP) forming a bridge for Hsp90's (90) binding into the complex. As the nascent polypeptide travels through the asymmetrical complex the immunophilins (I) bind in a competitive fashion to Hsp90 (90) allowing for a conformational change. Further, the mature complex forms as HIP, HOP, SGTA, fall off and a 23 kDa cochaperone (p23) stabilizes the receptor. Once the receptor is in the native state hormone is bound with high affinity. The receptor is then able to translocate to the nucleus, dimerize and bind to hormone response elements (HRE) to initiate gene transcription.

1.2.2 Intermediate Complex

The client protein enters the intermediate complex when Hsp40 introduces it to the substrate binding domain of Hsp70 (*57*). Hsp70 binds a multitude of proteins through the EEVD recognition sequence, which is a conserved region where interaction with most TPR-containing cochaperones occurs. Heat shock protein interacting protein (HIP) is a cochaperone that facilitates substrate transfer from Hsp40 to Hsp70 in an ATP-dependent manner (*58*). Mutagenesis studies demonstrate that the TPR region of HIP is critical for binding Hsp70, which is a determinant for the fate of the client protein.(*59*). Depending on the fold of the receptor, Hsp70 can send the substrate to degradation pathways via the triage complex involving carboxyl terminus of Hsp70-interacting protein (CHIP) and Bcl-2- associated athanogene (BAG) or progress the substrate to the mature complex. Recent studies have suggested that these pathways are critical. The family of BAG's is fairly large and is composed of various isoforms, which seem to have a role with the chaperones or SHRs. For instance, BAG1M can inhibit GR, MR, and PR, and BAG 1L can inhibit the aforementioned receptors including AR. It is believed that it functions through Hsp70's ATPase activity (*60, 61*). Moreover, competition occurs for Hsp70's ATPase domain. BAG1 and HIP often compete for this domain and BAG1 has a preference of destabilizing Hsp70 (*50*). Further, the main protein important for quality control, the carboxyl-terminus of Hsc70-interacting protein (CHIP) is an E3 Ubiquitin ligase, which has a critical role in detecting misfolded proteins; thereby sending them to degradation pathways (*62, 63*). Nonetheless, if the client protein is ready to move to the mature complex, Hsp70-Hsp90 organizing protein (HOP) introduces the client protein to Hsp90 via its TPR region at the carboxy-terminus (*64, 65*). A more recently identified cochaperone, Small Glutamine Rich-TPR Containing Protein Alpha (SGTA), is a TPR-containing protein that can bind both Hsp90 and

Hsp70 but has a higher affinity towards Hsp70. SGTA can be introduced within the intermediate steps due to its high affinity for Hsp70 (*66-68*). In addition, SGTA can negatively regulate AR, GR, and PR (*67, 69*). Although the dogmatic chaperone cycle seems to be straightforward, there is much cross-talk between cochaperones through competition for binding the chaperone proteins and other possible mechanisms. Cyclophilin 40 (Cyp40) is an immunophilin that plays a major role in the mature complex, yet studies have also demonstrated that it can bind to Hsp70 and modulate its role. However, Cyp40 does not bind to the Hsp70 ATPase domain (*70*). Further studies are needed to understand if the other immunophilins act in this manner. The TPR domain allows them to interact with Hsp70 and/or Hsp90, but domain organization is key to their functional and physiological relevance.

1.2.3 CHIP Degradation Pathways

Protein quality control within the chaperoning pathway is crucial and CHIP serves as the bridge for undesired substrates. CHIP has a TPR (3 TPR motifs) domain at the amino terminus, a middle helical hairpin region, and a carboxy U-box. The structure posed by CHIP gives it flexibility and adaptability for recruiting substrates via its TPR domain and sending that substrate to degradation pathways via the U-box due to its E3 Ubiquitin ligase activity, which polyubiquitinates substrates leading to their degradation in the 26S proteasome (*71, 72*). CHIP competes with HOP for Hsp70 binding; this is a rate-limiting step for substrates because they will either go towards re-folding or degradation processes (*73*). BAG1 is a cochaperone that collaborates with CHIP for Hsp70 binding. BAG1 binds to the 26S proteasome and is able to send Hsp70 substrates to this degradation pathway (*74*). CHIP and BAG1 provide the maintenance for protein quality control and could serve as therapeutic targets for diseases involving protein aggregation including the neurodegenerative diseases.

1.2.4 Mature Complex

Hsp90 is a highly abundant chaperone that has been extensively studied. It plays major cellular roles and has massive implications in diseases such as cancer (*75, 76*). In the mature complex, Hsp90 receives client proteins from Hsp70 via HOP (*77*). Once Hsp90 binds to the client protein, Hsp70 and its associated cochaperones dissociate. Upon p23 binding the protein complex becomes stable and once the immunophilin protein binds the receptor assumes a high affinity hormone binding competent state (*78*). Further, immunophilins such as FKBP51, FKBP52, Protein Phosphatase 5 (PP5), and Cyp40 compete for binding to the conserved EEVD motif in the carboxyl terminus of Hsp90 via their common TPR domain (*79-81*). FKBP52 competes with Cyp40 for Hsp90 binding via the TPR (*81*). Additionally, GCUNC-45 is an interactor of PRA and PRB, which binds to Hsp90 ATPase domain and prevents activation of the ATPase activity by Aha1. It is hypothesized that the immunophilin component can translocate the receptor. More so, FKBP52 can displace GCUNC-45 from HOP (*82*). Ultimately, FKBP52 and p23 bind to Hsp90 and stabilize the complex (*83*). Protein quality control is always in place and these dynamic steps allow for receptor recycling or activation. Upon hormone binding the SHR translocates to the nucleus, dimerizes, and binds to the hormone response element where gene transcription occurs accordingly (*84*). The question of whether the Hsp90 heterocomplex dissociates upon hormone binding as suggested by the *in vitro* models is currently a matter of debate as there are a number of evidences suggesting that the molecular chaperones are required for receptor interaction with the nuclear pore, and may associate with the receptor on the DNA. In addition, the immunophilin components of the complex may have a role in these processes.

1.3 Immunophilins FKBP51 and FKBP52

The Immunophilins belong to a group of proteins that can bind to immunosuppressive drugs (rapamycin, FK506, and cyclosporine A) through their functional peptidylprolyl cis-trans isomerase (PPIase) enzymatic domain (*85*). Immunophilins can be further divided into two categories based on the drug they bind. For instance, cyclophilins bind to cyclosporine A and regulate various cellular processes, and FK506 Binding Proteins (FKBPs) can respond to FK506 and rapamycin, and participate in protein folding (*86, 87*). These multi-functional proteins are present in plants, yeast, bacteria, fungi, and mammals, and possess immunomodulatory activity where they can regulate T cell proliferation and act as molecular cochaperones to regulate AR, GR, and PR.

The family of immunophilin proteins consists of an assortment of proteins with a size range of 12- 52 kDa in weight whose architecture is composed of three regulatory domains: FK1 at the N- terminus, FK2 in the middle region, and a TPR at the C- terminus (*80*). Studies performed by the Smith lab were the first to associate FK506 Binding Protein 51kDa (FKBP51) and FK506 Binding Protein 52kDa (FKBP52) with PR complexes, and to detail their regulatory role based on their structural composition (*80, 87, 88*). The most closely related immunophilins are FKBP51 and FKBP52 due to their roles within the Hsp90 heterocomplex. It is well established that the chaperone and cochaperone proteins work in an orchestrated manner to assist proper folding and regulation of SHRs (*89*). Particular focus has been on FKBP52 as a potential drug target given its ability to potentiate AR, GR, and PR activity (*87, 90*). On the other hand, FKBP51 is approximately 60% identical to FKBP52, yet FKBP51 suppresses SHR activity (*79, 91-93*).

Studies over the past three decades have focused largely on the FKBP12-like domain (FK1) domain, which is the critical functional domain for the regulation of SHR activity. FKBP51 FK1 is composed of a central alpha helix and surrounded by five antiparallel beta strands. This region contains a binding pocket (PPIase pocket) that is highly hydrophobic allowing drugs like FK506 and rapamycin to bind.

The FK1 has a proline-rich loop that overhangs a functional PPIase enzymatic pocket, although PPIase activity is not critical for FKBP52 regulation of receptor activity. To narrow down which region within the FK1 domain is the most critical for function, a library of random FKBP51 mutants was generated by error-pone PCR and these mutants were screened in receptor-mediated reporter assays in yeast. Interestingly, only two residue changes (A116V and L119P) within the FKBP51 proline-rich loop, which make the FKBP51 loop more like that of FKBP52, convert FKBP51 from a negative to a positive regulator of receptor activity (*49*). These data suggest that the proline-rich loop within the FK1 domain is critical for the regulation of receptor activity and may serve as an interaction surface within the receptor-chaperone complex. An analysis of FKBP sequence similarity across species suggests that FKBP51 and FKBP52 functionally diverged some time after the boney fishes.

A striking difference between FKBP51 and FKBP52 can be observed in the 7-9 residues linking the FK1-FK2 domains, also known as the FK linker. The FKBP52 FK linker has a Casein Kinase II (CKII) phosphorylation site, which is phosphorylated by CKII in cellular models (*95*). CKII phosphorylation was demonstrated to prevent FKBP52 binding to Hsp90 (*96, 97*) and to abrogate FKBP52 potentiation of receptor function (*93*). FKBP51 lacks the CKII phosphorylation site. The importance of CKII phosphorylation *in vivo* and the contribution of this difference to the distinct functions of FKBP51 and FKBP52 are currently unclear.

In addition to the FK1 region, the TPR is also critical for function in that it is required for FKBP52 binding to Hsp90's carboxy terminus EEVD motif (*95*). Site-directed mutagenesis studies further demonstrated that a single point mutation (FKBP51K352A and FKBP52K354A) abolished FKBP protein binding to Hsp90. Interestingly, not only is the TPR region important to bind Hsp90 but so are the upstream and downstream regions (*98*).

TPR-containing proteins have been extensively studied to understand the nucleo-cytoplasmic shuttling of SHRs. Although much insight has been provided, the exact mechanism is currently unclear. For instance, it remains unknown if the chaperone heterocomplex plays a role in the nuclear pore complex (*58*). Evidence suggests that dynein and FKBP52 work in concert for GR translocation into the nucleus (*99*). Confocal microscopy experiments have revealed that GR is unable to translocate to the nucleus when Hsp90 is inhibited by geldanamycin (*100*). Some evidence also suggests that FKBP52 may translocate to the nucleus with the SHR, and confocal microscopy studies demonstrated that FKBP52 co-localizes with receptors and additional transcription factors on the DNA independent of its interaction with Hsp90 (*102*). Thus, the dogmatic chaperoning cycle illustrated in Figure 1.1.1 is likely a drastic oversimplification regarding the roles of TPR-containing proteins within the SHR signaling pathways. In addition to the regulation of receptor activity within the Hsp90 complex, the FKBP proteins also have additional roles within cells. FKBP52 destabilizes microtubules, whereas FKBP51 promotes microtubule assembly, and the functional and physiological significance of these activities are currently unknown (*101*). More recently, FKBP52 was shown to interact with and regulate NF-kB. Taken together, the data has firmly established the FKBP proteins as relevant factors in SHR signaling and as attractive drug target for the treatment of hormone-dependent diseases. While the role of the FKBP proteins have been extensively studied, novel

TPR-containing proteins continue to be identified that may also have functionally important roles in SHR signaling.

1.4 Small Glutamine Rich Tetratricopeptide Repeat Containing Protein Alpha

Small Glutamine Rich Tetratricopeptide (TPR) Repeat Containing Protein Alpha (SGTA) is a 35 kDa cochaperone that is involved in numerous cellular processes from viral particle assembly to apoptosis, cell division, protein quality control, and steroid hormone receptor regulation (*103-105*). A complete list of the known protein interactors can be seen in Table 1.

1.4.1 SGTA's Involvement in Viral Pathways

Two groups independently identified SGTA as a protein interactor for a variety of viral proteins in yeast two-hybrid screens. Czieplucha *et al* first identified SGTA interacting directly with the NS1 of Parvovirus H-1 using an *in vitro* interaction assay. Fluorescence microscopy has also shown SGTA accumulation with NS1 H-1 nuclear bodies owing to specific recruitment. Since NS1 protein is vital for driving viral DNA replication, SGTA's association suggests a similar biological role (*106*). Furthermore, cellular fractionation studies reveal SGTA in the cytoplasm and nucleus of rat fibroblasts, while Western blot has demonstrated that SGTA is ubiquitously expressed in rat tissue (*104, 107*). SGTA is chromosomally located on 19p13 based on *in situ* hybridization, and is ubiquitously expressed in human tissue as shown by Northern blot (*108*). Given this, it appears that SGTA is associated with many maintenance pathways in a predominantly inhibitory role.

Callahan *et al* used a yeast two-hybrid screen to detect unknown interactors with Viral protein U (Vpu) and identified SGTA. They presented SGTA as U-binding protein (UBP) for its *in vitro* and *in vivo* interaction with Vpu and Gag protein of HIV-1 (*103*). Vpu and Gag proteins

have collaborative functions and are critical for viral entry and exit (*109, 110*). Interestingly, GST-UBP (SGTA) was able to co-precipitate with Gag protein directly *in vitro*. However, transiently transfected HeLa cell lysates were used for *in vitro* binding assays and in the presence of Vpu, GST-UBP (SGTA) was unable to bind Gag protein. Additionally, a p24 ELISA exhibited that UBP (SGTA) can negatively regulate HIV-1 particle release (*103*). The aforementioned experimental data suggests that UBP (SGTA) can mediate the interactions between these two proteins perhaps via its TPR. In an effort to further understand SGTA's regulation with Vpu and Gag, immunofluorescence studies demonstrated that SGTA associates with actin filaments and microtubules. Upon treatment with the microtubule-destabilizing agent, colchicine, SGTA remained associated with microtubules. However, when assessing SGTA's association with microtubules in a detergent-dependent manner, cellular fractions were unable to associate (*111*). Collectively, these studies have demonstrated that SGTA can inhibit viral particle release and is involved in distinct pathways from different viral families.

Severe acute respiratory syndrome coronavirus (SARS-CoV) 7a is another interacting viral partner of SGTA mediated by its TPR region (*112*). In addition to the human interaction, SARS-CoV7a co-immunoprecipitated with the African Green monkey SGTA from Vero E6 cells. Co-localization studies demonstrated that SGTA translocates to the nucleus with SARS-CoV7a and that SGTA could be an accessory protein important for viral particle formation. The presence of SGTA in the cytoplasm and nucleus are in line with the previously established reports.

The Rec protein of Human endogenous retroviruses HERV-K (HML-2) adds to the list of viral proteins interacting with SGTA by means of a yeast-two hybrid screen, and co-localize through SGTA's TPR domain (*113*). Since HERVs are endogenously expressed in human cells,

they have been implicated in cancer progression due to their oncogenic properties (*114, 115*). In prostate cancer cell lines, HERV-K transcripts and splice variants were present suggesting a role for these endogenous retroviruses in PCA progression (*116*). In addition to binding and co-localizing, HERV-K (HML-2) masks SGTA's ability to inhibit AR function. HERV-K (HML-2) up-regulates AR by preventing SGTA binding to the chaperone complex of AR leading to enhanced AR-mediated transcriptional activity. These interactions are functionally relevant because they can play a major role in tumor progression and lead to the next generation of drug targets.

1.4.2 SGTA's Functional Role with Hsp70 and Hsp90

SGTA binds to molecular chaperones and possesses cochaperone activity as evidenced by multiple biochemical studies. SGTA can bind to Hsp70's C-terminus, which has a conserved EEVD motif that is known for regulating chaperone activity mainly through its TPR domain (*117, 118*). Similar to Hsp70, SGTA's TPR domain is responsible for binding to Hsp90 (*66*). SGTA's binding affinity for Hsp70 is 6.1μM, whereas its affinity for Hsp90 is 11.0μM. Although SGTA has similar *in vitro* affinities to Hsp70 and Hsp90, it preferentially precipitates with Hsp70 (*67*). Furthermore, SGTA forms a synaptic protein chaperone complex with Hsc70 and Cysteine String Protein (CSP) where it has effects on misfolded proteins near the synaptic vesicle surface (*119*). In addition, SGTA shows suppressive toxicity effects through its interaction with intracellular β amyloid peptide (*120*). SGTβ, an isoform of SGTA was found to be exclusively in the rat brain and can bind to Hsc70 and CSP. SGTA and SGTβ operate in a similar fashion mainly by binding Hsc70 and CSP through their TPR domain, and it was suggested that they work in conjunction to regulate the central nervous system, which might be pertinent for neuronal protection (*121*). Moreover, based on co-immunoprecipitation

experiments, the N-terminal region of myostatin interacts with the TPR and the C-terminus of SGTA (*122*). Myostatin is mostly present in skeletal muscle and has a negative regulatory role (*123*). The association of SGTA with myostatin contributes to the list of proteins towards which SGTA has an inhibitory role.

Mounting evidence has suggested that SGTA plays a "housekeeping" role in cellular processes. Primarily, Winnefeld and colleagues observed that SGTA is required for cell cycle progression. A time-lapse microscopy video depicted that SGTAKDHeLa cells stayed longer in mitosis and exhibited delays in prometa- or metaphase in comparison to wild type HeLa cells. The complex formed by Hsp70, SGTA, and Bag-6 was able to co-precipitate in prometaphase cell extracts (*124*). In addition, Wang *et al* extended the previous observations and demonstrated that SGTA promotes apoptosis in 7721 cells and showed that the TPR motifs are critical for this function (*122*). The three structural units were identified and individually tested for functionality by Wang and colleagues. They concluded that the TPR interacts with Hsp90. Additionally, because of the close association with Hsp90 in HeLa cells, SGTA displays pro-apoptotic function (*105*). It can be reasonably concluded that the TPR region plays a pivotal role in cellular interaction (*125*).

Although the work cited above provides convincing evidence that SGTA's structural domains are relevant factors that contribute to cellular roles and protein-protein interactions, the precise functions are completely unknown in prostate cancer progression. For instance, Buchanan and colleagues demonstrate that SGTA down-regulates AR. They suggested that this effect retains AR in the cytoplasm and serves as a rheostat for its control. Moreover, *in silico* docking analysis predicted that SGTA interacts with AR's hinge region. However, definitive proof of this proposed mechanism is lacking. On the other hand, Paul *et al* sought to determine if

this novel regulatory role posed for SGTA works similarly for other nuclear receptors. A sequence alignment showed that human SGTA and *S. cerevisiae* Sgt2 share approximately 30% amino acid identity (Figure 2.3.3). Moreover, they have three regions required for function: N-terminus, TPR, which is the most conserved across species (*108*), and Q-rich region (*67*). SGTA is a negative effector of GR and PR, however, there was no effect on MR and ER activity. To further validate such interactions, HeLa SGTA KD cell lines were generated. In luciferase reporter experiments, the absence of SGTA increases receptor function. On the contrary, when SGTA is present the negative effect remains. Furthermore, a yeast two-hybrid analysis demonstrates SGTA associates with GR and PR. This result does not demonstrate a direct interaction with the receptor, but it does suggest an association with receptor-chaperone complex. The data indicate that SGTA is a specific negative regulator of AR, GR, and PR activity.

Based on SGTA's involvement with PCA, many efforts have been made to understand if SGTA is a contributor to PCA progression. The knockdown of SGTA in C4-2B cells had a significant alteration in AR target genes, and potentiates Akt activity (*126*). C4-2B cells have been derived from a LNCaP PCA cell line and exhibit castration resistant features (*127*). PI3K/Akt signaling has been implicated in PCA progression and activation is observed in CRPC (*128*). This line of evidence is in stark contrast to what Buchanan *et al* published since AR's activity was inhibited in PCA cells (*69*). Our lab has also observed that SGTA is a transcriptional repressor of AR (*67*). Perhaps this indicates SGTA is a protein reliant on tissue and system specificity for its regulation.

1.4.3 SGTA's Involvement in Protein Quality Control

The first report of SGTA in protein quality control pathways was performed by Schantl *et al*. They determined that SGTA's TPR region is critical for its interactions with the ubiquitin-dependent endocytosis (UbE) motif of the growth hormone receptor (*129*). Although it is not involved in the ubiquitin pathway, it seems this interaction is critical for the fate of the growth hormone receptor perhaps due to SGTA's interactions with Hsp70 and CHIP in the intermediate chaperone pathway. Moreover, the endoplasmic reticulum is the entry site for the transmembrane domain recognition complex of 40 kDa (TRC40) and this complex is driven by chaperones (*130*). Tail anchored (TA) proteins constitute a majority of biosynthetic pathways and function in an ATP-dependent manner (*131*). Sec61β is a TA protein that interacts with SGTA and facilitates membrane entry (*132*). The Bcl-2 associated athanogene-6 (BAG6) is a multifunctional cochaperone that collaborates with Hsp70 to enhance protein quality control by sending substrates to degradation pathways (*133*). Remarkably, SGTA plays a role in promoting deubiquitination of mislocalized proteins from BAG6-mediated protein triage by masking the hydrophobic regions (*134-136*). SGTA binds to Rpn13, which is a proteasomal ubiquitin receptor, and can prevent proteasomal degradation (*137*). The yeast homologue of SGTA, Sgt2, is involved in the TA protein pathways as well. The Guided Entry of TA proteins (GET) pathway is composed of Get3, Get4, and Get5 proteins that form a complex and are ATP-driven to direct newly synthesized proteins to their respective locations (*138, 139*). Sgt2 is involved in this pathway by loading the TA protein onto Get5, by binding to the Ubl domain of Get5 (*140, 141*). Based on structural studies, the dimerization domain of SGTA and Get5-UBL interaction is mainly driven by electrostatics (*142*). Thus far, these studies have demonstrated that SGTA along with partners from the BAG6/UBL containing protein complexes recognize and propel

proteins towards biosynthesis or degradation mechanisms. SGTA has become an increasingly relevant factor in protein quality control and it would be interesting to determine if SGTA can determine the fate of SHRs and thus, influence their negative regulation.

Table 1: SGTA Protein Interactors

	Protein Interactor	Method of Discovery	Bait	SGTA Relevant Regulatory Role	Year	Citation
1	NS1-Parvovirus H-1	Y2H	H-1virus NS1, FREJ4 cDNA library	Can be modified by parvovirus infection.	1998	(***104***)
2	Vpu and HIV-1 Gag	Y2H	Vpu, Human B-lymphocyte cDNA library	Plays a role in virus assembly or release and inhibits viral particle release.	1998	(***103***)
3	Hsp70	Y2H	Hsc70, human liver cDNA library	TPR associates with Hsp70.	1999	(***117***)
4	Cysteine String Protein	Y2H	rat CSP1 and rat brain library as prey	Forms a complex with Hsp70 and together as a complex work to inhibit neurotransmitter release.	2001	(***121***)
5	UbE motif of growth hormone receptor	2D-gel, MS	GHR and truncated GHR, HepG2 cells	SGTA first TPR specifically interacts with the UbE but does not have a role with ubiquitin system.	2003	(***129***)
6	N-terminal myostatin	Y2H		SGTA's third TPR motif was crucial for interaction with N-ter of myostatin, may play a role in myostatin secretion and activation.	2003	(***122***)
7	Hsp90B				2006	(***105***)
8	SARS-CoV7a	2Hybrid			2006	(***112***)
9	Bag6/Bat3/Scythe	Co-IP-MS	SGTA-FLAG, HeLa cells	SGTA might be involved in mitosis, as a complex, bag-6/bag-3/scythe could be required for complete chromosome progression.	2006	(***124***)
10	AR	Y2H	AR, pACT2-pooled prostate cDNA library	SGTA negatively regulates AR.	2007	(***69***)
11	Nuclear proteome	2D-gel, MaldiTOF	Embryonic Stem cells	Part of the nuclear proteome along with SUMO.	2010	(***143***)
12	PDGFRalpha	phosphoproteomic study	PDGFR alpha, in cancer cell lines-	S305 SGTA critical for PDGFRalpha stabilization and cell	2010	(***144***)

				survival.		
13	TRC40 Substrate: Sec61βOPG	Purified recombinant pull down		SGTA helps with accommodating substrates with PEGylated TA region, and helps integration.	2011	(***132***)
14	HERV-K(HML-2) Rec	Co-IP in HEK293T cells		Rec protein disrupts SGTA's negative role in AR and leads to a vicious cycle increasing cell proliferation and inhibition of apoptosis eventually leading to tumorigenesis.	2013	(***113***)
15	SV40	Purified recombinant pull down		Completes ER membrane penetration in a nonenveloped virus.	2014	(***145***)
16	GR and PR	Y2H		Down-regulates GR and PR.	2014	(***67***)
17	Rpn13	Y2H	Purified recombinant pull-downs with Rpn13	SGTA is involved in protein quality control with BAG6 complex and operates in 19S regulatory particle. Helps to escape proteasomal degradation and selectively modulates substrate degradation.	2015	(***137***)
18	REIC/DKK-3	Y2H	REIC/DKK-3, normal human heart and prostate cDNA library	Binding to REIC/DKK-3 this interferes with SGTA dimerization, promotes dynein-dependent AR transport then upregulates AR signaling.	2016	(***146***)

1.5 SGTA, FKBP51, and FKBP52's Role in Disease

TPR-containing proteins have the potential to impact a diverse set of hormone-dependent physiological processes and diseases. In terms of understanding these diseases at the molecular level, molecular chaperones and cochaperones have been extensively studied since they are involved in the SHR regulation. Acquiring knowledge on how these proteins associate with and regulate the receptors will provide novel targets and strategies for the treatment of diseases.

The first studies to relate FKBP52 in a physiological context were performed by Cheung-Flynn and colleagues where a FKBP52 knockout (52KO) mouse model was generated. They characterized the critical importance of FKBP52 in the male and female reproductive tract. An apparent difference in the FKBP52KO model compared to the wild type was the presence of nipples and internally, the seminal vesicles and anterior prostate were mainly absent creating a link to Androgen Insensitivity Syndrome (AIS). AIS is characterized by the lack of androgens present in males where symptoms such as ambiguous external genitalia, a dysgenic prostate, and nipples are notable. Interestingly, mice lacking FKBP51 and FKBP52 were embryonically lethal suggesting redundant roles for these two proteins in embryonic development (*147*).

It has been established that FKBP52 is critical for normal male and female reproductive development and success. Congenital anomalies such as hypospadias have been affiliated with FKBP52, and an increase in infant birth defects has been reported (*148*). Anatomical defects have been affiliated with FKBP52 based on the previous FKBP52KO mouse studies. In addition, in human samples, immunohistochemistry studies from the epidermis of the penile skin demonstrated the presence of FKBP52. Nonetheless, genetically, there were no FKBP52 mutations in these samples (*149*). In addition, it has been reported that FKBP52 plays a relevant role along with AR for urethra morphogenesis. *In situ* hybridization showed that there were

higher levels of FKBP52 present in the ventral rather than the dorsal aspect of the male penis (*150*).

In female mice, FKBP52 is critical for implantation given that embryos failed to implant after fertilization in 52KO mice. This phenotype is consistent with FKBP52's positive role in PR signaling based on cellular and biochemical evidence (*151*). Studies have established that FKBP52 also plays a role in Endometriosis. Immunohistochemistry studies performed by the Dey group showed that 52KO female mice, as compared to the wild type, had endometriotic lesions. They sought to determine if angiogenesis played a collaborative role with FKBP52. In the 52KO mice there was increased inflammation and angiogenesis. The extent as to which FKBP52 influences angiogenesis is not well understood. In a clinical setting, immunohistochemistry revealed that FKBP52 expression was low in human endometriosis samples (*152*). More recently, a more detailed role for FKBP52 in reproduction has been established; depending on the stage of pregnancy FKBP52 forms a complex with hormone-bound PR (*153, 154*).

A role for FKBP52 is not exclusive to sexual development, but it also appears to be a critical component of other diseases such as prostate cancer. In human prostate cancer tissues, up-regulated expression of FKBP52 is observed (*155*). Thus far, the emphasis for targeting prostate cancer has relied heavily on Hsp90, but a novel approach is to target immunophilins based on their molecular and physiological importance. With this in mind, De Leon and colleagues screened a small molecule library from which the lead compound MJC13 shows a decrease in cancer cell proliferation. The lead compound was capable of “freezing” the mature Hsp90-FKBP52-AR complex and retaining the complex in the cytoplasm (*156*). The data demonstrate that targeting the regulation of AR by the FKBP52 cochaperone is an effective

strategy that could by-pass mechanisms of disease resistance observed with the current antiandrogen therapies currently used in the clinic.

The neuroendocrine effects that involve FKBP52 are minor as compared to the closely related FKBP51 protein, which results from FKBP51's negative regulation of GR in a tissue-specific manner. However, FKBP52 can regulate GR as well and behavioral studies have shown that 52KO mice demonstrate an anxiety-related behavior. In addition, 52KO mice had higher levels of stress as compared to wild type suggesting that FKBP52 has a specific role with GR in the HPA axis. This regulatory role remains unknown and it would be interesting to understand the difference that FKBP52 and FKBP51 have on GR specificity in neuroendocrine disorders (*157*). Moreover, based on the interaction FKBP52 has with tau proteins this interaction is likely to be critical for Alzheimer's Disease (AD). Indeed, in AD, FKBP52 is present in extremely low levels in the frontal cortex of patients with AD as compared to controls (*158*). Although the role of tauopathies is well studied, the role of FKBP52 remains elusive. A metabolic role for FKBP52 with GR has also been established. A study mimicked the metabolic syndrome in mice lacking FKBP52, as well as in wild type mice. 52KO mice became GR-resistant leading the liver to retain fat (*159*). Mounting evidence based on animal and cellular studies demonstrate that FKBP52 has a meaningful role in physiological processes. Thus, using FKKBP52 as a molecular target for numerous diseases can be extremely useful and, yet understanding the exact mechanism as to how FKBP52 can regulate receptor is needed.

FKBP52, a positive regulator, shares the same specificity as SGTA for receptor regulation. A receptor-mediated reporter assay in yeast demonstrated that SGTA abrogates FKBP52-regulated receptor function. Further, a human tissue blot, based on their physiological relevance to AR, GR, and PR, was used to assess tissue-specific expression patterns of FKBP52

and SGTA and a similar pattern of expression in the tissues was observed. Higher expression is present in the testis, brain, ovaries, and liver, and its expression is lowest in the ovary. Moreover, SGTA and FKBP52 both possess TPR regions and this effect could be due to a competition for binding the EEVD motif on Hsp90. Collectively, these data suggest that there is a physiological relevance and that SGTA can have multiple functions in the cell. The immunophilin FKBP51 that is highly similar to FKBP52 does not have a dramatic effect on receptor function like SGTA (*67*).

SGTA has been implicated in various diseases such as Polycystic Ovary Syndrome (PCOS), and based on its regulation with the AR-chaperone complex, it may contribute to the pathogenesis of PCOS (*160-162*). Unfortunately, gynecological carcinomas are a major threat for woman in the United States as the SGTA/AR ratio is altered and this alteration influences subcellular localization (*163*). The SGTA/AR ratio seems to be low in reproductive cancers contributing to progression. Immunohistochemistry studies demonstrated that SGTA is expressed in Non-Hodgkin's Lymphomas (*164*), esophageal squamous cell carcinoma (*165*), human hepatocellular carcinoma (*166*) and, non-small-cell lung cancer (*167*). Collectively, these studies made SGTA a contributor of tumor cell proliferation, differentiation, and poor prognosis.

1.6 Prostate Cancer Mechanism of Action: Classical and Contemporary Approaches

Prostate cancer is a moral and economic burden to families in the United States. In 2015, PCA accounted for 220,800 newly diagnosed cases and approximately 27,540 deaths according to the American Cancer Society. African American males are at higher risk than other races, making this a health disparity that requires immediate research attention. Prostate cancer is typically terminal once it becomes castration-resistant. For early stage cancers, current effective

treatments include antiandrogens, which antagonize the androgen receptor. However, as PCA progresses to castration resistance these treatment options become ineffective. AR is a promising target for PCA, yet the mechanisms of androgen-independence remain unclear (*168*).

There is substantial evidence showing an important role for the Hsp90 chaperone machinery in 'client' protein (*e.g.* AR) folding and function. Hence, Hsp90 also serves as a therapeutic target for PCA. Hsp90 inhibitors have been in clinical trails since 1999 where only three molecules have been introduced in the clinic. Trepel *et al* suggest that cancer cells are addicted to chaperones like Hsp90 due to a cancerous (stressed) state (*169*). Development of strategies like androgen antagonism, blocking androgen synthesis, and Hsp90 inhibitors to degrade AR are revolutionizing the fields as well (*170*). Moreover, mutations in AR are present in primary tissue samples and cell lines where the exploitation of this fact has served to investigate novel mechanisms and alternate sites for PCA. AR structural regions are also under investigation where it is believed that by blocking functionally relevant coactivators of AR better therapeutic approaches can be achieved (*43, 171, 172*).

Other strategies to target PCA are through the roles AR splice variants (AR-V7) have on CRPC. The most recent findings in this area show that AR splice variants remain resistant to inhibitors as compared to full length AR and are constitutively active (*11*). The difference between full-length and AR-V7 is that the ligand domain which is located at the C- terminus in AR is lacking (*173*). This means that even though its specificity for and activation by a ligand is lacking, AR-V7 can homodimerize or heterodimerize with the full-length AR and thus initiate transcription of target genes (*174*). The splice variant mechanism is suspected to contribute to the escape of the normal AR mechanism due to its truncated domain (*175*). This constitutive AR signaling bypasses the classical therapies.

Novel therapies involving the androgen synthesis pathway, AR signaling inhibition, and degradation of AR seem to be the most effective strategy for targeting the splice variants (*176*). Unfortunately PCA signaling will find means to bypass the novel therapies. In PCA sample tissues, an overexpression and up-regulation of AR-V7 is observed mainly in the CRPC stage (*177*). The exact mechanism as to how these contribute to progression and can remain constitutively active remains unknown. One interesting hypothesis is that AR-V7 is developed as a compensatory mechanism when a patient undergoes Androgen Deprivation Therapy (ADT) (*178*).

In addition to AR, GR has been speculated to be a driving force for CRPC. GR belongs to the nuclear receptor superfamily and can activate an analogous transcriptional sequence (*179*). An interesting study was performed by Xie and colleagues in which they demonstrate, through a PCA tissue microarray, an upregulation of GR genes in CPRC. However, these genes were not altered in a pre-castration model suggesting that GR is repressed by AR (*180*). In a similar manner, PR has the capacity to activate CRPC and nuclear PR was present in PCA sample suggesting that it may be associated with the transition from a pre-CRPC to CRPC (*181*). The SHRs share structural domains and have the capacity to activate similar pathways in a unique manner. An exciting approach is being developed in Dr. Cox's laboratory in which the targeting of the FKBP52 cochaperone directly would inhibit a variety of protein known or thought to have a role in PCA progression including AR, GR, and PR.

1.7 Current Research Focus

In the present study, I demonstrate the binding affinities of SGTA for Hsp70/90. A PR reconstitution assay demonstrates that SGTA does not affect chaperone complex formation and is not vital for receptor hormone binding. In studies comparing full-length versus a ΔQ-rich

SGTA mutant at the C- terminus, the ΔQ-rich mutant fails to abrogate AR activity in a yeast receptor-mediated reporter assay. This demonstrates the importance of the Q-rich region at the C-terminus of SGTA for AR signaling, and that SGTA regulation of SHRs is not based solely on its ability to interact with Hsp70/90. Additionally, SGTA antagonizes Peroxiredoxin 1 potentiation of AR activity in HeLa-SGTAKO and 22RV1-SGTAKO cell lines. SGTA and PRDX1 can interact directly *in vitro* in the absence of other proteins, as demonstrated by a FLAG-pull down assay using purified recombinant proteins. Thus, SGTA remains a relevant factor due to its ability to associate with and antagonize positive-regulators of AR.

1.8 Hypothesis

Molecular chaperones are responsible for regulating the folding and activation of steroid hormone receptors (SHRs). The dynamic exchange of factors, and the type of protein-protein interactions involved is critical for SHR regulation in physiological processes. However, the precise molecular mechanism that drives these SHRs to function remains poorly understood. This knowledge is necessary because in late stage prostate cancer the androgen receptor can be activated upon exposure to molecules other than ligand. Because of this, the receptor can be continually activated as seen in castration resistant prostate cancer. The cochaperone SGTA is crucial in the down-regulation of androgen, progesterone, and glucocorticoid receptors. Moreover, our results have also indicated that when SGTA is co-expressed with the immunophilin FKBP52, SGTA can partially abrogate receptor function. However, receptor reconstitution assays *in vitro* demonstrate that SGTA is an independent regulator in receptor function because hormone-binding levels were not affected. We hypothesize that SGTA is acting as a non-competitive inhibitor of FKBP52 function by binding to intermediate receptor chaperone complexes preventing the receptor from reaching the native folded state on which

FKBP52 acts. In prostate cancer, SGTA levels are down-regulated and FKBP52 levels are up-regulated, thus implying that SGTA may play a key role in governing negative feedback (Figure 1.1.2).

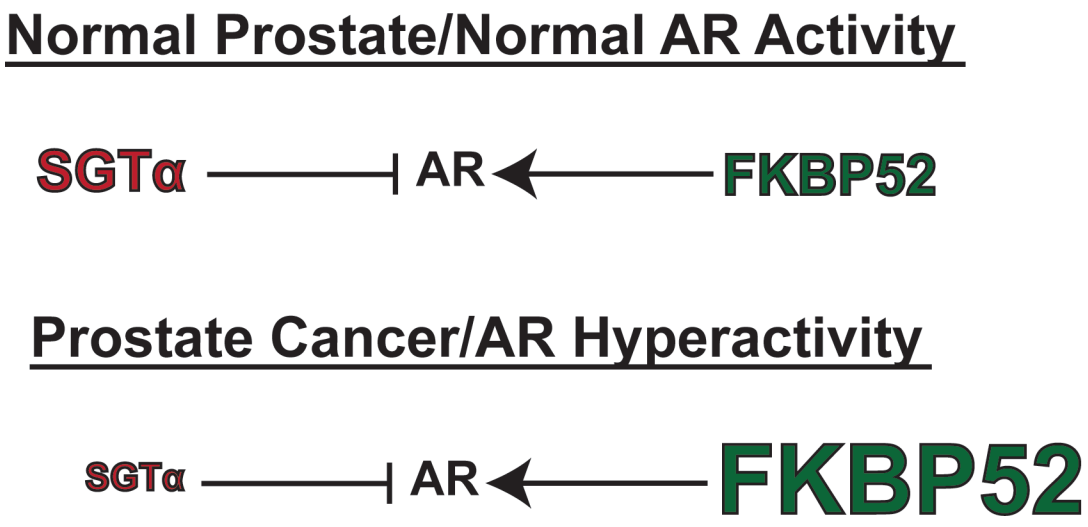

Figure 1.1.2 SGTA Regulatory Hypothesis in Normal versus Prostate Cancer Activity

In a normal prostate, SGTA inhibits AR regulation while FKBP52 promotes it to maintain homeostasis in a normal prostate setting. In Prostate Cancer, AR hyperactivity is observed in which SGTA expression levels are decreased and FKBP52 expression levels are up-regulated which drives AR to a hyperactive state and disrupt this homeostatic balance.

1.9 Dissertation Goals

The overall target of this work is to understand the structural and functional role SGTA plays in androgen receptor signaling. Based on our knowledge that SGTA can abrogate androgen receptor function, and that it is down-regulated in prostate cancer, it is relevant to understand the important SGTA functional domains and/or residues. In addition, the identification of SGTA interactors that could abrogate the negative regulation of AR by SGTA could lead to novel drug targets for the treatment of PCA. An effort has been made to understand SGTA's regulation towards the androgen receptor by addressing the following questions:

1. Which domain is important for SGTA's functional role?

2. Does SGTA belong to the intermediate/mature complex in the chaperone machinery?

3. What are the global SGTA interacting proteins in prostate cancer cells and do any of these interactions antagonize SGTA regulation of AR?

In addressing these questions, we will contribute to the knowledge by which a specific domain is regulating AR and its role in the chaperone machinery towards receptor folding and regulation. Additionally, we will provide evidence of previously unknown SGTA interacting partners and of their putative functional role. In testing our hypothesis, we will have an understanding of SGTA's role in prostate cancer progression.

Chapter 2: Functional Characterization of SGTA Interactions with the Androgen Receptor

2.1 Rationale

Initial studies demonstrated that SGTA is a novel cochaperone that interacts with Hsp70 and Hsp90, and down-regulates AR by binding to its hinge region (*68, 69, 105, 118*). More recently, our laboratory demonstrated that SGTA associates with and negatively regulates GR and PR complexes as well (*67*). SGTA is comprised of a unique N- terminal dimerization domain, a middle TPR domain, and a glutamine-rich C-terminus (*66, 125*). Currently, SGTA is known to interact with Hsp70 and Hsp90 through the conserved C-terminal EEVD motif (*66, 68, 118*). Nevertheless, it is unknown whether the binding affinity towards Hsp70/90 interaction is essential for the steroid hormone receptor maturation process, or whether the regulatory domains are capable of having a functional effect. Here we sought to determine the binding affinities of SGTA and Hsp70/90 to better understand if these affinities play a role in the receptor maturation process.

Another TPR-containing protein, FKBP52, is similar in that the TPR mediates interactions with Hsp70 and Hsp90 to regulate AR activity (*49, 93, 182*). Based on these similarities, we sought to determine whether SGTA had the ability to influence FKBP52 regulation of AR (*67*). Our previous studies in a yeast reporter assay in which we co-transformed FKBP52 and SGTA showed SGTA had an antagonistic effect on FKBP52's ability to regulate AR and GR. Initially, we hypothesized that SGTA and FKBP52 were competing for Hsp70/Hsp90 MEEVD binding motif through their TPR domains. To further understand this we utilized a well-established *in vitro* progesterone receptor reconstitution assay to investigate whether SGTA associates with intermediate complexes, thus preventing the receptor from reaching the mature complex (*183*).

In addition to SGTA's role in the chaperoning pathway, we assessed which SGTA domain(s) were critical for regulation of AR activity. The extent to which the down-regulatory effect on nuclear receptor activity is dependent on SGTA's structural domains has not been established. Therefore, we generated truncation mutants and tested them in a well-established functional yeast reporter assay system (*184, 185*).

2.2 Materials and Methods

2.2.1 CONSTRUCTS

Construction of Truncation Mutants: Dutta et al. were the first to determine the structure of SGTA (*125*). However, the extent of each domain's function remains elusive. Therefore, to assess the significance of the three distinct domains, truncation mutants were generated. A translation stop codon was introduced at the desired location to produce each truncation mutant. To obtain these constructs, we used the QuickChange kit (Stratagene) and standard procedures. The full-length SGTA yeast expression vectors served as the template. Upon completion of the yeast truncation mutants, the plasmids were transformed into the yeast strains. A hormone-inducible β-galactosidase reporter plasmid, a *LEU2*-marked high copy number plasmid constitutively expressing the androgen receptor from a glyceraldehyde phosphate dehydrogenase (GPD) promoter, and a *HIS3*-marked high copy number plasmid with the truncation mutant, thus allowing for growth and assessment of function. Transformants were selected with medium containing synthetic complete dextrose lacking leucine, uracil, and histidine. Confirmation of the construct was performed by DNA sequencing at UTEP's BBRC DNA Analysis Core Facility.

2.2.2 Receptor-Mediated Reporter Assays in Yeast

Yeast reporter assays are used to record steroid hormone receptor activity by means of measuring β-galactosidase. Standard procedures were followed as with Balsiger *et al*. and modified as necessary (*184*). Three independent isolates were grown overnight in 5 ml of selective medium lacking leucine, uracil, and histidine in a shaking incubator at 30°C. To ensure that the yeast exhibit logarithmic growth, overnight cultures were diluted to an OD_{600} of 0.08, and growth was monitored by spectrophotometry approximately 20 minutes after dilution. Next, dihydrotestosterone (DHT) was added and incubated in the shaking incubator at 30°C for two

hours. To measure β-galactosidase activity, in a 96-well plate, 100 μl of culture and 100 μl of Gal-Screen TM substrate (Appplied Biosystems) were mixed, covered to avoid evaporation, and incubated for two hours at room temperature. Post two-hour incubation, the plate was read in a luminometer (BioTek). Relative light units were normalized to the optical density of the cultures and plotted as a percentage of the activity in the presence of the empty vector alone (lacking SGTA expression). The normalized data were plotted in GraphPad Prism Software. The data reported is performed in triplicate clonal isolates and in at least three separate experiments. The empty yeast expression vector (p423-GPD) served as our control, and full-length SGTA was used to compare the functional differences of the truncation and chimeric proteins.

2.2.3 Western Blot Analysis

Overnight yeast cell culture was pelleted upon exponential phase growth. The pelleted yeast cells were washed using HyPure Grade Molecular Water (Thermo) then resuspended in yeast cell lysis buffer (20mM Tris-HCl, pH 7.4, 50 mM NaCl, 5% Glycerol) containing EDTA-free protease inhibitor cocktail (Thermo). To disrupt the yeast cell walls, glass disruption beads 0.5 mm for yeast/fungi (Research Products International Corp.) were used and vortexed rigorously with the yeast cells containing lysis buffer plus protease inhibitor 7 times for 1 minute each while placing the lysates on ice in between disruptions. The cells were then centrifuged for 20 minutes at 4°C at maximum speed to remove cell debris. The supernatant was saved and used to perform a Bradford Assay using Coomassie Plus (Bradford) Assay Kit (ThermoScientific, Pierce) according to manufacturer's instructions. 30 μg of total cell lysate was loaded in a 10-20% Criterion Gel (BioRad), and transferred to a PVDF membrane. The presence of SGTA was detected using anti-SGTA antibody (ProteinTech), Androgen Receptor (Santa Cruz Biotechnology; mouse monoclonal), and our loading control: L3, a mouse monoclonal antibody (*186*). L3 is a ribosomal protein encoded by the TCMI gene and is the largest ribosomal protein in *S. Cerevisiae*. All the above antibodies were alkaline phosphatase conjugated for use with the Immun-Star AP Substrate (BioRad) upon exposure to X-Ray Film (Phoenix Research Products).

2.2.4 Statistical Analysis of Yeast Assay Data

Statistical analysis was performed using GraphPad Prism software. The data was normalized to the vector and the mean assessed by one way analysis of variance followed by a Bonferroni post-test and a value of $p< 0.05$ determined statistically significant values.

2.2.5 Recombinant Protein Expression and Purification

Purified recombinant human Hsp90∝ and Hsp70 were previously purified in the Buchner lab (Department Chemie, Technische Universität München, Garching, Germany). SGTA was cloned into pET28a(+) vector with a C-terminal His_6 tag and into pGEX-4T-1 (a kind gift from Dahai Zhu, Chinese Academy of Medical Sciences) with an N-terminal GST tag. The His_6-tagged and GST-tagged SGTA were both shown to be functional in the yeast reporter assays (data not shown). For purification, the His_6-tagged SGTA was expressed in *Escherichia coli* BL21 (DE3). 30 ml of each overnight culture were grown in 1 liter of medium in a shaking incubator at 37°C until the A_{600} reached 0.6. Protein expression was induced with isopropyl β–D-1-thiogalactosidase to a final concentration of 1mM. The cultures were grown for an additional 4h and centrifuged at 6,000 rpm for 20 min. The pellets were resuspended in 12 ml of lysis buffer (20 mM Tris-HCl, 300 mM NaCl, 10 mM imidazole, pH 8) and divided into three 4-ml aliquots. 40 µl of 100 mg/ml lysozyme was then added to each 4-ml cell suspension and incubated for 20 min at 30°C. To lyse the cells, each of the four samples were then sonicated and kept on ice. The four aliquots were pooled together and centrifuged at 15,000 rpm for 20 min at 4°C. To purify the protein, the 12-ml lysate was loaded onto the nickel-nitrilotriacetic acid column pre-equilibrated with lysis buffer and mixed for 1h at 4°C. The resin was then washed with buffer (20mM Tris-HCl, 300 mM NaCl, 250 mM imidazole, pH 8) was used to elute the proteins. All proteins were dialyzed extensively against 50 mM HEPES, 50 mM KCl, 10 mM

$MgCl_2$, 1 mM DTT (pH 7.4) prior to sample concentration and storage at -80°C. GST-tagged SGTA was purified in a similar manner, except a glutathione resin was used and the buffer formulations were as follows: lysis and wash buffer (50 mM Tris-HCl, 150 mM NaCl, 0.05% Nonidet P-40, pH 7.5), elution buffer (10 mM reduced glutathione, 50 mM Tris-HCl, 1 mM EDTA, pH 7.4).

2.2.6 PR-Chaperone Complex Reconstitution and Hormone Binding Assays

Purified PR was adsorbed onto PR22-protein A-Sepharose resin beads and reconstituted into multiprotein complexes as described previously (*183*). Briefly, ~0.05 μM of PR was incubated with 1 μM each of Hsp90β, Hsp70, Hop, Hsp40, p23, and indicated concentrations of His_6-tagged SGTA in 200 μL of reaction buffer A (20mM Tris-HCl, pH 7.5, 5 mM $MgCl_2$, 2mM DTT, 0.01% Nonidet P-40, 50 mM KCl, and 5 mM ATP) for 30 min at 30°C, resuspending beads every 3-4 min. 0.1μM [^{3}H] progesterone (American Radiolabeled Chemicals, Inc.) was then added, and the reaction mixture was incubated for 3 h at 4°C on a gentle shaker. PR multiprotein complexes were washed with 1 ml of reaction buffer B (20 mM Tris-HCl, pH 7.5), 0.01% Nonident P-40, 50 mM KCl) three times and assessed for bound progesterone using Microbeta plate reader (PerkinElmer Life Sciences). The remaining samples were incubated with SDS sample buffer, and protein complexes were resolved using SDS-PAGE (10% gel) and Coomassie Blue staining. One-fifth fraction of each sample was run on SDS- PAGE (10% gel) and transferred to PVDF membrane.

2.2.7 Isothermal Titration Calorimetry

Isothermal titration calorimetry was performed using a MicroCal VP-ITC instrument (Microcal Inc., Northampton, MA). For the binding of human SGTA to Hsp90 or Hsp70,

recombinant human GST-SGTA was titrated from the syringe into the cell containing human Hsp90 or human Hsp70. The concentration of SGTA was 270 μM and the Hsp90 or Hsp70 concentration was 40 μM. In the case of Hsp90, the nucleotide dependence of SGTA binding was tested by measuring the binding under the same conditions but in the presence of 2mM AMP-PNP (Roche) in the cell. The buffer used in the syringe and the cell was 40 mM HEPES (pH 7.5), 20 mM KCl, 5 mM $MgCl_2$ at 25°C. 40 injections of ligand solution were performed to fully saturate the protein in the cell. Data analysis was performed using Origin software (OriginLab Corporation, Northampton, MA)

2.2.8 Isolation of His-Cpr6 and Ura2-TAP Complexes

Plasmids expressing wild type Sgt2 or Cpr6 containing an N-terminal His_6 tag and Xpress epitope expressed under the strong constitutive GPD promoter were transformed into an hsc82hsp82 strain expressing untagged WT hsc82 or Hsc82ΔMEEVD. His-Sgt2 or His-Cpr6 complexes were isolated as described (*187*). Briefly, cells were grown overnight and harvested at an A_{600} of 1.2-2.0. Cell pellets were resuspended in lysis buffer (20 mM Tris, pH 7.5, 100 mM KCl, 5 mM $MgCl_2$, 5 mM imidazole containing a protease inhibitor tablet (Roche Applied Science)) and were disrupted in the presence of glass beads with eight 30-s pulses. Cell lysates were incubated with nickel resin (1 h with rocking at 4°C) followed by washes with lysis buffer plus 35 mM imidazole and 0.1% Tween 20. Proteins were eluted from nickel resin by boiling in SDS-PAGE sample buffer, and protein complexes were separated by gel electrophoresis (10% acrylamide) followed by Coomassie Blue staining. Alternatively, proteins were transferred to nitrocellulose, and chemiluminescence immunoblots were performed according to the manufacturer's suggestions (Pierce). Anti-Xpress antibody was obtained from Invitrogen. Anti-Hsp70 (Ssa isoform) was a gift from Dr. Elizabeth Craig.

2.3 Results

2.3.1 SGTA and Sgt2 interaction with Hsp70 and Hsp90

Previous studies demonstrated that SGTA interacts with Hsp70 and weakly with Hsp90 in coimmunoprecipitation experiments, and these interactions were mapped to the three tandem TPRs between residues 95 and 195 on SGTA (*68*). To get a more quantitative measure of SGTA binding to Hsp70 and Hsp90, we performed isothermal titration calorimetry with recombinant human SGTA, Hsp70, and Hsp90 (Figure 2.3.1) These results indicate that SGTA binds Hsp70 with an affinity of 6.1 μM (Figure 2.3.1A) and to Hsp90 with an affinity of 11.0 μM (Figure 2.3.1B) *in vitro*. Despite the similar affinities *in vitro*, previously published data suggested that SGTA precipitates predominately with Hsp70 in co-immunoprecipitations from mammalian cell lysates (*68*). To further corroborate these findings, we isolated His-Sgt2 complexes to determine whether Sgt2 interacts predominantly with Hsp70 or Hsp90 in yeast extracts. For comparison, we also isolated His-Cpr6, which is known to interact with both Hsp70 and Hsp90, but not Hsp90ΔMEEVD because of the deletion of the TPR binding site (*187*). As shown in Figure 2.3.1C, similar levels of Hsp70 bound His-Sgt2 and His-Cpr6. There was no noticeable effect of the Hsp90ΔMEEVD mutation, suggesting that little or no Sgt2 directly binds Hsp90 in yeast extracts.

2.3.2 SGTA Acts Independently of Receptor Maturation and Hormone Binding

Our data support the idea that SGTA acts at an early stage in receptor folding. Based on this idea, we sought to determine whether SGTA influences receptor-chaperone complex assembly and the folding of the receptor to a hormone-binding competent conformation. Thus, we assessed the ability of increasing concentrations of recombinant SGTA to affect the assembly

of PR-chaperone complexes in a progesterone receptor reconstitution assay using the five purified proteins (Hsp90, Hsp70, Hop, Hsp40, and p23) known to be required for PR to reach a hormone-binding competent conformation *in vitro* (Figure 2.3.2A). Although SGTA was able to associate with PR-chaperone complexes, SGTA supplemented into the assay up to 16 μM had no effect on PR-chaperone complex assembly. It is possible that additional endogenous factors are required for SGTA function. Thus, in addition to the "five purified protein system," we also performed these assays in rabbit reticulocyte lysate (Figure 2.3.2B). SGTA did not affect PR-chaperone complex assembly in both systems. In addition, SGTA had no effect on PR folding to the hormone-binding competent conformation in reticulocyte lysate (Figure 2.3.2B, *left panel*) and in the five purified protein system (data not shown). Thus, although SGTA can associate with receptor chaperone complexes and functionally affect receptor activity, these effects are not due to the alteration of receptor folding and hormone binding.

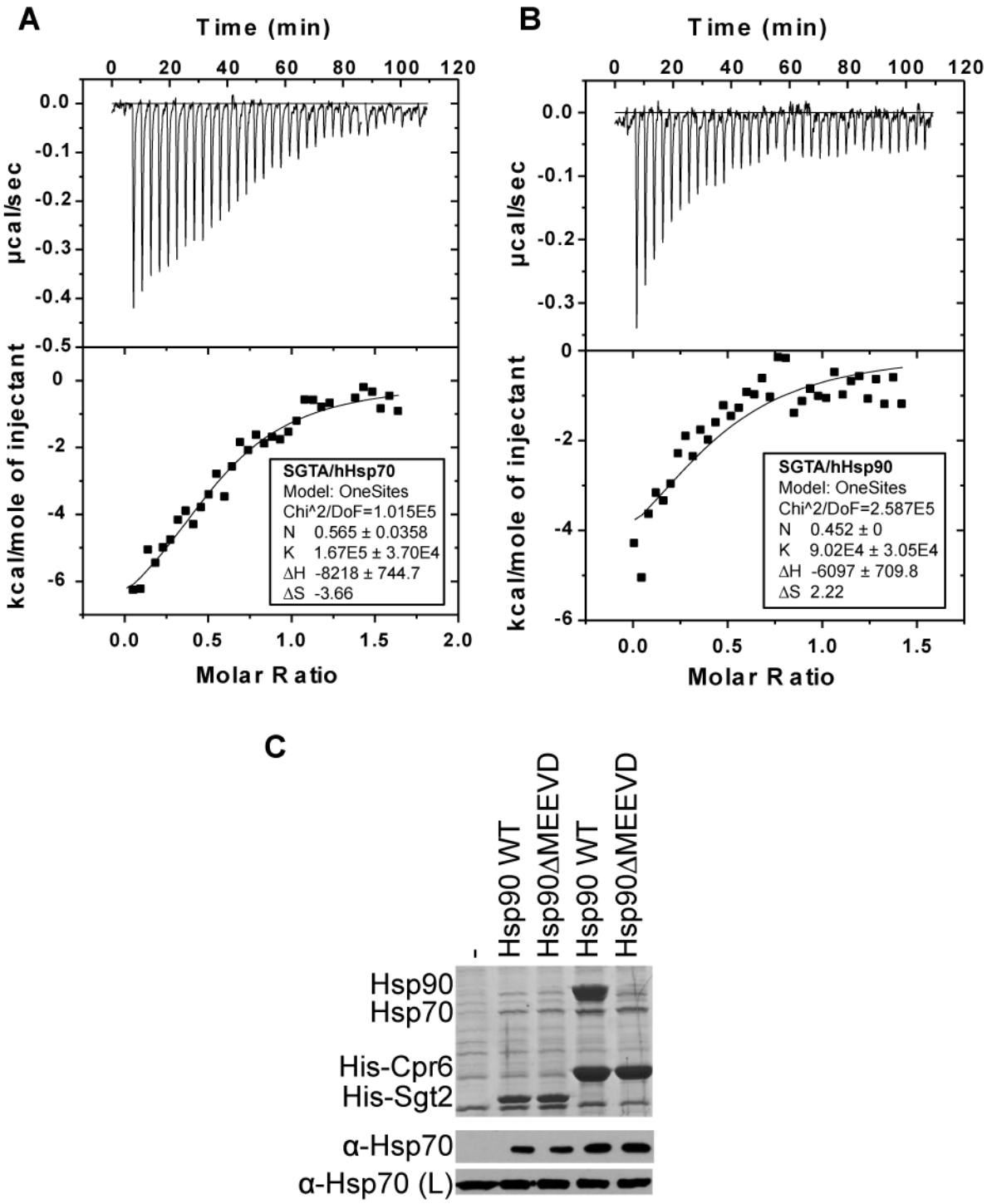

Figure 2.3.1 SGTA and Sgt2 interaction with Hsp70 and Hsp90.

Figure 2.3.1: SGTA and Sgt2 interaction with Hsp70 and Hsp90.

A and *B*, isothermal titration calorimetry was performed with recombinant SGTA (270 μM) and either human Hsp70 (*A*) or human Hsp90 (*B*) (40μM each). Titrations were performed with 40 injections of 8 μl of SGTA in the injection syringe. *C*. His-Sgt2 or His-Cpr6 was isolated from hsc82hsp82 cells expressing WT Hsp90 or Hsp90ΔMEEVD. Cell extracts were incubated with nickel resin, and complexes were analyzed using SDS-PAGE and immunoblot analysis. The upper panel displays the Coomassie Blue-stained gel of the resin samples, whereas the lower panels show immunoblot analysis. Immunoblots of the lysate (L) are provided as a loading control. The band in the stained gel that migrates below His-Sgt2 is an unknown protein that binds nonspecifically to nickel resin.

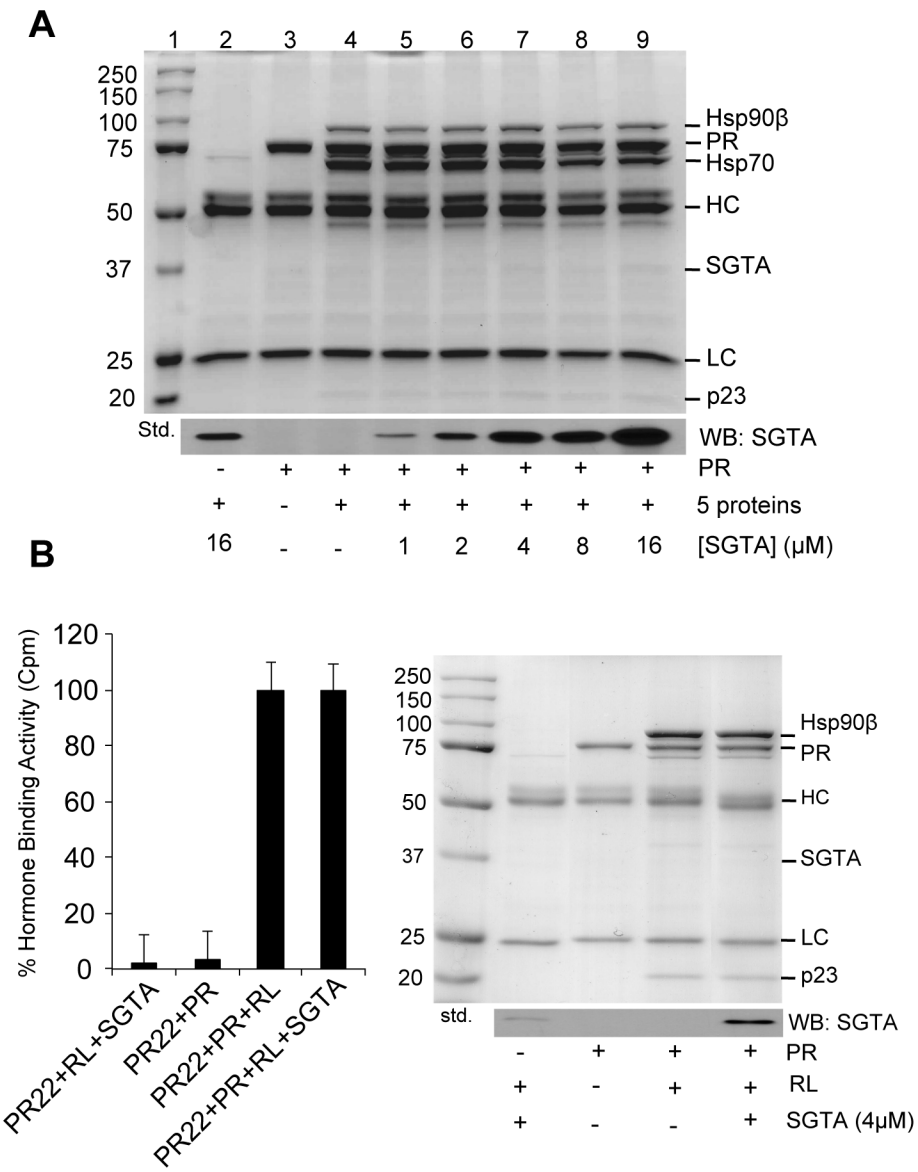

Figure 2.3.2 SGTA Does Not Affect Chaperone Complex Formation and Receptor Hormone Binding in a Cell-Free System.

Figure 2.3.2 SGTA Does Not Affect Chaperone Complex Formation and Receptor Hormone Binding in a Cell-Free System.

A, an *in vitro* PR-chaperone complex reconstitution assay with serial SGTA protein concentrations. The five purified proteins known to be required for PR to reach a hormone-binding competent conformation *in vitro* include Hsp90, Hsp70, Hop, Hsp40, and p23. Binding buffer was supplemented with or without the indicated recombinant proteins and immunoprecipitated with the PR-specific antibody, PR22. The *upper panel* is the Coomassie dye-stained gel, and the *lower panel* is a Western blot (*WB*) for SGTA. *Lane 1* is the molecular weight standard and lanes 2-4 are negative controls with or without PR, the five proteins, and/or SGTA. Increasing concentrations of SGTA from 1 to 16 μM (*lanes 5-9*) had no effect on PR-chaperone complex assembly. *B*, an *in vitro* PR-chaperone complex reconstitution assay in reticulocyte lysate, which contains the five proteins known to be required for PR to reach a hormone-binding competent conformation. The *right panel* shows the Coomassie-stained gel and the Western blot for SGTA. PR within the reconstituted complexes was assessed for hormone binding using [^{3}H] progesterone (*left panel*).

2.3.3 The Q-Rich Domain is Important for SGTA Regulation of AR Activity

Previous studies in mammalian cells suggested that SGTA modulates activity through its TPR domain based on Hsp70/90 binding (*68, 69, 118*). The other domains have not been linked to a regulatory role. Therefore, we performed a sequence alignment with human SGTA and yeast Sgt2 and found that they share the three domains: dimerization at the N-terminus, middle TPR, Q-rich region at the C-terminus (Figure 2.3.3). In addition, they have 30% amino acid identity. However, the C-terminus of human SGTA is significantly more glutamine-rich as compared to the yeast homologue Sgt2. Thus, we tested SGTA truncation mutants to understand which domains were critical for the regulation of AR activity. To assess SGTA structural domains in AR activity, we generated β-galactosidase reporter strains in a W303a background and assayed for receptor function in the presence of empty vector, full-length SGTA, or the truncated SGTA expression vector. The truncation mutants were engineered according to the structural map created by Dutta et al (*125*). Full-length SGTA overexpression significantly reduced AR activity as compared with the empty vector control (Figure 2.3.4B). Deletion of half the glutamine-rich region at the C-terminus or the dimerization domain did not have an effect in AR regulation as compared to full-length SGTA. Elimination of the glutamine-rich region at the C-terminus and deletion of the linker between the TPR and the Q-rich region failed to abrogate AR activity. The effect observed was not due to receptor destabilization (Figure 2.3.4B, *inset*).

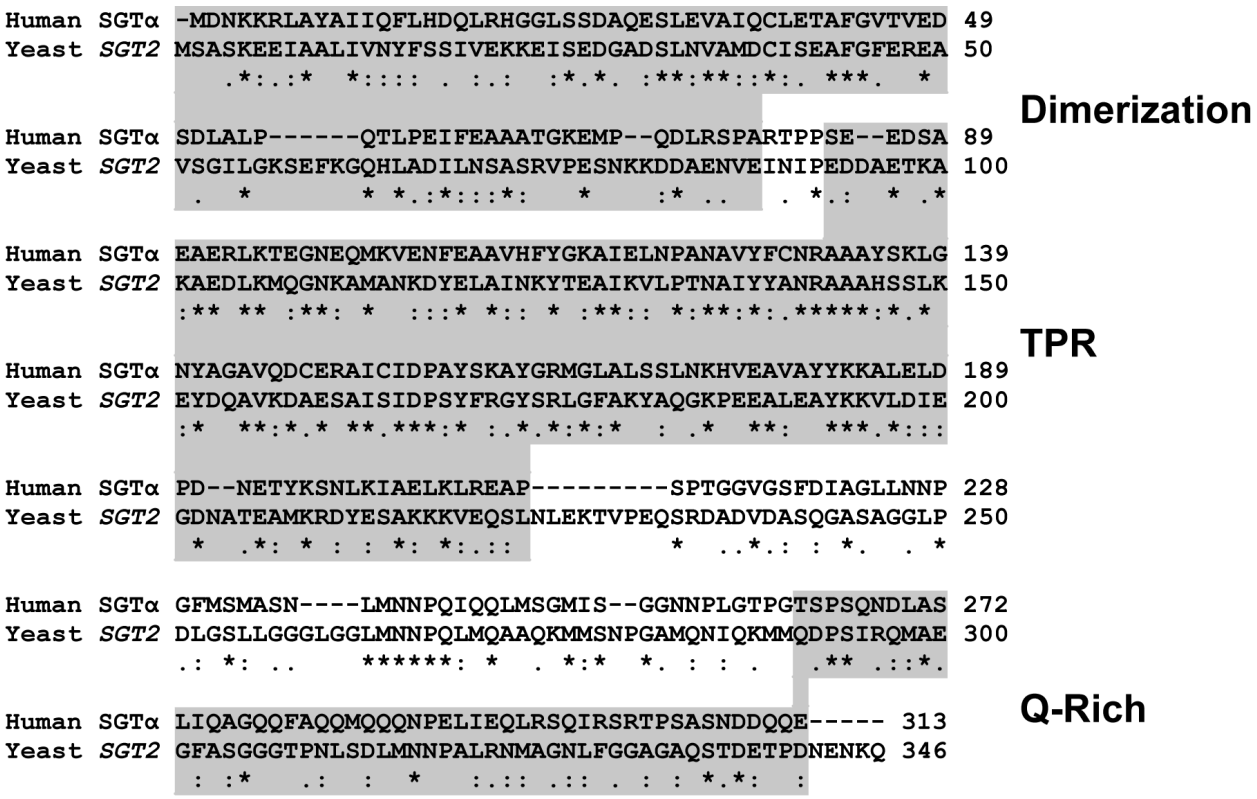

Figure 2.3.3. Human SGTA and Yeast Sgt2 Amino Acid Sequence Alignment.

An amino acid comparison was made with human SGTA and yeast Sgt2 in which they share the three domains, which are shaded and are 30% amino acid identical. At the N-terminus is the dimerization domain, the middle TPR, and at the C-terminus a glutamine-rich region. However, the yeast Sgt2 contains less glutamines at the C-terminus.

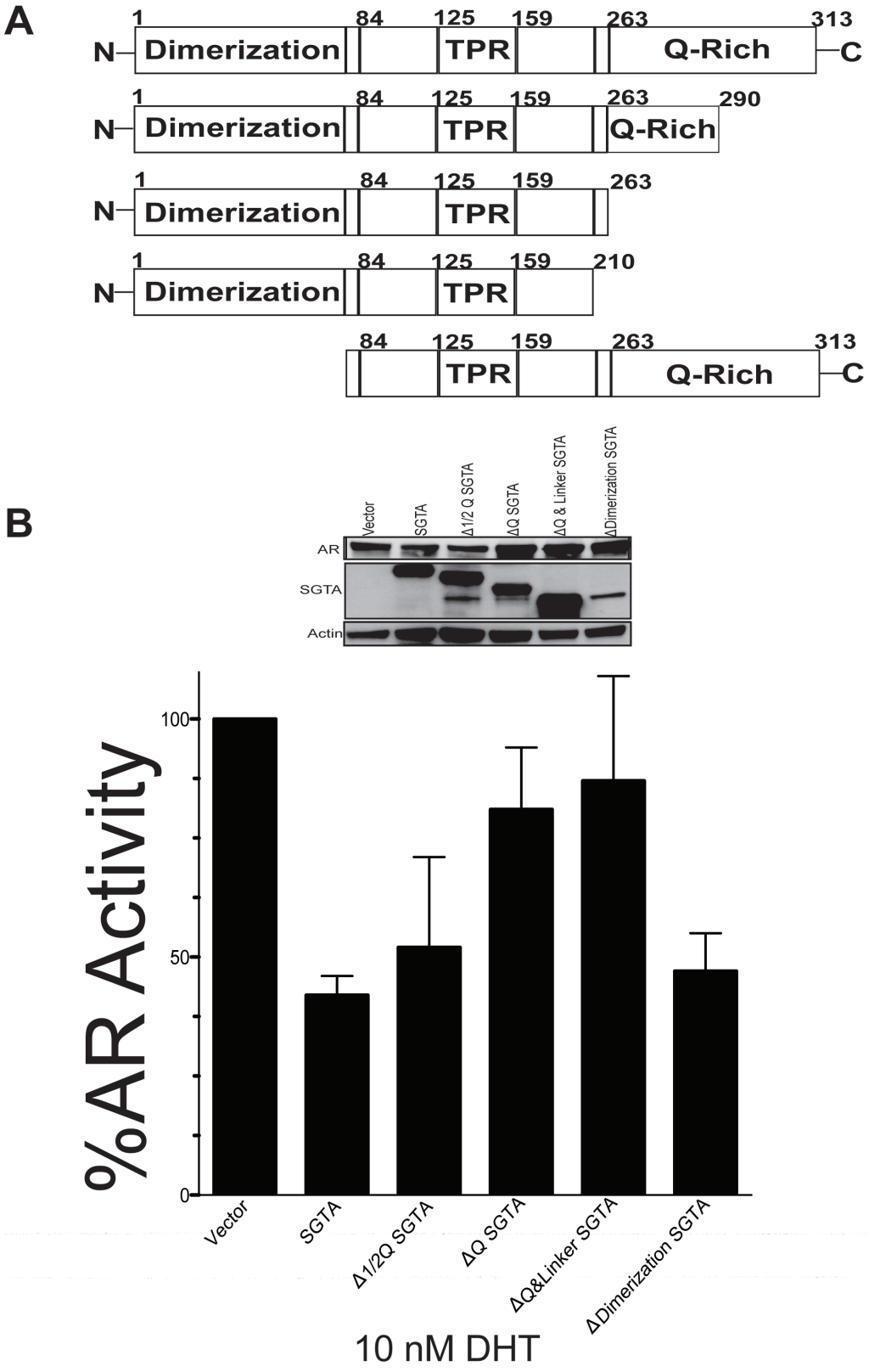

Figure 2.3.4 SGTA-specific effects on AR in yeast.

Figure 2.3.4. SGTA-Specific Effects on AR in Yeast.

A, structural map encompassing full-length and truncated domains of SGTA based on amino acid positions. *B*, yeast reporter strains for AR in a W303a genetic background were transformed with empty plasmid vector or a plasmid expressing human full-length or truncated SGTA. The cells were treated with 5 nM DHT and assessed for receptor-mediated β-galactosidase expression. Full length SGTA negatively regulated AR as compared to the empty vector. Elimination of half of the glutamine rich domain at the C- terminus or the dimerization domain at the N-terminus region had no statistically significant difference in AR activity in comparison to the full-length SGTA. Deletion of the Q-rich region at the C-terminus failed to abrogate AR activity as compared with the full-length SGTA. Yeast lysates were prepared and immunoblotted for AR, SGTA, or actin as a loading control (*insets*).

2.4 Discussion

SGTA binding to Hsp70/90 in mammalian cell lysates was previously documented and it was speculated that SGTA regulates receptor function through its TPR-Hsp interaction. The previous information available for SGTA binding to Hsp70/90 was performed in yeast and mammalian cell lysates. In this chapter, we demonstrate a direct interaction with Hsp70 and Hsp90 in the absence of other factors and determined the binding affinities of SGTA interaction with Hsp70 and Hsp90 *in vitro* (Figure 2.3.1A,B). The measured affinity for Hsp70 binding is two-fold higher than that for Hsp90 binding. Consistent with these results, SGTA preferentially co-precipitated with Hsp70 in yeast (Figure 2.3.1C). In addition, SGTA modulation of Hsp70 ATPase activity was previously shown (*68, 119, 188*).

The specificity shown by SGTA is remarkably similar to that of FKBP52. Both proteins have a TPR domain, which permits protein-protein interactions. However, the fact that SGTA negatively affects receptor in yeast lacking FKBP52, and the fact that SGTA had no effect on receptor maturation and hormone binding ability, which is regulated by FKBP52, suggest that it is not acting through simple competition with FKBP52 for binding Hsp90. This chapter has shown that SGTA binds Hsp70 with a two-fold higher affinity than Hsp90, which suggests that SGTA is acting on the receptor in intermediate complexes through its interaction with Hsp70.

SGTA is known for its down-regulatory effect on AR, GR, and PR (*67*). Its structural composition is comprised of three regulatory domains (*66*). Yeast and human SGTA share the three domains but the yeast homologue is less Q-rich at the C-terminus (Figure 2.3.3). This chapter has demonstrated that deletion of the Q-rich region fails to abrogate receptor function (Figure 2.3.4). Even though this does not seem to be due to receptor destabilization as the Figure

2.3.4 insets shows, it is important to note that this should be further investigated given that the results could possibly be due to misfolding of the truncation mutants.

These findings present exact binding affinities of SGTA towards the Hsp70/90 proteins and its involvement in the chaperone pathway, in which it is not required for hormone assembly or regulation. In addition, the glutamine-rich C-terminus fails to abrogate AR activity. Further studies are needed to continue to characterize the other pathways in which SGTA regulates receptor activity. These pathways are critical for better understanding the role it has in prostate cancer progression.

Chapter 3: Identification of Global SGTA Interacting Proteins in LNCaP Human Prostate Cancer Cells

3.1 Rationale

Molecular chaperone and cochaperone proteins have a dynamic role in steroid hormone receptor (SHR) assembly, repair, and transcriptional regulation (*189*). SGTA was initially linked to SHRs through a yeast-two hybrid screen with AR and a prostate cDNA library. After functionally characterizing these interactions, they demonstrated that SGTA down-regulated AR activity in prostate cancer cells and, based on *in silico* modeling, it was predicted that SGTA interacts with AR's EEVD-like sequence in the hinge region, thus, retaining AR in the cytoplasm (*69*). Since AR, GR, and PR are members of the nuclear receptor superfamily and have highly conserved structural domains, we sought to determine whether SGTA would regulate these receptors as well (*190*). To this end, our laboratory was the first to demonstrate that SGTA associates with PR and GR complexes through yeast-two hybrid analysis and PR reconstitution assays *in vitro* (*67*). Thus, we hypothesized that SGTA's regulation of AR, GR, and PR is based on its ability to interact with Hsp70/90 via its TPR domain. Although GR and PR associated with SGTA, the regulation posed by SGTA may not be solely in the hinge region since GR and PR do not have an EEVD-like sequence in this region. SGTA's association with AR, GR, and PR is also noteworthy because these complexes are highly dynamic and were recently implicated in prostate cancer (*191*).

While studies have identified SGTA as an emerging protein interactor with viruses, neurons, protein quality control partners, and AR, the relevance of SGTA's importance for SHR regulation in PCA has not been studied extensively. The majority of studies identifying SGTA as an interacting partner were conducted utilizing a yeast-two hybrid model system. For instance, SGTA's interaction with viral proteins such as VpU, HIV-1 Gag, NS1-Parvovirus H-1, SV40, and SARS-CoV7a led to the understanding that SGTA is important in viral particle assembly and

release, inhibition of viral release, and ER membrane incorporation (*103, 104, 112, 145*). Since SGTA has a middle TPR domain, the first biological role was based on the idea that TPR proteins can moderate apoptosis (*192, 193*). Fluorescence microscopy revealed that the full middle TPR domain was essential to stimulate apoptotic functions based on deletion mutants (*194*). On the other hand, Winnefeld *et al* showed that SGTA has anti-apoptotic properties in an SGTA knock down NBE cell line (*124*). In light of this conflicting dataset, it appears that SGTA displays both anti- and pro-apoptotic functions in a tissue-dependent manner. SGTA is also responsible for cell division in which its interaction with Bag6/Bat3/Scythe can prevent mitosis (*195*). All told, it is believed that SGTA can serve as a "housekeeping" protein.

SGTA also interacts with the N- terminus of myostatin (*122*), cysteine string protein (CSP) (*119*), UbE motif of growth hormone receptor (*129*), TRC40 substrate Sec61β (*132*), and SV40 (*145*). These interactions have mainly been observed through yeast-two hybrid studies, which showcase SGTA's multifaceted roles. A list of published SGTA interacting proteins is shown in Table 1.

Proteomic approaches have significantly advanced many scientific fields through their sensitivity and unbiased method of detecting proteins. While our current understanding of molecular chaperone association in prostate cancer is evolving, there remains a need to understand co-regulators within androgen receptor signaling pathways possibly contributing to prostate cancer progression. Based on this idea, we used a proteomic approach to discern global protein interactors of SGTA in LNCaP prostate cancer cells. Although there is an increasing amount of known SGTA interactors in noncancerous settings, mainly through yeast-two hybrid screens, little is known about SGTA's interactors in prostate cancer cells.

Our initial hypothesis centered on SGTA working in unison with unidentified proteins known to promote PCA progression through links in AR signaling pathways. In order to test this hypothesis, we performed a top-down proteomics approach using tandem affinity purification in LNCaP PCA whole-cell lysates, and then functionally characterized these interactions.

3.2 Materials and Methods

3.2.1 Construct of SGTA-6XHis-Gly-FLAG

Using PCR recombinant techniques, a full-length SGTA cDNA was tagged at the N-terminus with a 6X His-tag followed by tagging with a FLAG (DYKKDDDDK) epitope. The construct was cloned into a mammalian expression vector (pCI-Neo), which contains a CMV promoter and a Neomycin marker using XbaI and XmaI restriction enzymes.

3.2.2 MEF52KO Receptor- Mediated Reporter Assay

Mouse Embryonic Fibroblasts (MEF52KO) is a cell line that has been used to determine SGTA down-regulation of AR (*67*). MEF52KO cells were maintained in Minimal Essential Medium (MEM) supplemented with 10% Fetal Bovine Serum (FBS) at 37°C in a 5% CO_2 atmosphere. Cells were plated at a $1x10^5$ density/ well in a 6-well tissue culture plate. Cells were transfected using Lipofectamine Reagent 2000 (Invitrogen) and followed standard procedures once 60-80% confluence was reached. The plasmids used for these assays were a hormone-responsive firefly luciferase reporter (400 ng per well), a mammalian expression vector (pCI-Neo) expressing wild type SGTA and tagged SGTA (800 ng per well), and a constitutive β-galactosidase expression plasmid that served as a transfection control (50 ng per well). The transfection was performed at a DNA (μg) to lipofectamine ratio of 1:3 in MEM-EBS lacking FBS. Four hours post-transfection, the medium was changed to MEM supplemented with 10%

Charcoal-Treated (CT) FBS. Twenty-four hours after transfection, the cells were treated with 100 nM dihydrotestosterone (DHT). Sixteen hours later, the cells were lysed using 100 uL of Mammalian Protein Extraction Reagent (M-PER) with a Protease Inhibitor Cocktail without EDTA (Thermo) and incubated at room temperature for ten minutes. Next, the cells were scraped and transferred to a cold microfuge tube. The cells were then centrifuged at 135Xg at 4°C for 20 minutes. The supernatant was used directly in the luciferase and β-galactosidase assays. To measure luciferase activity, 40 μL of sample and 100 μL of luciferase assay reagent (Promega) were added to individual wells on an opaque 96-well plate and the light emission was measured in a luminescence plate reader (Gen5 BioTek) immediately. For β-galactosidase activity, 10 μL of sample was incubated with 100 μL of Tropix Gal-Screen reagent (Applied Biosystems) in a 96-well plate and incubated for 2 hours at room temperature. β-galactosidase was measured using a luminescence plate reader (Gen5 BioTek). To measure any transfection efficiency differences, the data was normalized by dividing the relative light units (RLU) by β-galactosidase activity. This experiment was performed in duplicate and three independent experiments were performed (*156*).

3.2.3 Tandem Affinity Purification in Human LNCaP Cells

LNCaP cells are an early stage PCA cell line that was derived from a 50-year old Caucasian male. These cells serve as a representation of an early stage prostate cancer setting, thus serving as an excellent model to look at SGTA interacting partners (*196*). LNCaP cells were maintained in RPMI-1640 Medium supplemented with 10% FBS at 5% CO_2 and 37°C. LNCaP cells were plated in a tissue culture petri dish at a density of $8.0x10^5$ cells/dish. After 48 hours, at 60-80% confluence, cells were transfected using Lipofectamine 2000 reagent (Invitrogen) and

manufacturer's procedure was followed. The transfection was performed using 800 ng of mammalian expression empty vector (pCI-neo) as our control, and 800 ng of tagged SGTA was also transfected with RPMI-medium lacking FBS. 4-6 hours post-transfection, the medium was changed to RPMI with 10% FBS. After 48 hours, the cells were washed with cold PBS three times and 1 ml of ice-cold lysis buffer (50 mM Tris-HCl pH 7.6, 10 mM NaCl, 0.5% NP-40, Protease Inhibitor Cocktail-EDTA Free (Thermo)) was added and incubated for 30 minutes. The cells were scraped and transferred to a microcentrifuge tube (AMGDAD) and centrifuged at 135xg for 30 minutes at 4°C. The supernatant was used immediately for nickel purification. 10% of supernatant was used for verification of expression of tagged SGTA and wild type SGTA vector via Western blot using anti-hSGTA 1:1000 (ProteinTech), anti-OctA (FLAG) Probe (D-8) sc-807 1:1000 (Santa Cruz Biotechnology). The tandem affinity purification was performed in batch. The cell lysate was incubated with 100 µL of nickel beads (4 vs 16 hrs) with 1 mg of cell lysate and a final volume of 20 mM of Imidazole was added to the reaction at 4°C with gentle rotation. The resin-lysate was washed 5 times with wash buffer (25 mM Tris-HCl pH 7.4, 150 mM NaCl, 0.1% NP-40, 20 mM Imidazole) we ensured the buffer was in a pH of 7.0. The elution was performed with 275 µL with elution buffer pH 8.0 (25 mM Tris-HCl pH 7.4, 150 mM NaCl, 300 mM Imidazole). The FLAG co-immunoprecipitation was performed following Krogan *et al* protocol (*197*). The eluate was further analyzed using 40 µl of Anti-FLAG M2 Affinity gel (Sigma) and left overnight with gentle rotation at 4°C. The next day, the resin cell-lysate was centrifuged at 8200xg for 30 seconds and incubated 2 minutes before handling the samples. The supernatant was carefully removed and the resin was washed 5 times with cold lysis buffer followed by one wash with lysis buffer without detergent. The samples were eluted

with 40 μL of 100 μg/ml 1X FLAG peptide (Sigma F3290), 0.05% RapiGest (Waters) in 50 mM Tris-HCl pH 7.6, 150 mM NaCl.

3.2.4 Sample Preparation for LC-MS/MS

LNCaP eluate samples were prepared for LC-MS/MS proteome analysis using the filter aided sample preparation (FASP™) Protein Digestion Kit (Expedeon) and modified accordingly. Samples were digested using 1 μg of SIGMA Trypsin Proteomics Grade and incubated overnight at 37°C. Digested samples were eluted into a clean collection tube with 0.1% formic acid. The final solution was concentrated in the vacufuge and frozen until LC-MS/MS analysis.

The complex peptide mixture from individual samples were then analyzed by LC/MS/MS at UTEP's Biomolecule Analysis Core Facility. Samples were loaded onto a pico C18-12 cm media (Luna, New Objective). Once loaded, the column was moved in-line with a U3000 HPLC (Dionex, subsidiary of Thermo Fisher Scientific) split to obtain ~300 nL/min flow rate over the nano-analytical column. The resolving column was housed in a nanospray sourse (Proxeon, Thermo Fisher Scientific) attached to a QExactive mass spectrometer (Thermo Fisher Scientific). An automated 22 h LC-MS/MS run was programmed into Xcalibur (Thermo Fisher Scientific) and each sample was analyzed with a separation scheme consisting of eleven salt pulses followed by a 2 hour C18 separation. During each analysis and all sample runs, the QExactive settings were as follows: the normalized collision energy for HCD was 28eV, a full scan resolution of 70,000 K from 400-1600 m/z, a HCD MS/MS resolution of 17,500 with an isolation width of 3 m/z, and the dynamic exclusion was set at 15 seconds. Peptides were not excluded based on charge state and 1 microscan for both full and MS/MS scans were acquired. All MS and MS/MS data were acquired in profile mode.

3.2.5 Proteome Informatics

All resultant MS/MS spectra from individual 24 hour runs were searched with Proteome Discoverer 2.0 (Thermo Fisher Scientific) and filtered via reverse database searching with maximum false positive rate of 0.5. The Proteome Discoverer settings were as follows: HCD MS/MS, included a fixed modification for carboxyamidomethylated cysteines, a variable modification for urea carbamylation of arginine and lysine residues, fully tryptic peptides only, 4 missed cleavages, a precursor mass tolerance of 10 ppm and a fragment mass tolerance of 0.6 Da. Only proteins identified with two fully tryptic peptides from a 22 run were considered for further analysis. Tandem MS/MS spectra were searched against a combined protein database of *Homo sapiens*.

Hierarchical clustering was performed on the resultant filtered proteome dataset using Cluster 3.0. Clustered data were depicted graphically (Heatmap). GO terms were used to generate the Search Tool for the Retrieval of Interacting Genes/Proteins (STRING) network for interacting partners graphic representation (*198*).

3.2.6 Co-Immunoprecipitations in LNCaP Cells

For the Co-IP experimentation, 200 µL of magnetic beads (Thermo Scientific) suspended resin per assay condition was added to microcentrifuge tubes, tubes were placed into the magnet and supernatant was removed. Resin beads were washed twice in ice-cold TBS and resuspended in 500 µL 0.1%Milk in TBST. 6 µl of SGTA antibody (Santa Cruz) was added to the mixture and incubated for two hours at 4°C. Meanwhile, the cells were washed three times with cold PBS and incubated with lysis buffer (150 mM NaCl, 50 mM Tris, 0.1% NP-40, Protease Inhibitors) for 30 minutes. The cells were then transferred to a microcentrifuge tube and centrifuged at

maximum speed at 4°C for 20 minutes. The cell lysate was pre-cleared twice using the magnetic beads (Thermo). The pre-cleared cell lysate and antibody-resin complex was incubated for 3 hours at 4°C with gentle shaking. The complex was then washed 5 times with TBST with 5 minute incubation intervals. Then 50 μL of 4X sample buffer and β-mercaptoethanol was added to each sample including the inputs. Proteins were separated by electrophoresis, transferred to a PVDF membrane (Millipore) and immunoblots were performed. 10% of supernatant was used for verification of expression of SGTA via Western blot using anti-hSGTA 1:1000 (ProteinTech) and human PRDX1 1:2000 (ProteinTech).

3.2.7 FLAG In Vitro Assays

For the FLAG-pull down assay, ANTI-FLAG® M2 Magnetic beads (Sigma-Aldrich) were used and followed manufacturers protocol. Briefly, 20 μL of packed gel volume were thoroughly resuspended and equilibrated with 5 packed gel volumes of TBS (50 mM Tris-HCl, 150 mM NaCl, pH 7.4). Beads were washed twice with TBS. The purified proteins were added alone or in conjunction. 2 nM/500μL of recombinant hSGTA (*67*), PRDX1-FLAG (Origene) was incubated with the beads for 2 hours at 4°C with gentle mixing. Upon completion of binding, the magnetic beads were collected using the magnetic separator. The resin beads were washed with TBS three times. The elution performed by adding 50 μL of 4X sample buffer and β-mercaptoethanol was added to each sample including the inputs. Proteins were separated by electrophoresis, transferred to a PVDF membrane (Millipore) and immunoblots were performed. 10% of supernatant was used for verification of expression of tagged SGTA and wild type SGTA vector via Western blot using anti-hSGTA 1:1000 (ProteinTech), anti-OctA (FLAG) Probe (D-8) sc-807 1:1000 (Santa Cruz Biotechnology) and anti-human PRDX1 1:2000 (ProteinTech).

3.2.8 Generation of SGTA Knock Out HeLa and 22Rv1 Human Cells

The CRISPR/Cas9 system has become a widely used biotechnology due to its ability to knock out genes from cells (*199*). Here, we exploited this system and utilized the Santa Cruz Biotechnology SGTAKO plasmids to knock out SGTA in HeLa and 22Rv1 cell lines. The SGTA CRISPR/Cas9 KO (sc-404399) plasmid was obtained with the SGTA HDR plasmid (sc-404399-HDR). Briefly, both cell lines were seeded at $2.0x10^6$ and incubated for 24 hours prior transfection. The following day, cells were transfected in a medium lacking FBS with equivalent ratios of DNA (1 μg) with Lipofectamine transfection reagent and was used at a 1:3 plasmid to DNA ratio. 4 hours-post transfection the medium was changed to normally used medium to culture the cells (+10%FBS). Selection was started for two weeks in which, 72 hours post-transfection, 3 μg/μl of Puromycin (InvivoGen) was added to the cells and the medium was changed every 2-3 days. The cells were then selected based on colony formation and further expanded. Successful colony selection was then confirmed via Western Blot and probing against human SGTA. The cells were maintained and cultured with their respective mediums used for maintenance without antibiotic.

3.2.9 Receptor-Mediated Reporter Assay

In a 6-well plate $3.0x10^6$ cells were plated using medium supplemented with 10% FBS. The following day, the cells were checked for complete attachment and once they reached a 60-80% confluence, transient transfection was performed using Lipofectamine 2000 Reagent (Invitrogen) according to manufacturer's instructions. The transfection was performed in duplicates for 4 hours using an equal amount of DNA and a DNA to Lipofectamine ratio of 1:3 in medium lacking FBS. The following plasmids were mixed as follows: 400 ng of pT81

(American Type Culture Collection, Manassas, VA) hormone-responsive firefly luciferase reporter, 50 ng of constitutive pCMVβ β-galactosidase expression plasmid (Clonetech, Mountain view, CA), which served as our transfection control, 800 ng of mammalian expression vector pCI-neo (Promega, Madison, WI), expressing human AR (note: no exogenous AR was utilized in 22Rv1 SGTAKO cells), SGTA and PRDX1. pCI-neo empty vector was used as a control, SGTA and PRDX1 were mixed alone or in combination. Four hours post-transfection the medium was changed to 10% Charcoal Treated FBS. Twenty-four hours after transfection, the cells were treated with 1 nM DHT for 16 hours.

The cells were washed three times with PBS and incubated with 100 μL of M-PER (Pierce, Rockford, IL) supplemented with Complete EDTA-free Mini Protease Inhibitor (Thermo) incubated for 10 minutes with rocking. The cells were then scraped and transferred to a microcentrifuge tube. The cells were spun using a microcentrifuge to remove debris at 15,000 rpm for 20 minutes at 4°C. 40 μL of the cell lysate with 100 μL of luciferase assay reagent (Promega, Madison, WI) were mixed in a single well for each sample on a 96-well plate, which was used to measure luciferase expression and read immediately in a microplate luminometer (Luminoskan Ascent, Thermo Labsystems). 10 μL of the cell lysate with 100 μL of Gal-Screen Reagent (Tropix, Bedford, MA) was used to measure β-galactosidase expression. This mixture was performed in a 96-well plate and incubated for two hours at room temperature, followed by quantification in the microplate luminometer. Luciferase RLU/β-galactosidase RLU were normalized and the transfection efficiency was demonstrated in graphical form utilizing GraphPad Prism software. The data is presented as the mean (+/- standard deviation) of duplicate samples and at least three independent experiments were performed.

3.2.10 Mammalian Cell lines

LNCaP cells were maintained using RPMI + 10% FBS. 22Rv1SGTAKO cells were maintained using RPMI-EBSS + 10% FBS + 1% NEAA + 1% NaPyr. For LNCaP and 22Rv1 cells transfections were performed with RPMI-EBSS lacking FBS. Upon transfection, 22Rv1 cells were maintained in RPMI-EBSS + 10% CT-FBS + 1% NEAA + 1% NaPyr. HeLa SGTAKO cell lines were maintained in MEM-EBS 10% FBS and upon transfection, the cells were changed to MEM-EBSS + 10% CT-FBS.

3.3 Results

3.3.1 A Schematic Representation of Analyzed LC-MS/MS Samples

To identify unknown protein interactors that preferentially co-precipitate with SGTA, we performed a label-free spectral count quantitative proteomics and utilized it to compare SGTA-6XHis-FLAG tag with an empty vector in LNCaP Cells. An overall visual representation of the approach can be seen in Figure 3.3.1A in which LNCaP cells were transiently transfected with either an empty vector or SGTA tag. The cells were lysed and purified first using a batch nickel purification followed by a FLAG Co-IP. The eluates were trypsin digested using a FASP Kit. The digested samples were further analyzed by LC-MS/MS. To affirm that tagged SGTA would not alter SHR function, we conducted luciferase reporter assays in MEF52KO. Figure 3.3.1B is a representative of at least three separate assays. The vehicle control demonstrates that the activity being measured is hormone-induced receptor activity. The data demonstrate that there is no significant difference between wild type and tagged SGTA. LNCaP cell lysates were successfully transiently transfected as shown in Figure 3.3.1C. Cells were lysed and expression of wild type and tagged SGTA were observed. Transfection did not alter the cells because the band in the vector indicates the presence of SGTA due to the endogenous expression in LNCaP

cells. Furthermore, there is no band seen in the vector with anti-FLAG in the eluates. The 3 hour versus the overnight incubation demonstrated a similar level of SGTA. These eluates were sent for further analysis in the LC-MS/MS.

3.3.2 SGTA Associated Proteins Visualized in a Heat Map

To assess preferential binding interactors with SGTA, a hierarchical clustered analysis was performed using SAINT analysis on the spectral count generated from PD 2.0. The resulting heat map in Figure 3.3.3 indicates sets of genes expressed predominantly with SGTA based on a 0.5% FDR. Two biological replicates with four technical replicates within each biological sample were analyzed. A total of 31 genes associated with SGTA in both biological replicates and in both conditions (3 vs 16 hours). Interestingly, a significant log fold change demonstrated that SGTA has a preference to the B2R4P2 gene, which was present in all conditions suggesting this interaction can be both transient and strong. The B2R4P2 gene encodes Peroxiredoxin-1 (PRDX1) protein. PRDX1 has been previously functionally associated with the AR pathway by interacting with and enhancing AR transactivation (*200, 201*). Within this cluster, SAINT analysis revealed enrichment with the chaperones Hsp70 and Hsp90, validating our interactors list since previous reports have established these interactions. General housekeeping proteins such as ribosomal proteins were also present in high abundance. A limitation with ribosomal proteins can be their abundance in Co-IP experiments since they are able to "stick" to resin and many proteins. Even though it has been established that SGTA contributes to protein quality control (Refer to Section 1.4.3 for details), we decided to pursue PRDX1 based on its relevant functional biological role with AR.

3.3.3 SGTA's String Network

From the resulting heat map (Figure 3.3.2), the associated gene sets were subsequently classified using GO terms that convey genes to biological functions. STRING interaction network in Figure 3.3.3 illustrates the association of SGTA with the total interacting proteins that were pulled out from the QSPEC analyzed files. The associations are made based on reported interactions in the literature. In the STRING network, a cluster of ribosomal proteins is observed and no known link with SGTA has been established. In addition, Hsp90 forms a complex with SGTA in which previous groups and ours have established this interaction. Moreover, the network analysis reported 14 proteins that are not ribosomal or chaperones to be SGTA binding partners (Figure 3.3.4). Interestingly, PRDX1 was associated previously with Hsp90 but no direct link with SGTA nor Hsp70 has been reported.

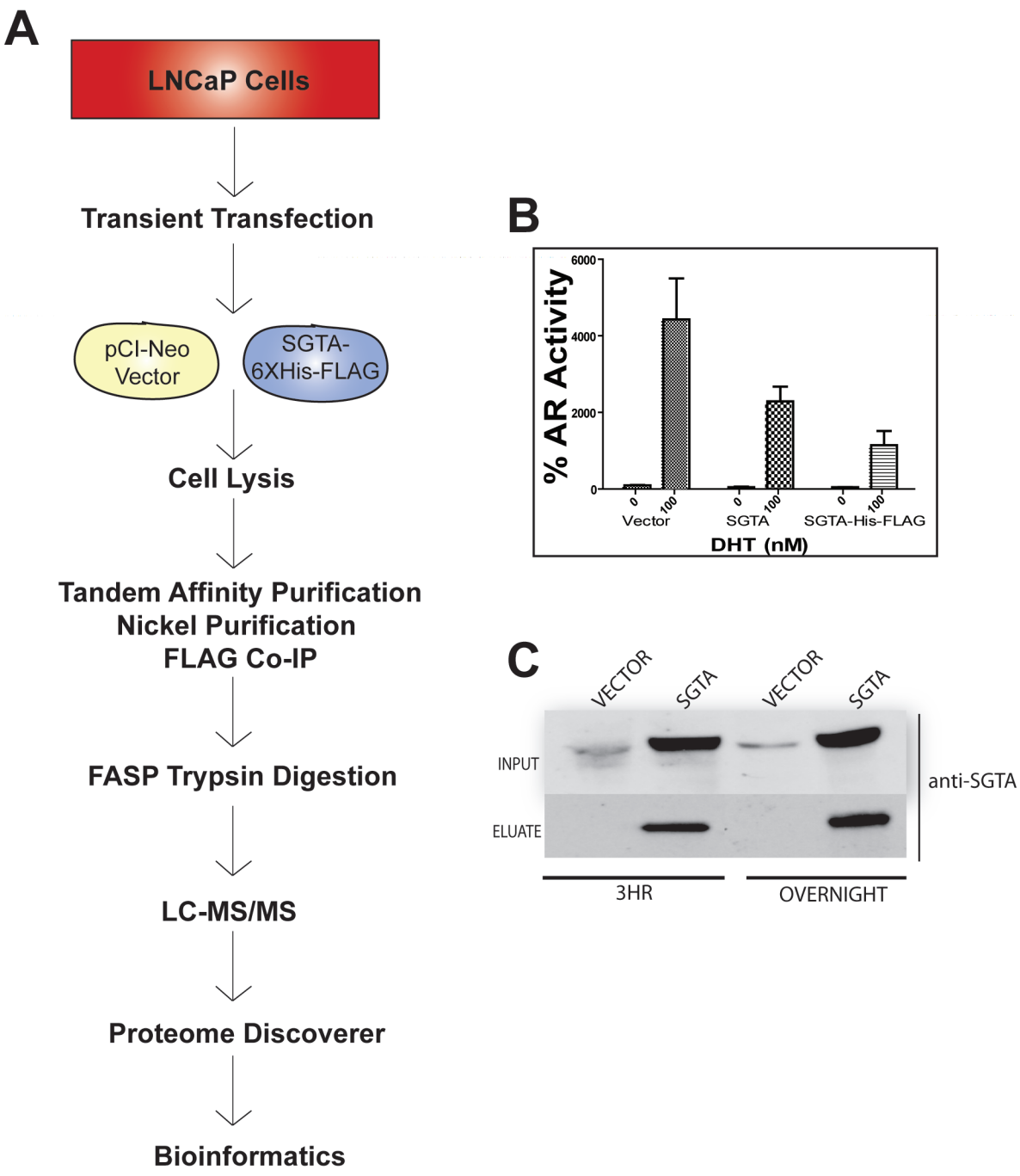

Figure 3.3.1 Schematic Representation of Proteomic Workflow.

Figure 3.3.1. Schematic Representation of Proteomic Workflow.

A. LNCaP Cells were plated and upon 70% cell confluence, transfection of the empty vector (pCI-Neo) and SGTA-6XHIS-FLAG was performed using Lipofectamine 2000. Cells were then lysed and a nickel purification was performed followed by a FLAG-Co-IP overnight. The eluates were Trypsin digested using a FASP Kit and analyzed by LC-MS/MS. Quantification of the spectral count was performed and networks were generated and assessed. *B*. MEF52KO cells were used to perform a luciferase reporter assay. In comparison to the empty vector (pCI-neo) wild type SGTA and tagged SGTA did not alter receptor activity. *C***.** SGTA protein expression is verified using immunoblots for the input and eluate experiments in both conditions 3 hours vs overnight.

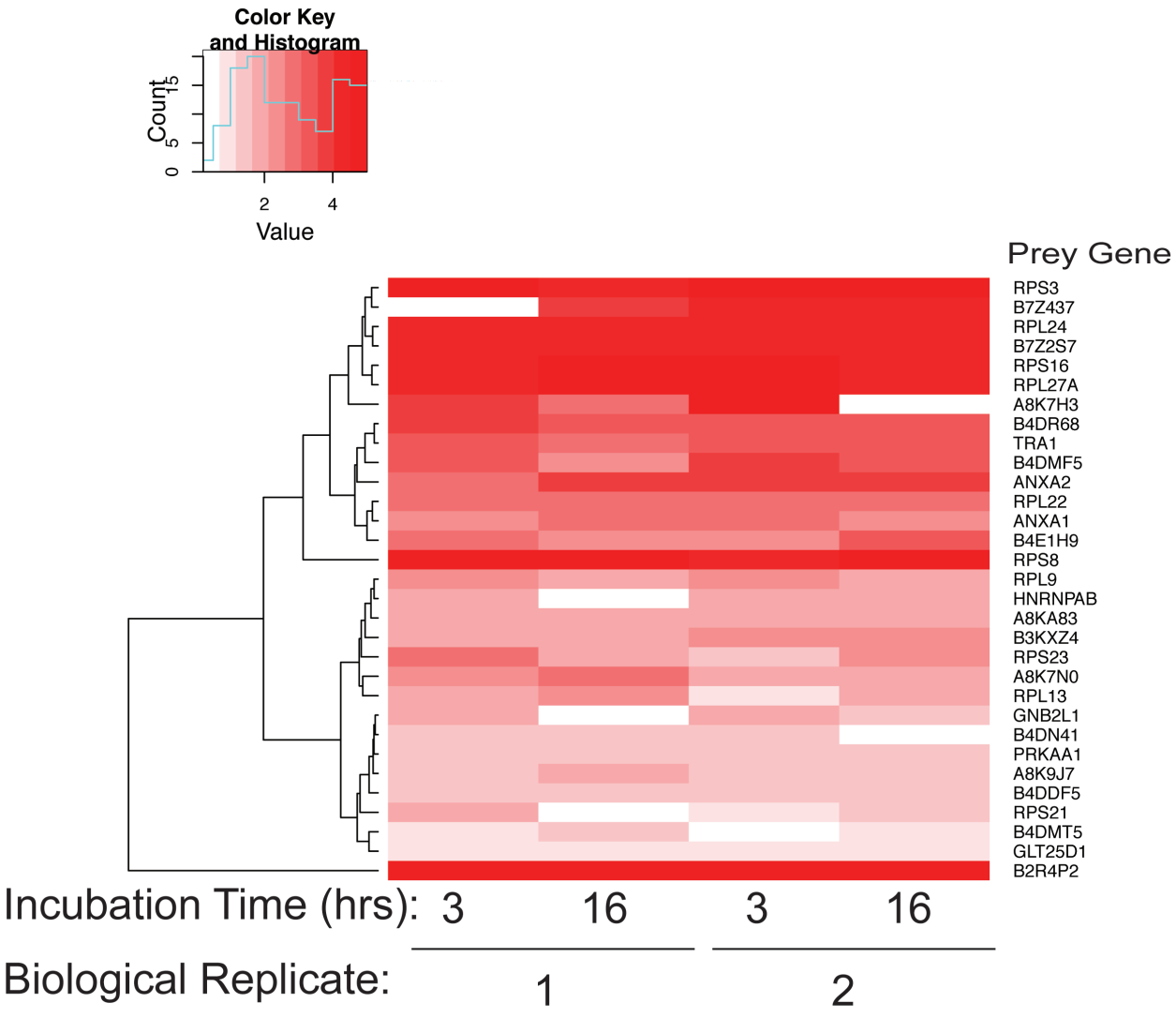

Figure 3.3.2 Heat Map of SGTA Associated Protein Network

SAINT analysis was performed on spectral count and GO term enriched values with a 0.5% FDR were used to generate the heat map. 31 proteins preferentially bound SGTA in the two biological replicates and four technical replicates within each biological set.

Table 2: Description of Identified Protein Interactors of SGTA

Number	Prey Gene Name:	Protein Name:	MW (kDa)	Biological Function:
1	RPS3_HUMAN	Ribosomal protein S3 40s	27	Translation
2	B7Z437_HUMAN	cDNA: FLJ53435, highly similar to Ezrin	51	Cytoskeletal Structure
3	RPL24_HUMAN	60S ribosomal protein L24	18	Translation
4	B7Z2S7_HUMAN	cDNA: FLJ58499, highly similar to Radixin	53	Translation
5	RPS16_HUMAN	Ribosomal protein S16 40s	17	Translation
6	RPL27A_HUMAN	60S ribosomal protein L27	17	Translation
7	A8K7H3_HUMAN	cDNA: FLJ77670, highly similar to H.s. ribosomal protein s15a	15	Translation
8	B4DR68_HUMAN	Heat shock protein 75kDa, mitochondrial	80	Chaperone
9	TRA1_HUMAN	Tumor Rejection Antigen aka HSP90B	92	Protein Folding
10	B4DMF5_HUMAN	Glutamate dehydrogenase	57	Metabolism
11	ANXA2_HUMAN	Annexin A2	39	Ca regulated membrane binding protein
12	RPL22_HUMAN	60S ribosomal protein L22	15	Translation
13	ANXA1_HUMAN	Annexin A1	39	Calcium/phospholipid-binding protein which promotes membrane fusion and is involved in exocytosis.
14	B4E1H9_HUMAN	phosphoglycerate kinase	35	PTM
15	RPS8_HUMAN	40S ribosomal protein S8	24	Translation
16	RPL9_HUMAN	60S ribosomal protein L9	22	Translation
17	HNRNPAB_HU	Heterogeneous	36	Transcription

	MAN	nuclear ribonucleoprotein A/B		
18	A8KA83_HUMAN	cDNA: FLJ78586, similar to HS VAMP	27	Protein Transportation and membrane organization
19	B3KXZ4_HUMAN	cDNA: FLJ53435, highly similar to DNA replication licensing factor MCM2	91	DNA Replication
20	RPS23_HUMAN	40S ribosomal protein S23	16	Translation
21	A8K7N0_HUMAN	cDNA: FLJ53435, highly similar to H.s. ribosomal protein L14	24	Translation
22	RPL13_HUMAN	60S ribosomal protein L13	24	Translation
23	GNB2L1_HUMAN	Guanine nucleotide-binding protein subunit beta-2-like 1	35	Translation, Cell division
24	B4DN41_HUMAN	cDNA: FLJ53435, highly similar to Probable ATP-dependent RNA helicase DDX5	68	ATP Binding
25	PRKAA1_HUMAN	5'-AMP-activated protein kinase catalytic subunit alpha-1	64	PTM-Cell Energy Metabolism
26	A8K9J7_HUMAN	Histone H2B	14	DNA Binding
27	B4DDF5_HUMAN	cDNA: FLJ53435, highly similar to DNA replication licensing factor MCM7	73	DNA Replication
28	RPS21_HUMAN	40S ribosomal protein S21	9	Translation
29	B4DMT5_HUMAN	Eukaryotic translational initiation factor 3 subunit F	33	Translation
30	GLT25D1_HUMAN	GLT25D1 protein	26	LPS Biosynthesis
31	B2R4P2_HUMAN	cDNA: FLJ53435, highly similar to H.s. peroxiredoxin 1	22	Transcription

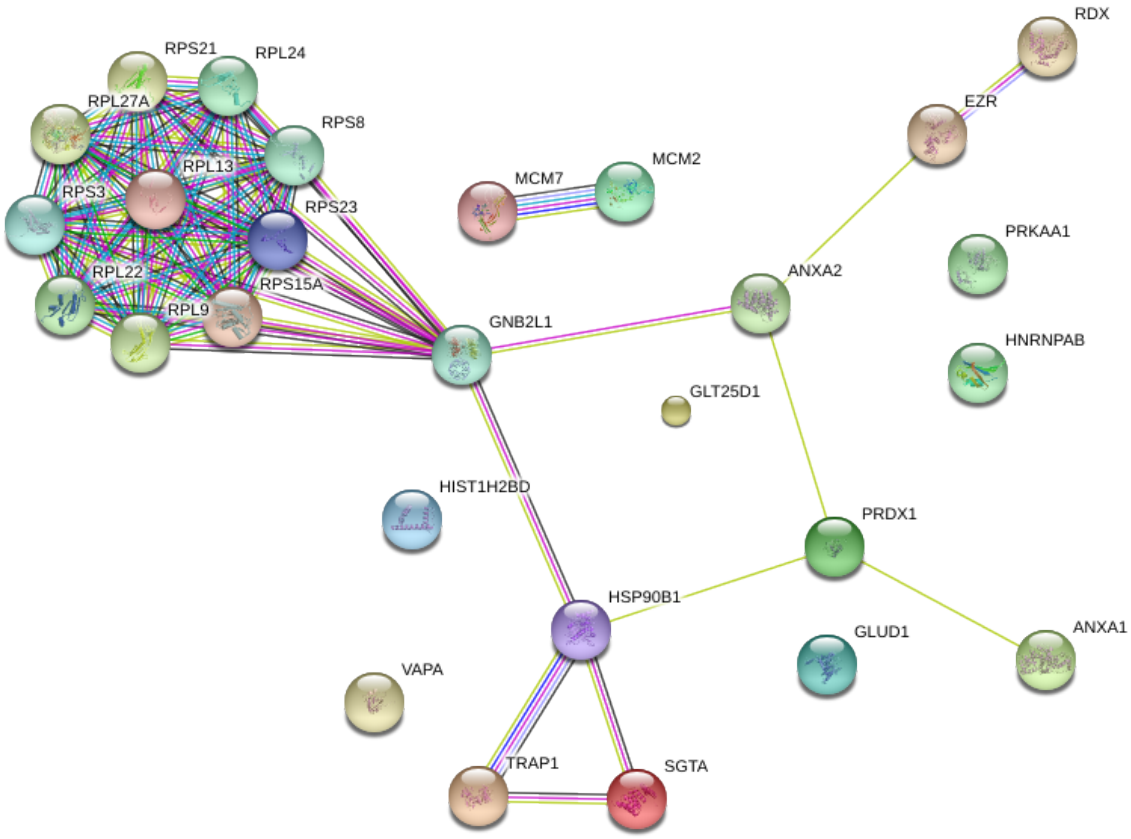

Figure 3.3.3 SGTA STRING Network Analysis

The STRING network analysis was generated based GO terms and on the total proteins generated by the heat map. The analysis depicts the known interactions of Hsp70 and Hsp90 to SGTA as observed in a triangular fashion. A ribosomal clustered analysis is also present. The other unknown protein interactors of SGTA have not been previously published.

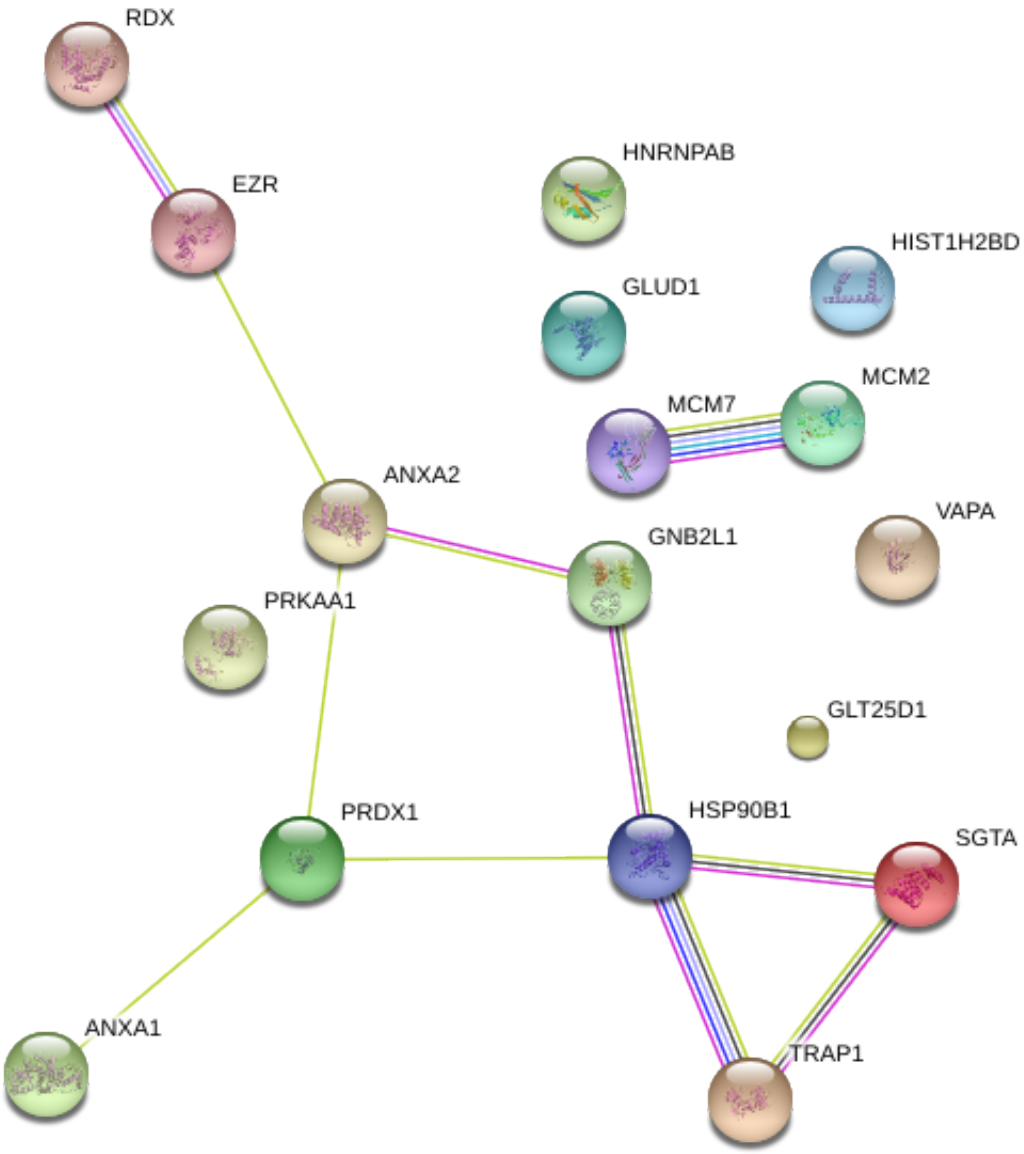

Figure 3.3.4 SGTA Non-Ribosomal STRING Network Analysis

A STRING network analysis generated from the heat map based on GO terms lacking ribosomal proteins cluster.

3.3.4 PRDX1 Interacts with SGTA in LNCaP Cells and In Vitro

Previous studies in mammalian cells suggested that PRDX1 is an AR modulator based on its ability to enhance transactivation and allow AR to facilitate binding to DHT with higher affinity. Thus, we assessed SGTA's association with PRDX1 in LNCaP cells and *in vitro* using human purified recombinant protein. To validate the interaction demonstrated by the Heat Map (Figure 3.3.2), we co-immunoprecipitated endogenous SGTA with PRDX1 from LNCaP prostate cancer cell lysates (Figure 3.3.5A). PRDX1 co-immunoprecipitaed with SGTA and no visible interaction was seen in the negative control IgG. To further validate this interaction, we assessed the ability of SGTA to interact directly with PRDX1 *in vitro* in the absence of other proteins. Recombinant human SGTA co-precipitated with recombinant FLAG-tagged PRDX1 in a cell-free system, but failed to precipitate on the FLAG resin in the absence of other proteins (Figure 3.3.5B). These interactions demonstrate that SGTA directly interacts with PRDX1.

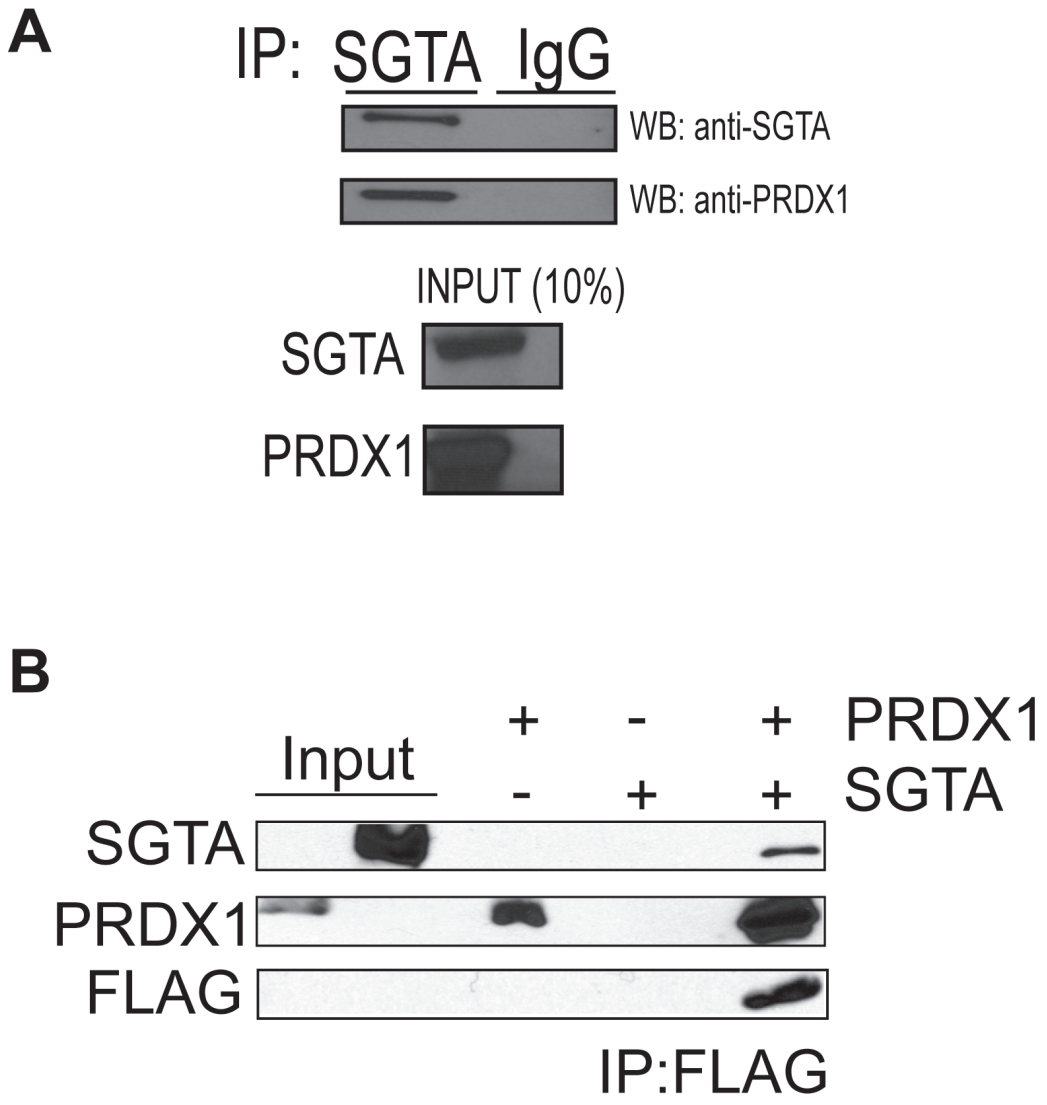

Figure 3.3.5 Interactions with PRDX1 and SGTA

A A co-immunoprecipitation was performed in LNCaP cell lysates to detect SGTA and PRDX1 interaction. SGTA was co-immunoprecitated and blots probed for SGTA and PRDX1. Inputs are shown at the bottom. *B In vitro* FLAG-pull down assays were performed with purified, recombinant human PRDX1-FLAG alone, and SGTA-HIS tag alone, and in combination. Proteins were visualized on Western Blots using primary antibodies specific to human SGTA, PRDX1, and FLAG.

3.3.5 Effects of SGTA on PRDX1 Regulation of AR Function

Our previous data indicate that SGTA and PRDX1 have a direct interaction. SGTA is a specific negative regulator of AR, GR, and PR. Interestingly, PRDX1 is a positive regulator of AR in prostate cancer cells (*200*). To functionally assess whether SGTA and PRDX1 are relevant interactors, we developed SGTA knockout HeLa and 22RV1 cell lines using the CRISPR/Cas9 system. We assessed the effects of SGTA and PRDX1 co-expression on exogenous AR activity in HeLa cells (Figure 3.3.6A) and endogenous AR 22Rv1 (Figure 3.3.6B) SGTAKO cell lines. Receptor-mediated luciferase assays were performed in the presence of empty vector or plasmids expressing SGTA and PRDX1 either alone or in combination. SGTA expression alone significantly reduced receptor activity, PRDX1 expression alone significantly enhanced receptor activity, and in the presence of SGTA and PRDX1 receptor activity was unchanged. Thus, in the presence of SGTA, PRDX1-mediated potentiation was completely abrogated. Immunoblots for SGTA, PRDX1 and the loading control GAPDH were performed on the samples used in the luciferase assays (insets). Interestingly, the same trend has been observed with the TPR-containing FKBP52, which is a positive regulator of AR, GR, and PR. This data suggests SGTA is a potent inhibitor of receptor function and has antagonistic properties.

The data indicate that this co-regulatory mechanism is pertinent in a prostate cancer setting as performed in the 22RV1 SGTAKO cells. This cell line is known to have the endogenous splice variant ARV7 that constitutively activates AR function. An interesting observation was made in Figure 3.3.6B, in which PRDX1 up-regulated endogenous AR activity with no DHT present. In addition, it can be noted that there was an increasing up-regulation of PRDX1 with increasing concentrations of DHT.

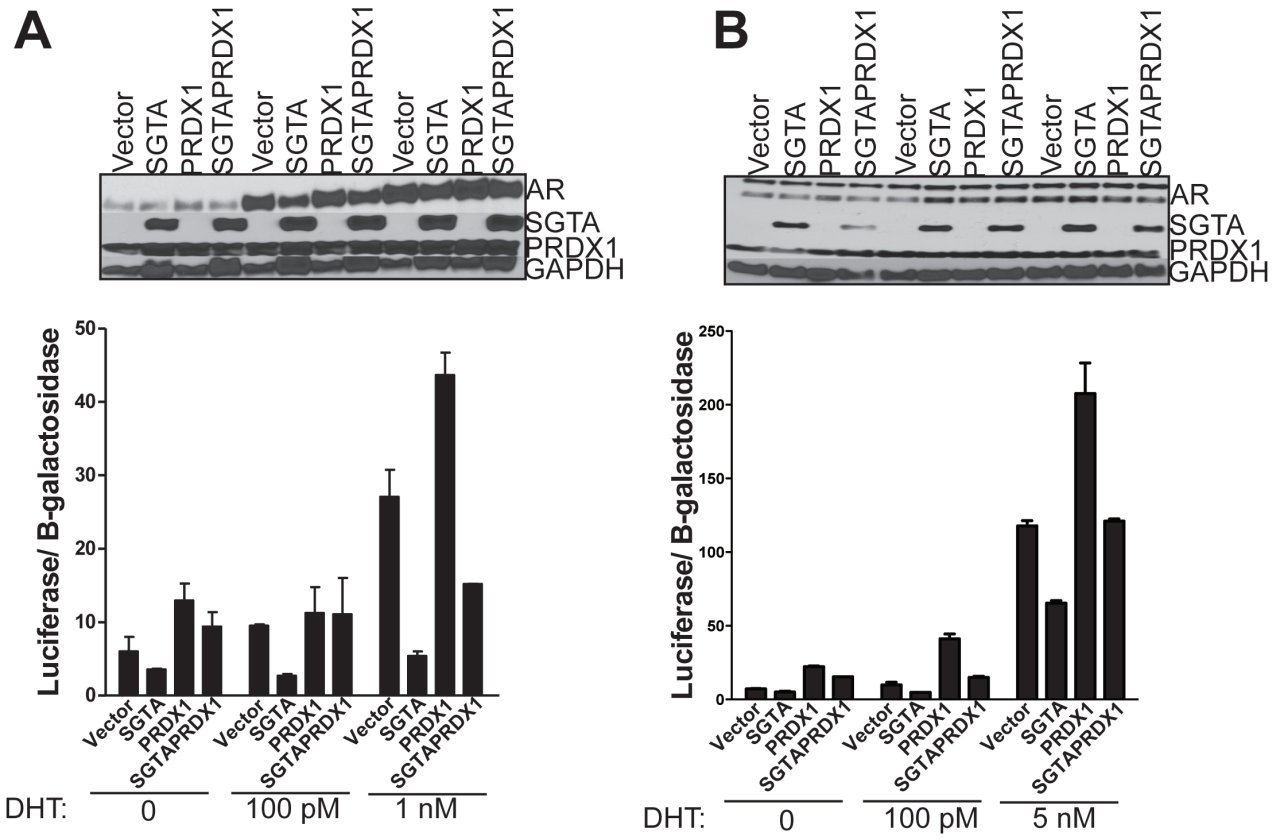

Figure 3.3.6 Effects of SGTA on PRDX1 Regulation of AR Function in HeLa and 22Rv1 SGTA KO Cells

Figure 3.3.6 Effects of SGTA on PRDX1 Regulation of AR Function in HeLa and 22Rv1 SGTA KO Cells

A. AR-mediated luciferase assay in HeLa SGTA KO cells in the presence of an empty vector, SGTA, PRDX1, or SGTA and PRDX1 combined with or with 0, 100 pM or 1 nM of DHT. AR potentiation by PRDX1 was observed in the presence of DHT. AR activity was suppressed by SGTA alone, and in combination, SGTA inhibits PRDX1 enhancement of AR activity. Immunoblots for AR, SGTA, PRDX1, SGTA, and GAPDH in HeLa SGTAKO observed in the insets. *B.* Endogenous AR activity was measured with a luciferase reporter assay in 22Rv1 SGTAKO cells in presence or absence of an empty vector, SGTA, PRDX1, or SGTAA and PRDX1 in conjunction with 0, 100 pM, or 5 nM DHT. SGTA decreased AR activity, PRDX1 potentiated and in combination, AR remained unchanged. Upper panels demonstrate the immunoblots against human AR, SGTA, and PRDX1.

3.4 Discussion

Previously, we utilized yeast two-hybrid to understand SGTA's association with GR and PR complexes (*67*). Although SGTA does not affect chaperone complex formation and receptor hormone binding *in vitro* (Chapter 2), it remains ubiquitously expressed predominately in human tissues relevant to reproductive processes. This also led to the belief that there are other mechanisms in which SGTA acts, which made it clear that a proteomic approach in LNCaP cells is applicable. The use of a label-free quantitative proteomic screen in LNCaP cells revealed SGTA significantly associates with Peroxiredoxin I, Hsp70, and Hsp90 in the conditions (3 vs 16 hours) tested. Hsp70 and Hsp90 have been previously reported to bind with SGTA and in our study, we were able to observe the presence of these proteins suggesting that our proteomic screen was reliable.

Our heat map revealed that PRDX1 had a high value of spectral count in all the conditions tested (Figure 3.3.2). We validated that SGTA directly interacts with PRDX1 and in LNCaP cells (Figure 3.3.4). PRDX1, a 22kDa protein, is known for its antioxidant properties and its ability to potentiate AR. Our data firmly establish the suppressive effect of SGTA on AR and the potentiation of PRDX1 in AR in both HeLa and 22Rv1 SGTAKO cells. Receptor-mediated reporter studies in prostate cancer cells have contributed to the current knowledge of progression and drug targeting. Interestingly, in an SGTAKO cell line, PRDX1 was able to potentiate AR activity, however, when co-expressed, SGTA abrogated PRDX1's ability to potentiate AR.

This study is the first to demonstrate SGTA's interaction with PRDX1 and the antagonistic effects it possesses with AR activity. The exact mechanism by which SGTA and PRDX1 mediate AR remains to be characterized, but the results of this chapter suggest that SGTA can antagonize PRDX1 regulation of AR activity.

Chapter 4: Validation and Application of a Four-Hour Yeast Bioassay for Screening Estrogenic Activity in Human Pregnant Female Urine

4.1 Rationale

Multiple studies have previously utilized *S. Cerevisiae* as a tool to identify and functionally characterize steroid hormone receptors (*185*), and to screen wastewater (*184*) and sediment samples in aquatic systems (*202*). Other assays such as the nAES assay has been used for the same purposes (*203*). As aforementioned, our laboratory previously developed a modified yeast estrogen screen to assess estrogenic activity in samples in a physiologically relevant timeframe. While the physiological relevance of the assay time (only a two-hour hormone treatment before cell lysis) was an important factor for the study of steroid hormone receptor signaling mechanisms including the characterization of SGTA functional domains, it was also realized that the short assay time and sensitivity of the assay were ideal for application to environmental samples. Thus, our group previously published the modified 4-hour yeast bioassay for the direct measure of estrogenic activity in wastewater without the need for sample extraction, concentration and sterilization. Prior to the studies conducted here, the four-hour yeast bioassay has only been applied to water, sediment, and herbal extract samples. Since then, it has been established that human urine provides another noninvasive manner to detect endocrine disrupting chemicals, which alter estrogenic activity (*204*). The ability of the yeast bioassay to directly detect estrogenic activity in environmental samples at picomolar concentrations suggests that this assay could also be applied to urine samples. Given the short assay time the yeast would only need to be grown directly in the presence of the urine for a 2-hour period minimizing the chance of cellular toxicity. Thus, we hypothesized that the four-hour yeast bioassay could be used as a tool to directly assess estrogenic activity in urine samples without the need for extraction. In order to test this hypothesis we employed the 4-hour yeast bioassay for the detection of expected estrogenic "spikes" in human pregnant female urine.

Estrogens bind to ERα/β, which are present in females and males, to mediate cellular functions important for cell differentiation and growth (*205*). Known as the 'female' hormone, these estrogens along with other hormones exert multiple functions throughout pregnancy allowing for development, maturation, and protection of the fetus (*206, 207*). Estrogens are the natural ligands of the estrogen receptor and are divided in three classes: estrone, estradiol, and estriol (*208*). In the case of pregnancy, estradiol is the most potent and common (*209*). The first trimester is characterized by an influx of hormones such as estradiol and progesterone. In the second trimester, estradiol levels continue increasing until reaching an apex during the third trimester. Estradiol is the major circulating estrogen in the urine and thus can be measured as a metabolite (*210-212*). Here, we used a recombinant yeast-based assay to screen for estrogenic activity in human urine. The convenience of this assay is highlighted by the rapid growth rate of yeast, relative low-cost, and highly conserved regulatory mechanisms between yeast and human in this system. Thus, the assay could serve as a low-cost, invaluable research tool for the monitoring of estrogen levels in urine from a wide variety of higher vertebrate species.

4.2 Materials and Methods

4.2.1 Urine Preparation

Normal human urine was purchased from Innovative Research Biologicals and stored in the -80°C until further use. The urine was freshly collected from single donors according to FDA regulations. Female donors were in their first, second, or third trimester during pregnancy. For the negative control urine from all three trimesters, dextran-coated charcoal was used to remove endogenous estrogens, growth factors, and cytokines from the urine. The urine was stripped using 200 mg/10 mL of dextran-coated Charcoal (Sigma C:6241) and was incubated overnight at 4°C with gentle shaking. The following day, the charcoal was removed by cold (4°C)

centrifugation 2000xg for 15 minutes and the supernatant was removed carefully by aspiration. The charcoal-treated urine was used immediately for the yeast bioassays.

Given that estrogen metabolites within the urine can be conjugated after phase II metabolism, we also assessed the importance of pre-treating with deconjugating enzymes prior to assay. To deconjugate estrogen metabolites, urine was treated with β-Glucuronidase and sulfatase enzymes. 1 Fishman unit liberated 1.0 μg of phenolphthalein from phenolphthalein glucuronide per hour. The urine was treated with 1000 units/mL for 30 minutes at 37°C and used immediately for yeast bioassay.

4.2.2 Yeast Reporter Assay

For details of the basic receptor-mediated reporter assay refer to section 2.2.3.The four-hour yeast bioassay (Figure 4.3.1) was modified from (*184*). Briefly, the parent strain was co-transformed with a TRP-marked constitutive human ERα expression plasmid (pG/ER) and a URA3-marked estrogen-inducible β-galactosidase reporter plasmid (pUCΔSS-ERE, both plasmids generously provided by Didier Picard, University of Geneva) and maintained in synthetic complete media lacking uracil and tryptophan (SC-UW). For all assays, the yeast were cultured overnight in SC-UW at 30°C in a shaking water bath incubator (Figure 4.3.1). The following day, the yeast cells were measured and diluted to an optical density of 0.08 at 600 nm and incubated until the optical density reached to 0.1. The yeast culture measured in log phase was aliquoted into 14 ml-snap cap tubes at 1 ml per tube and centrifuged at 2000rpm for 3 minutes. The yeast cells were resuspended with 1 ml of a mixture containing 750 μL of urine (CT/enzyme treated/none) and 250 μL of 4X concentrated SC-UW for each assay performed. The culture was incubated for two hours at 30°C shaking incubator. 100 μL from each culture

was then transferred to an opaque 96-well plate and substrate was added. A standard 17β-estradiol dose response curve was performed in parallel by "spiking' negative control urine with the indicated concentrations of 17β-estradiol. The standards were prepared by diluting 17β-estradiol into distilled, deionized water and handled in the same manner as urine samples. For the "plate" assays, 100μL per well of the logarithmic phase yeast culture was added to the opaque 96-well plate. 1 μL of urine (CT/enzyme treated/none) was added and incubated for 2 hours in a 30°C incubator. After a 2 hour incubation period, 100 μL of Tropix Gal-Screen in Buffer B (Applied Biosystems, Foster City, CA) was added to each well, and the wells were covered and further incubated for 2 hours at room temperature. The chemiluminescent signal was detected using a Luminoskan Ascent microplate luminometer (Thermo Fisher Scientific Inc., Waltham, MA).

4.3 Results

4.3.1 Human Urine Yeast BioAssay

Our laboratory and others have extensively utilized yeast-based methodology for the functional characterization of steroid hormone receptor-associated cochaperones (*49, 67, 90, 156, 185*). Given the utility of this assay in assessing SHR function and regulation, we reasoned that this assay could also be employed to assess hormone activity in human urine samples. A graphic illustration of the methodology tested is described in Figure 4.3.1. Similar to the yeast bioassay described by Balsiger *et al*. (*184*), in 4 hours the assay can be performed to analyze the urine samples with minimal sterilization and sample preparation time. The log-phase yeast cells are incubated with urine that has been previously diluted to a ratio of 1:4 in 4X-concentrated yeast medium for 2 hours in a shaking incubator at 30°C prior to addition of β-galactosidase

substrate (Figure 4.3.1, *left side*). The cells were further incubated for 2 hours for maximal chemiluminescent signal and read by a microplate luminometer. An advantage of our yeast bioassay is the minimal amount of urine needed, in which, 300 μl of urine sample was sufficient to detect estrogenic activity in the large scale tube assay (Figure 4.3.1, *left side*). Other yeast assays require large volumes (5 liters per batch) and can be time-consuming (12 hours - 3 days) (*213*). For smaller scale assays this protocol can be scaled down to a 96-well plate format in which urine extracts could be tested (Figure 4.3.1, *left side*). However, it should be noted that the plate format would likely require sample extraction adding sample preparation time to the protocol. The use of a "plate" assay for the direct measure of estrogenic activity without urine extraction was also tested to determine if 1 μl of urine was sufficient to give a signal. The log-phase yeast were incubated with concentrated urine for 2 hour in a 30°C incubator with no movement and the cells were further lysed and incubated with β-galactosidase substrate for 2 hours. Similar to the left side of Figure 4.3.1, the plate was then read in a luminometer machine.

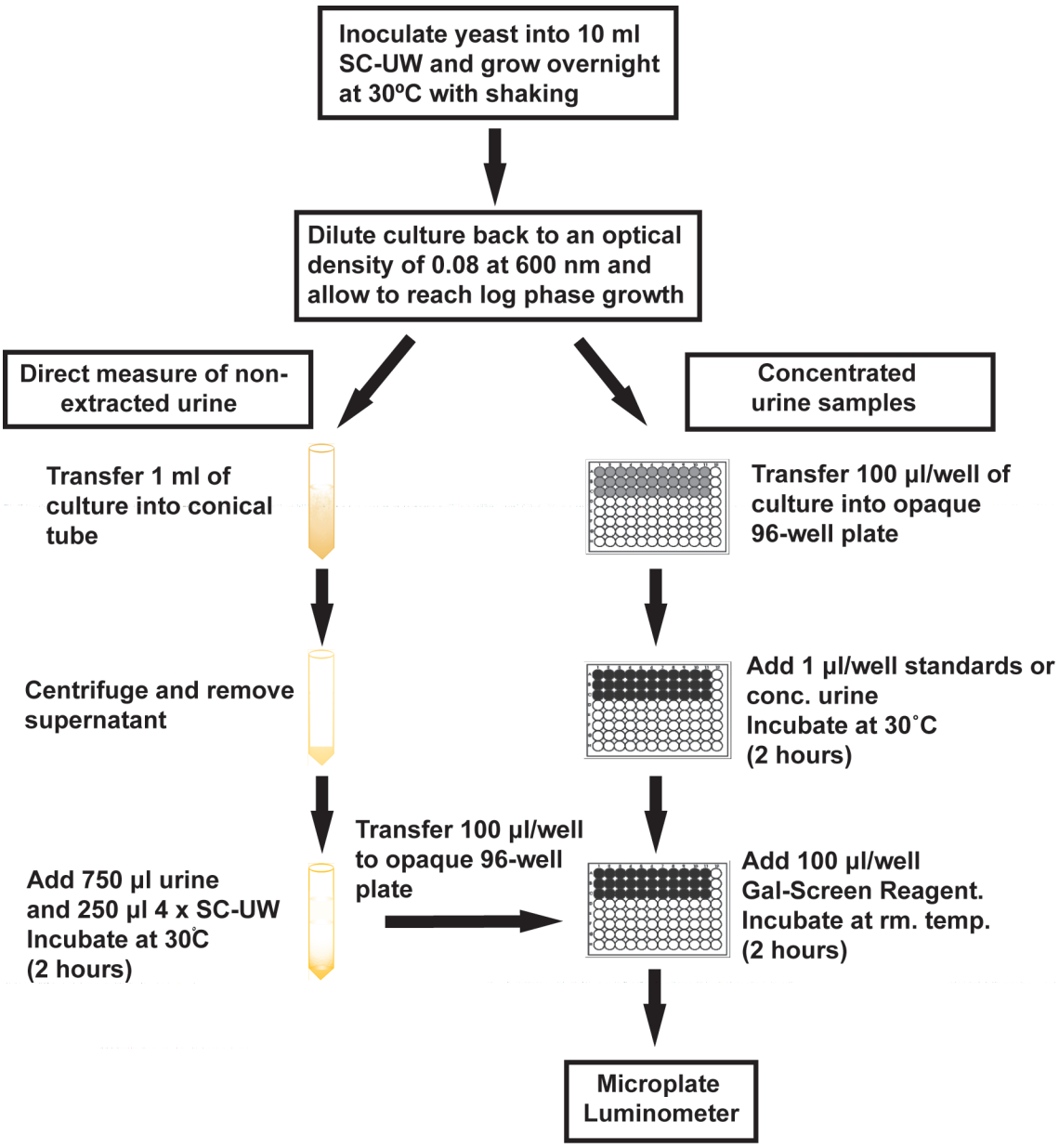

Figure 4.3.1 Schematic Representation of Yeast Bioassay Protocol.

Figure 4.3.1. Schematic Representation of Yeast bioassay protocol

An overnight culture was inoculated in 10 ml of SC-UW. The following day, it was diluted back to an $O.D._{600}$ of 0.08 and allowed to reach logarithmic phase growth before the addition of urine sample. The three trimesters can be assayed directly by mixing with concentrated yeast medium and placed on the cells for 2 hours (left panel). 100 μl of the non-extracted sample is then transferred to a 96-well plate, covered and incubated for 2 hours and analyzed with a microplate luminometer. The concentrated samples can be examined similarly to the traditional method of a yeast assay in which the minimal amount of 1 μl of urine required was tested (left panel). The yeast cells are only treated with urine sample for 2 h and then incubated with 100 μl of β-galactosidase substrate for an additional 2 hours at room temperature and read in a microplate luminometer.

4.3.2 Human Urine Yeast Assay

To demonstrate that there is an increasing activity of estrogenic signal in our yeast cells, we performed a hormone dose response with yeast only and increasing concentrations of 17β-Estradiol diluted in ethanol in parallel to our yeast assay (Figure 4.3.2A). To assess whether the direct measure of estrogenic activity in human urine was plausible, we performed the yeast assay with human urine from pregnant females in their first, second, or third trimester. We decided to use human urine from pregnant females based on evidence that correlates the increase in estrogenic activity as the trimester's progress (*212*). To control for hormone induction, we charcoal-stripped all three trimesters and used them as our negative control. In Figure 4.3.2B, the third trimester showed the highest amount of estrogenic activity in comparison to the first and second. In addition, the CT-treated urine was successful and minimal amounts of estrogenic activity were detected. Given the short amount of incubation time needed for the urine and yeast cells, we sought to determine whether using a "plate" yeast assay in which 1 µl of urine could be employed and tested for estrogenic activity (Figure 4.3.2C). Similarly to the direct measure of urine in the yeast assay, we observed the trend of the highest estrogenic activity in the third trimester. Although, the first and second trimester compared to the CT-urine treated did not display a significant change. Thus, this data set is the first to show the direct measure of human urine in the yeast bioassay and established that the assay is a valid means to be further investigated.

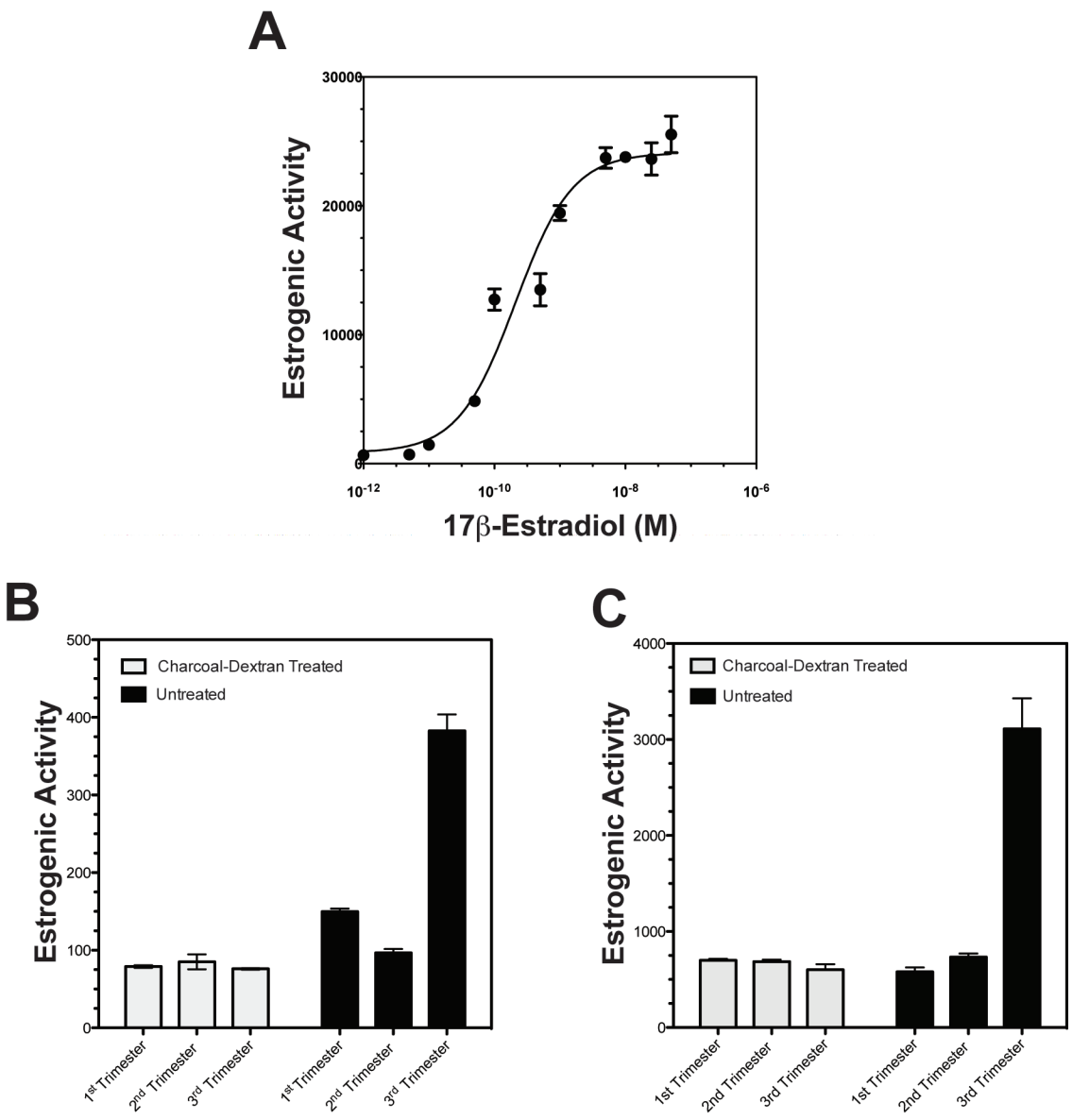

Figure 4.3.2 Yeast Bioassay is Applicable in Urine.

Figure 4.3.2 Yeast Bioassay is Applicable in Urine

A. Representative dose response curve for typical estrogenic activity using 17β-Estradiol as the ligand in yeast cells using the four-hour yeast bioassay. *B*. Urine samples taken from the three trimesters were assayed directly and tested for estrogenic activity in yeast bioassay. Dextran-treated charcoal was compared to untreated urine. *C*. A non-direct way to measure estrogenic activity was performed with dextran-treated charcoal and untreated urine as described in Figure 4.3.1, *right side*. All data points are averages of three independent replicates with error bars representing standard deviation.

4.3.3 Human Urine Yeast After Enzyme Pretreatment

Representative dose-response curves of typical estrogenic ligand, 17β-Estradiol, spiked into the charcoal-treated 1st, 2nd and 3rd trimester urine is shown in Figure 4.3.3A. These data demonstrate that the 17β-Estradiol dose-response performed in conjunction with the assay of unknown samples can be performed drectly in the control urine and also validates the assay for use in directly screening urine samples. Given that estrogenic metabolites are excreted in conjugated form we sought to assess whether pretreatment with deconjugating enzymes would improve the sensitivity and reliability of the assay. For a prototypical comparison, we pretreated the urine with β-Glucuronidase and sulfatase enzymes for 30 minutes to assess liberated hormones and increased activity. Untreated, CT-, and β-Glucuronidase and sulfatase-treated urine was assessed using the yeast bioassay (Figure 4.3.3B). The measured estrogenic activity as previously demonstrated had an increasing trend per trimester with untreated urine. The urine treated with β-Glucuronidase and sulfatase exhibited an increase in activity. Interestingly, there was a noticeable effect in the 1st trimester as there were more hormones liberated than in the rest. Although the 2nd trimester had a slight increase as well, the trend similar to that found in untreated urine remained. No significant change was observed in the 3rd trimester with treated vs untreated urine. All three trimesters exhibited minimal estrogenic activity in the CT-urine samples from all three trimesters. It is clear that addition of β-Glucuronidase and sulfatase enzymes is not necessary to observe estrogenic activity, nor to observe the expected trend in the data. While pretreatment with these enzymes increased the maximal level of estrogenic activity detected, it did not change the conclusions that could be drawn from the data. Thus, the pretreatment with deconjugating enzymes is likely unnecessary for comparison of estrogenic

activity across samples, but may be desired if the goal is to assess total estrogenic activity from both free and conjugated estrogens.

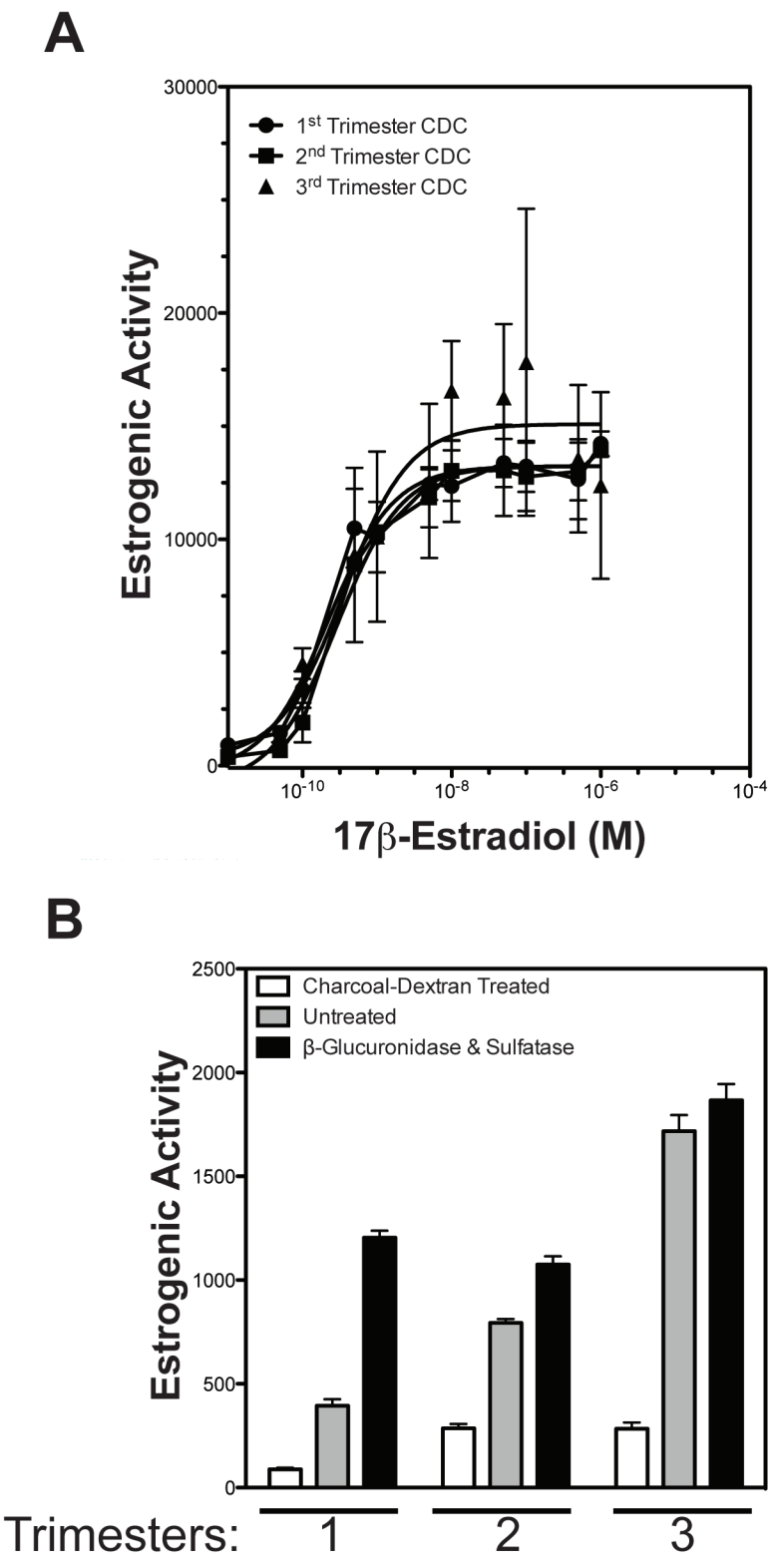

Figure 4.3.3 Urine Treated with β-Glucuronidase and Sulfatase Enzymes

Figure 4.3.3. Urine Treated with β-Glucuronidase and Sulfatase Enzymes

A. Representative 17β-Estradiol dose response curve in which the ligand solubilized with ethanol vehicle was added straight to the wells containing either 1st, 2nd, or 3rd trimester CT-urine. *B.* Urine samples taken from the 1st, 2nd, and 3rd trimester were either charcoal-treated or β-Glucuronidase and sulfatase treated, and untreated samples were directly measured using the yeast bioassay. The untreated and β-Glucuronidase and sulfatase treated urine were significantly higher than the CT-treated urine. Each data point is an average of triplicates with error bars representing standard deviation.

4.4 Discussion

The four-hour recombinant yeast bioassay has been utilized for the direct measure of environmental water, wastewater, and sediment samples in a time and cost-efficient manner. In this chapter, we have validated the easy and sensitive method to detect estrogenic activity in human pregnant urine. We observed the increasing estrogenic activity with the three different trimesters, and the estrogens can be removed efficiently upon charcoal treatment. A limitation in this study is that the urine was purchased and the way the urine was collected may not have been properly controlled for. In addition, the trimesters are months long and there is no indication at which time within the trimester the urine was collected. Thus, these studies did not aim to determine the exact estrogenic activity present within the trimesters, but instead aimed to demonstrate that the yeast-based assay could be used to directly assess estrogenic activity within the urine. This assay will be a powerful tool for endocrine disruption studies in animal models given the low volume of urine generated in mice and rats as compared to human samples. Collectively, the data presented here demonstrate an inexpensive, short assay for use in screening for estrogenic activity in urine that could be adapted to a high throughput format.

Chapter 5: Conclusions

5.1 SGTA is a Participant in the Early Complexes of the Chaperone-Mediated Receptor Folding Pathway

The data presented in Chapter 2 provides the first evidence of a role for SGTA in the chaperone-steroid hormone receptor complex. Similar to what was observed in previous reports, SGTA binds to Hsp70 and Hsp90 (*68, 105*). We are the first to demonstrate direct interaction *in vitro* and to determine binding affinities for the interactions between SGTA and Hsp70 or Hsp90 (Figure 2.3.1). Using isothermal titration calorimetry, we demonstrated that human recombinant SGTA binds Hsp70 with an affinity of 6.1 μM and to Hsp90 with an affinity of 11.0 μM *in vitro*. A co-immunoprecipitation performed in yeast lysates (Figure 2.3.1C) exhibited that the His-Sgt2, SGTA's yeast homologue, bound Hsp70, yet did not bind Hsp90ΔMEEVD, implying that SGTA does not likely bind to Hsp90 within a cellular context. Moreover, *in vitro* PR reconstitution assays demonstrated that SGTA is not a participant in the folding of the receptor to the hormone-binding competent conformation in reticulocyte lysate. The data suggests that SGTA can associate with chaperone complexes, although this is not due to the alteration of receptor folding and hormone binding (Figure 2.3.2). In addition, deletion of the glutamine-rich region at the carboxy-terminus of SGTA resulted in failure to abrogate AR function in yeast when compared to full-length SGTA (Figure 2.3.4).

While it was clear that SGTA has a functional role in AR, GR, and PR signaling, the exact functional domains and/or residues critical for this function were unknown. Thus, we assessed SGTA truncation mutants to determine the contributions of the SGTA domains to regulation of receptor activity. It is clear that the TPR domains, which are highly conserved, are critical for Hsp binding and function. However, we sought to determine the contributions of the Q-rich region in the C-terminus and the N-terminal dimerization domain. Our data demonstrate

that the C-terminal Q-rich domain, but not the N-terminal dimerization domain, is critical for receptor regulation (Figure 2.3.4). However, we make this conclusion with some caution given that misfolding of the truncation mutants could also lead to a loss of activity. Further studies are needed to firmly establish the importance of the Q-rich domain in the SGTA regulation of steroid hormone receptor signaling. However, if verified this would suggest a unique mechanism for SGTA given that it is the only TPR-containing cochaperone that utilizes a Q-rich domain. AR's structure is composed of four functional domains, and Buchanan *et al* hypothesized that SGTA regulates through binding to the hinge region (*69*). However, if the truncation failed to abrogate AR activity, perhaps SGTA regulates through the NTD with corepressors. It has been shown that coactivators/repressors with a Q-rich region bind preferentially to DNA (*214-216*). It could be possible that SGTA is interacting with other corepressors and influencing the AR-dependent cistrome and transcriptome. This could also explain why SGTA can regulate GR and PR since the NTD communicates with the DBD and is the most conserved region in the nuclear receptor superfamily.

5.2 SGTA Interacts with and Antagonizes PRDX1 in AR Function

The fact that SGTA associates with Hsp70/90 complexes was well known and further confirmed and quantitated by our laboratory (Chapter 2). Furthermore, yeast-two hybrid screens have extensively contributed to the repertoire of binding partners of SGTA (Table 1). Thus, the functional role for Hsp70, Hsp90, and viral proteins with SGTA has given SGTA a key role in cellular processes (*e.g.* cell cycle progression and apoptosis). However, the role SGTA played in a prostate cancer scenario with other binding partners was relatively unknown. Thus, we employed a label-free quantitative proteomics approach using a 6X-His-FLAG-SGTA in LNCaP PCA cells in an attempt to answer this question (Chapter 3). In agreement with studies conducted

previously (*105, 117*), a 0.5% FDR hierarchical clustered analysis revealed that Hsp70 and Hsp90 preferentially bind to SGTA (Figure 3.3.2 and Figure 3.3.3), thus, providing a confident screen for unknown protein interactors with SGTA. Our results showed that a total of 31 proteins preferentially bound SGTA in both biological replicates and the four technical replicates within each biological replicate. Remarkably, a strong interaction appeared with the prey gene B2R4P2, which encodes PRDX1. A cluster of ribosomal proteins was also present and observed in the STRING network analysis (Figure 3.3.3). Ribosomal proteins can account for 30% of the cell's total mass and are critical for protein synthesis (*217*). However, due to their sticky nature, in proteomics, ribosomal proteins are often considered false positives (*218*). Nevertheless, more recently Hsp90 and Hsp70 were shown to interact with the intact ribosome and have been demonstrated to be relevant in protein synthesis (*219, 220*). It is possible that SGTA could be a participant in these mechanisms, and further validation of these proteins with SGTA would be required to assess relevance.

The heat map generated for SGTA was validated with co-immunoprecipitation in LNCaP cells, and an *in vitro* FLAG pull-down assay with human recombinant SGTA and PRDX1 (Figure 3.3.5). To assess whether this interaction was functionally relevant, we performed an AR-mediated reporter assay with co-expression of SGTA and PRDX1. SGTA antagonizes PRDX1 effects on AR in HeLa and 22RV1 SGTAKO cell lines (Figure 3.3.6). Interestingly, PRDX1 up-regulated AR activity even in the absence of DHT in 22Rv1 cells (Figure 3.3.6B). Given that 22RV1 cells have a truncated, constitutively active AR and are used as a model to mimic CRPC, this might suggest that PRDX1 regulates AR through the N-terminus and could have effects on the AR splice variants that can drive the hormone refractory state in CRPC. Future studies are needed to further assess this observation. Future studies should assess this

mechanism in a cell line in which SGTA and PRDX1 are both deleted, which would eliminate endogenous PRDX1 activation and allow for us to better assess the functional interplay between these two proteins. Experiments designed to determine if the catalytic function of PRDX1 is involved with SGTA regulation are also warranted. If this were the case, this could be another functional role for SGTA in cellular homeostasis.

Our data suggests that SGTA is a strong inhibitor of AR function and can antagonize FKBP52 and PRDX1 (Figure 5.1.1). FKBP52 and PRDX1 are known to be strong positive regulators of AR function. SGTA is expressed at low levels in LNCaP cells, and interestingly, PRDX1 was found to be a positive regulator here. Thus, SGTA could be part of a functional rheostat mechanism that works to maintain a balance between strong positive regulation of AR activity by up-regulation of a negative regulatory factor. In prostate cancer this balance is upset as FKBP52 and PRDX1 are found to be highly up-regulated whereas SGTA is found to be down-regulated leading to hyperactivity of the AR signaling pathway, thereby promoting tumor growth and progression.

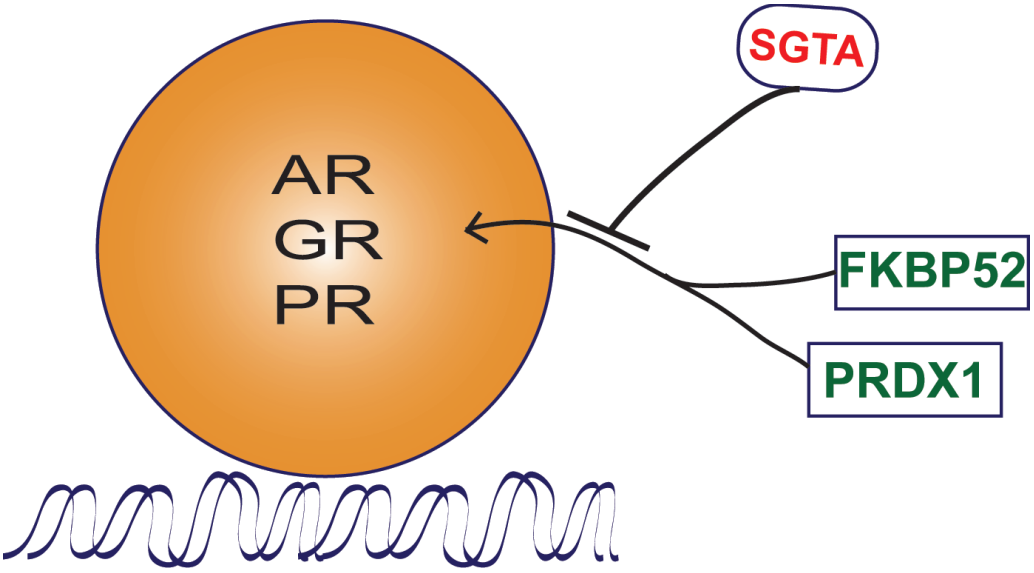

Figure 5.1.1 SGTA Portrays Antagonistic Effects on FKBP52 and PRDX1.

FKBP52 exerts a positive regulatory effect on AR, GR, and PR. PRDX1 up-regulates only AR in prostate cancer cells. Thus far, our model suggests that SGTA can antagonize FKBP52 and PRDX1 function in AR.

5.3 The 4-Hour Yeast Bioassay is Valid for Testing Estrogenic Activity in Human Urine

The four-hour receptor-mediated reporter assay in yeast has been used extensively to identify and characterize chaperone and cochaperone regulation of SHRs (*185*), screen compounds (*156*), and assess estrogenic activity in wastewater (*184*) and sediment samples (*202*). The data presented in Chapter 4 are the first to establish that the four-hour yeast bioassay is applicable in testing human urine directly without urine extraction and concentration. Remarkably, there was no toxicity observed in the yeast cells growing directly in the urine for two hours (Figure 4.3.2). A hormone dose response (HDR) curve was generated directly in the urine to ensure that hormone induction was present and was not influenced by the urine treatment, which further validates our assay in assessing the increasing estrogenic activity within the three trimesters from human urine. For yeast assay quality control, we tested the CT-treated urine, which eliminated estrogenic activity. Thus, it is likely that the activity observed is due to organic molecules present within the urine.

It has been documented that treating urine with β-Glucuronidase and sulfatase liberates estrogens and other hormones, and is sufficient to increase sensitivity in screening estrogenic activity (*213*). First, we assessed an HDR with CT-urine and observed an increase of estrogenic activity as the dose increased (Figure 4.3.3A), thus, demonstrating that even with spiked CT-urine, the yeast were responsive and displayed no toxicity. To test for liberated hormones, in Figure 4.3.3B, we demonstrated that the treatment of urine with β-Glucuronidase and sulfatase dramatically raised the yields of the activity in comparison to the untreated urine. The most dramatic increase of liberated estrogens was in the first trimester of β-Glucuronidase and sulfatase treated urine. Interestingly, the second and third trimester did not liberate as much ligand as the first. All together, these assays provide a valid method for testing estrogenic

activity in human urine. Although we are aware that handling the urine samples may increase variability, our assay shows that human urine is not toxic to yeast cells and can be used to assess estrogenic activity in human urine samples. Future studies should aim to fractionate the urine samples coupled to mass spectrometry to identify the active metabolites within the urine.

References

1. **E. V. Jensen, E. R. Desombre, D. J. Hurst, T. Kawashima, P. W. Jungblut, Estrogen-receptor interactions in target tissues. *Arch Anat Microsc Morphol Exp* 56, 547 (1967).**
2. **G. N. Eick, J. W. Thornton, Evolution of steroid receptors from an estrogen-sensitive ancestral receptor. *Mol Cell Endocrinol* 334, 31 (Mar 1, 2011).**
3. **M. E. Baker, D. R. Nelson, R. A. Studer, Origin of the response to adrenal and sex steroids: Roles of promiscuity and co-evolution of enzymes and steroid receptors. *J Steroid Biochem Mol Biol* 151, 12 (Jul, 2015).**
4. **M. Beato, P. Herrlich, G. Schutz, Steroid hormone receptors: many actors in search of a plot. *Cell* 83, 851 (Dec 15, 1995).**
5. **N. Z. Lu *et al.*, International Union of Pharmacology. LXV. The pharmacology and classification of the nuclear receptor superfamily: glucocorticoid, mineralocorticoid, progesterone, and androgen receptors. *Pharmacol Rev* 58, 782 (Dec, 2006).**
6. **D. J. Mangelsdorf *et al.*, The nuclear receptor superfamily: the second decade. *Cell* 83, 835 (Dec 15, 1995).**
7. **W. L. Miller, Molecular biology of steroid hormone synthesis. *Endocr Rev* 9, 295 (Aug, 1988).**
8. **J. T. Sanderson, The steroid hormone biosynthesis pathway as a target for endocrine-disrupting chemicals. *Toxicol Sci* 94, 3 (Nov, 2006).**
9. **D. M. Stocco, StAR protein and the regulation of steroid hormone biosynthesis. *Annu Rev Physiol* 63, 193 (2001).**
10. **A. S. Johansson, B. Mannervik, Human glutathione transferase A3-3, a highly efficient catalyst of double-bond isomerization in the biosynthetic pathway of steroid hormones. *J Biol Chem* 276, 33061 (Aug 31, 2001).**
11. **A. A. Shafi, A. E. Yen, N. L. Weigel, Androgen receptors in hormone-dependent and castration-resistant prostate cancer. *Pharmacol Ther* 140, 223 (Dec, 2013).**
12. **A. Aranda, A. Pascual, Nuclear hormone receptors and gene expression. *Physiol Rev* 81, 1269 (Jul, 2001).**
13. **P. E. Lonergan, D. J. Tindall, Androgen receptor signaling in prostate cancer development and progression. *J Carcinog* 10, 20 (2011).**
14. **T. W. Moore, C. G. Mayne, J. A. Katzenellenbogen, Minireview: Not picking pockets: nuclear receptor alternate-site modulators (NRAMs). *Mol Endocrinol* 24, 683 (Apr, 2010).**
15. **L. Clinckemalie, D. Vanderschueren, S. Boonen, F. Claessens, The hinge region in androgen receptor control. *Mol Cell Endocrinol* 358, 1 (Jul 6, 2012).**
16. **G. Jenster, H. A. van der Korput, J. Trapman, A. O. Brinkmann, Identification of two transcription activation units in the N-terminal domain of the human androgen receptor. *J Biol Chem* 270, 7341 (Mar 31, 1995).**
17. **C. Helsen *et al.*, Structural basis for nuclear hormone receptor DNA binding. *Mol Cell Endocrinol* 348, 411 (Jan 30, 2012).**
18. **D. J. Mangelsdorf, R. M. Evans, The RXR heterodimers and orphan receptors. *Cell* 83, 841 (Dec 15, 1995).**

19. **D. M. Heery, E. Kalkhoven, S. Hoare, M. G. Parker, A signature motif in transcriptional co-activators mediates binding to nuclear receptors. *Nature* 387, 733 (Jun 12, 1997).**
20. **F. Schaufele *et al.*, The structural basis of androgen receptor activation: intramolecular and intermolecular amino-carboxy interactions. *Proc Natl Acad Sci U S A* 102, 9802 (Jul 12, 2005).**
21. **I. J. McEwan, D. Lavery, K. Fischer, K. Watt, Natural disordered sequences in the amino terminal domain of nuclear receptors: lessons from the androgen and glucocorticoid receptors. *Nucl Recept Signal* 5, e001 (2007).**
22. **S. M. Dehm, K. M. Regan, L. J. Schmidt, D. J. Tindall, Selective role of an NH2-terminal WxxLF motif for aberrant androgen receptor activation in androgen depletion independent prostate cancer cells. *Cancer Res* 67, 10067 (Oct 15, 2007).**
23. **J. A. Dar *et al.*, N-terminal domain of the androgen receptor contains a region that can promote cytoplasmic localization. *J Steroid Biochem Mol Biol* 139, 16 (Jan, 2014).**
24. **T. Ueda, N. Bruchovsky, M. D. Sadar, Activation of the androgen receptor N-terminal domain by interleukin-6 via MAPK and STAT3 signal transduction pathways. *J Biol Chem* 277, 7076 (Mar 1, 2002).**
25. **J. K. Myung *et al.*, An androgen receptor N-terminal domain antagonist for treating prostate cancer. *J Clin Invest* 123, 2948 (Jul, 2013).**
26. **R. J. Andersen *et al.*, Regression of castrate-recurrent prostate cancer by a small-molecule inhibitor of the amino-terminus domain of the androgen receptor. *Cancer Cell* 17, 535 (Jun 15, 2010).**
27. **C. Helsen *et al.*, Evidence for DNA-binding domain--ligand-binding domain communications in the androgen receptor. *Mol Cell Biol* 32, 3033 (Aug, 2012).**
28. **M. E. van Royen, W. A. van Cappellen, C. de Vos, A. B. Houtsmuller, J. Trapman, Stepwise androgen receptor dimerization. *J Cell Sci* 125, 1970 (Apr 15, 2012).**
29. **Z. Chen *et al.*, Agonist and antagonist switch DNA motifs recognized by human androgen receptor in prostate cancer. *EMBO J* 34, 502 (Feb 12, 2015).**
30. **B. He *et al.*, Probing the functional link between androgen receptor coactivator and ligand-binding sites in prostate cancer and androgen insensitivity. *J Biol Chem* 281, 6648 (Mar 10, 2006).**
31. **S. Mukherjee, O. Cruz-Rodriguez, E. Bolton, J. A. Iniguez-Lluhi, The in vivo role of androgen receptor SUMOylation as revealed by androgen insensitivity syndrome and prostate cancer mutations targeting the proline/glycine residues of synergy control motifs. *J Biol Chem* 287, 31195 (Sep 7, 2012).**
32. **G. Gill, SUMO and ubiquitin in the nucleus: different functions, similar mechanisms? *Genes Dev* 18, 2046 (Sep 1, 2004).**
33. **M. Rytinki *et al.*, Dynamic SUMOylation is linked to the activity cycles of androgen receptor in the cell nucleus. *Mol Cell Biol* 32, 4195 (Oct, 2012).**
34. **Y. Yang *et al.*, Inhibition of androgen receptor activity by histone deacetylase 4 through receptor SUMOylation. *Oncogene* 30, 2207 (May 12, 2011).**
35. **T. M. Tanner *et al.*, A 629RKLKK633 motif in the hinge region controls the androgen receptor at multiple levels. *Cell Mol Life Sci* 67, 1919 (Jun, 2010).**

36. **Z. X. Zhou, J. A. Kemppainen, E. M. Wilson, Identification of three proline-directed phosphorylation sites in the human androgen receptor. *Mol Endocrinol* 9, 605 (May, 1995).**
37. **S. Chen, C. T. Kesler, B. M. Paschal, S. P. Balk, Androgen receptor phosphorylation and activity are regulated by an association with protein phosphatase 1. *J Biol Chem* 284, 25576 (Sep 18, 2009).**
38. **M. Fu *et al.*, p300 and p300/cAMP-response element-binding protein-associated factor acetylate the androgen receptor at sites governing hormone-dependent transactivation. *J Biol Chem* 275, 20853 (Jul 7, 2000).**
39. **L. Gaughan, I. R. Logan, S. Cook, D. E. Neal, C. N. Robson, Tip60 and histone deacetylase 1 regulate androgen receptor activity through changes to the acetylation status of the receptor. *J Biol Chem* 277, 25904 (Jul 19, 2002).**
40. **M. Fu *et al.*, Acetylation of androgen receptor enhances coactivator binding and promotes prostate cancer cell growth. *Mol Cell Biol* 23, 8563 (Dec, 2003).**
41. **J. M. Wurtz *et al.*, A canonical structure for the ligand-binding domain of nuclear receptors. *Nat Struct Biol* 3, 206 (Feb, 1996).**
42. **E. Estebanez-Perpina *et al.*, A surface on the androgen receptor that allosterically regulates coactivator binding. *Proc Natl Acad Sci U S A* 104, 16074 (Oct 9, 2007).**
43. **J. R. Gunther, A. A. Parent, J. A. Katzenellenbogen, Alternative inhibition of androgen receptor signaling: peptidomimetic pyrimidines as direct androgen receptor/coactivator disruptors. *ACS Chem Biol* 4, 435 (Jun 19, 2009).**
44. **G. V. Callard, P. Mak, Exclusive nuclear location of estrogen receptors in Squalus testis. *Proc Natl Acad Sci U S A* 82, 1336 (Mar, 1985).**
45. **M. Beato, R. Candau, S. Chavez, C. Mows, M. Truss, Interaction of steroid hormone receptors with transcription factors involves chromatin remodelling. *J Steroid Biochem Mol Biol* 56, 47 (Jan, 1996).**
46. **W. B. Pratt, D. O. Toft, Steroid receptor interactions with heat shock protein and immunophilin chaperones. *Endocr Rev* 18, 306 (Jun, 1997).**
47. **J. L. Johnson, Evolution and function of diverse Hsp90 homologs and cochaperone proteins. *Biochim Biophys Acta* 1823, 607 (Mar, 2012).**
48. **D. P. Edwards, The role of coactivators and corepressors in the biology and mechanism of action of steroid hormone receptors. *J Mammary Gland Biol Neoplasia* 5, 307 (Jul, 2000).**
49. **D. L. Riggs *et al.*, Noncatalytic role of the FKBP52 peptidyl-prolyl isomerase domain in the regulation of steroid hormone signaling. *Mol Cell Biol* 27, 8658 (Dec, 2007).**
50. **D. F. Smith, Tetratricopeptide repeat cochaperones in steroid receptor complexes. *Cell Stress Chaperones* 9, 109 (Summer, 2004).**
51. **D. F. Smith, D. O. Toft, Minireview: the intersection of steroid receptors with molecular chaperones: observations and questions. *Mol Endocrinol* 22, 2229 (Oct, 2008).**
52. **D. F. Smith, L. E. Faber, D. O. Toft, Purification of unactivated progesterone receptor and identification of novel receptor-associated proteins. *J Biol Chem* 265, 3996 (Mar 5, 1990).**
53. **P. J. Murphy *et al.*, Visualization and mechanism of assembly of a glucocorticoid receptor.Hsp70 complex that is primed for subsequent Hsp90-dependent opening of the steroid binding cleft. *J Biol Chem* 278, 34764 (Sep 12, 2003).**

54. A. J. Caplan, E. Langley, E. M. Wilson, J. Vidal, Hormone-dependent transactivation by the human androgen receptor is regulated by a dnaJ protein. *J Biol Chem* 270, 5251 (Mar 10, 1995).

55. C. Y. Fan, H. Y. Ren, P. Lee, A. J. Caplan, D. M. Cyr, The type I Hsp40 zinc finger-like region is required for Hsp70 to capture non-native polypeptides from Ydj1. *J Biol Chem* 280, 695 (Jan 7, 2005).

56. M. P. Hernandez, A. Chadli, D. O. Toft, HSP40 binding is the first step in the HSP90 chaperoning pathway for the progesterone receptor. *J Biol Chem* 277, 11873 (Apr 5, 2002).

57. J. H. Kim, T. R. Alderson, R. O. Frederick, J. L. Markley, Nucleotide-Dependent Interactions within a Specialized Hsp70/Hsp40 Complex Involved in Fe-S Cluster Biogenesis. *J Am Chem Soc* 136, 11586 (Aug 20, 2014).

58. M. D. Galigniana, P. C. Echeverria, A. G. Erlejman, G. Piwien-Pilipuk, Role of molecular chaperones and TPR-domain proteins in the cytoplasmic transport of steroid receptors and their passage through the nuclear pore. *Nucleus* 1, 299 (Jul-Aug, 2010).

59. S. P. Place, Single-point mutation in a conserved TPR domain of Hip disrupts enhancement of glucocorticoid receptor signaling. *Cell Stress Chaperones* 16, 469 (Jul, 2011).

60. R. T. Knapp *et al.*, BAG-1 diversely affects steroid receptor activity. *Biochem J* 441, 297 (Jan 1, 2012).

61. J. N. Rauch, J. E. Gestwicki, Binding of human nucleotide exchange factors to heat shock protein 70 (Hsp70) generates functionally distinct complexes in vitro. *J Biol Chem* 289, 1402 (Jan 17, 2014).

62. M. C. Smith *et al.*, The E3 ubiquitin ligase CHIP and the molecular chaperone Hsc70 form a dynamic, tethered complex. *Biochemistry* 52, 5354 (Aug 13, 2013).

63. S. F. Ahmed *et al.*, The chaperone-assisted E3 ligase C terminus of Hsc70-interacting protein (CHIP) targets PTEN for proteasomal degradation. *J Biol Chem* 287, 15996 (May 4, 2012).

64. S. Chen, D. F. Smith, Hop as an adaptor in the heat shock protein 70 (Hsp70) and hsp90 chaperone machinery. *J Biol Chem* 273, 35194 (Dec 25, 1998).

65. T. Kajander, J. N. Sachs, A. Goldman, L. Regan, Electrostatic interactions of Hsp-organizing protein tetratricopeptide domains with Hsp70 and Hsp90: computational analysis and protein engineering. *J Biol Chem* 284, 25364 (Sep 11, 2009).

66. S. T. Liou, C. Wang, Small glutamine-rich tetratricopeptide repeat-containing protein is composed of three structural units with distinct functions. *Arch Biochem Biophys* 435, 253 (Mar 15, 2005).

67. A. Paul *et al.*, The cochaperone SGTA (small glutamine-rich tetratricopeptide repeat-containing protein alpha) demonstrates regulatory specificity for the androgen, glucocorticoid, and progesterone receptors. *J Biol Chem* 289, 15297 (May 30, 2014).

68. P. C. Angeletti, D. Walker, A. T. Panganiban, Small glutamine-rich protein/viral protein U-binding protein is a novel cochaperone that affects heat shock protein 70 activity. *Cell Stress Chaperones* 7, 258 (Jul, 2002).

69. G. Buchanan *et al.*, Control of androgen receptor signaling in prostate cancer by the cochaperone small glutamine rich tetratricopeptide repeat containing protein alpha. *Cancer Res* 67, 10087 (Oct 15, 2007).
70. A. Carrello *et al.*, Interaction of the Hsp90 cochaperone cyclophilin 40 with Hsc70. *Cell Stress Chaperones* 9, 167 (Summer, 2004).
71. A. L. Edkins, CHIP: a co-chaperone for degradation by the proteasome. *Subcell Biochem* 78, 219 (2015).
72. S. E. Soss, K. L. Rose, S. Hill, S. Jouan, W. J. Chazin, Biochemical and Proteomic Analysis of Ubiquitination of Hsc70 and Hsp70 by the E3 Ligase CHIP. *PLoS One* 10, e0128240 (2015).
73. L. Kundrat, L. Regan, Identification of residues on Hsp70 and Hsp90 ubiquitinated by the cochaperone CHIP. *J Mol Biol* 395, 587 (Jan 22, 2010).
74. J. Luders, J. Demand, J. Hohfeld, The ubiquitin-related BAG-1 provides a link between the molecular chaperones Hsc70/Hsp70 and the proteasome. *J Biol Chem* 275, 4613 (Feb 18, 2000).
75. L. Sun, T. Prince, J. R. Manjarrez, B. T. Scroggins, R. L. Matts, Characterization of the interaction of Aha1 with components of the Hsp90 chaperone machine and client proteins. *Biochim Biophys Acta* 1823, 1092 (Jun, 2012).
76. Y. Miyata, H. Nakamoto, L. Neckers, The therapeutic target Hsp90 and cancer hallmarks. *Curr Pharm Des* 19, 347 (2013).
77. P. E. Carrigan, D. L. Riggs, M. Chinkers, D. F. Smith, Functional comparison of human and Drosophila Hop reveals novel role in steroid receptor maturation. *J Biol Chem* 280, 8906 (Mar 11, 2005).
78. N. Wayne, P. Mishra, D. N. Bolon, Hsp90 and client protein maturation. *Methods Mol Biol* 787, 33 (2011).
79. C. L. Storer, C. A. Dickey, M. D. Galigniana, T. Rein, M. B. Cox, FKBP51 and FKBP52 in signaling and disease. *Trends Endocrinol Metab* 22, 481 (Dec, 2011).
80. J. C. Sivils, C. L. Storer, M. D. Galigniana, M. B. Cox, Regulation of steroid hormone receptor function by the 52-kDa FK506-binding protein (FKBP52). *Curr Opin Pharmacol* 11, 314 (Aug, 2011).
81. T. Ratajczak, A. Carrello, Cyclophilin 40 (CyP-40), mapping of its hsp90 binding domain and evidence that FKBP52 competes with CyP-40 for hsp90 binding. *J Biol Chem* 271, 2961 (Feb 9, 1996).
82. A. Chadli *et al.*, GCUNC-45 is a novel regulator for the progesterone receptor/hsp90 chaperoning pathway. *Mol Cell Biol* 26, 1722 (Mar, 2006).
83. S. Bose, T. Weikl, H. Bugl, J. Buchner, Chaperone function of Hsp90-associated proteins. *Science* 274, 1715 (Dec 6, 1996).
84. Y. J. Tao, W. Zheng, Chaperones and the maturation of steroid hormone receptor complexes. *Oncotarget* 2, 104 (Mar, 2011).
85. G. S. Hamilton, J. P. Steiner, Immunophilins: beyond immunosuppression. *J Med Chem* 41, 5119 (Dec 17, 1998).
86. C. C. Trandinh, G. M. Pao, M. H. Saier, Jr., Structural and evolutionary relationships among the immunophilins: two ubiquitous families of peptidyl-prolyl cis-trans isomerases. *FASEB J* 6, 3410 (Dec, 1992).

87. **D. F. Smith, B. A. Baggenstoss, T. N. Marion, R. A. Rimerman, Two FKBP-related proteins are associated with progesterone receptor complexes. *J Biol Chem* 268, 18365 (Aug 25, 1993).**
88. **D. F. Smith, M. W. Albers, S. L. Schreiber, K. L. Leach, M. R. Deibel, Jr., FKBP54, a novel FK506-binding protein in avian progesterone receptor complexes and HeLa extracts. *J Biol Chem* 268, 24270 (Nov 15, 1993).**
89. **M. B. Yaffe *et al.*, Sequence-specific and phosphorylation-dependent proline isomerization: a potential mitotic regulatory mechanism. *Science* 278, 1957 (Dec 12, 1997).**
90. **D. L. Riggs *et al.*, The Hsp90-binding peptidylprolyl isomerase FKBP52 potentiates glucocorticoid signaling in vivo. *EMBO J* 22, 1158 (Mar 3, 2003).**
91. **P. D. Reynolds, Y. Ruan, D. F. Smith, J. G. Scammell, Glucocorticoid resistance in the squirrel monkey is associated with overexpression of the immunophilin FKBP51. *J Clin Endocrinol Metab* 84, 663 (Feb, 1999).**
92. **W. B. Denny, D. L. Valentine, P. D. Reynolds, D. F. Smith, J. G. Scammell, Squirrel monkey immunophilin FKBP51 is a potent inhibitor of glucocorticoid receptor binding. *Endocrinology* 141, 4107 (Nov, 2000).**
93. **M. B. Cox *et al.*, FK506-binding protein 52 phosphorylation: a potential mechanism for regulating steroid hormone receptor activity. *Mol Endocrinol* 21, 2956 (Dec, 2007).**
94. **F. Pirkl, J. Buchner, Functional analysis of the Hsp90-associated human peptidyl prolyl cis/trans isomerases FKBP51, FKBP52 and Cyp40. *J Mol Biol* 308, 795 (May 11, 2001).**
95. **C. R. Sinars *et al.*, Structure of the large FK506-binding protein FKBP51, an Hsp90-binding protein and a component of steroid receptor complexes. *Proc Natl Acad Sci U S A* 100, 868 (Feb 4, 2003).**
96. **Y. Miyata *et al.*, Phosphorylation of the immunosuppressant FK506-binding protein FKBP52 by casein kinase II: regulation of HSP90-binding activity of FKBP52. *Proc Natl Acad Sci U S A* 94, 14500 (Dec 23, 1997).**
97. **Y. Miyata, Protein kinase CK2 in health and disease: CK2: the kinase controlling the Hsp90 chaperone machinery. *Cell Mol Life Sci* 66, 1840 (Jun, 2009).**
98. **J. Cheung-Flynn, P. J. Roberts, D. L. Riggs, D. F. Smith, C-terminal sequences outside the tetratricopeptide repeat domain of FKBP51 and FKBP52 cause differential binding to Hsp90. *J Biol Chem* 278, 17388 (May 9, 2003).**
99. **T. H. Davies, Y. M. Ning, E. R. Sanchez, A new first step in activation of steroid receptors: hormone-induced switching of FKBP51 and FKBP52 immunophilins. *J Biol Chem* 277, 4597 (Feb 15, 2002).**
100. **M. D. Galigniana, C. Radanyi, J. M. Renoir, P. R. Housley, W. B. Pratt, Evidence that the peptidylprolyl isomerase domain of the hsp90-binding immunophilin FKBP52 is involved in both dynein interaction and glucocorticoid receptor movement to the nucleus. *J Biol Chem* 276, 14884 (May 4, 2001).**
101. **D. L. Cioffi, T. R. Hubler, J. G. Scammell, Organization and function of the FKBP52 and FKBP51 genes. *Curr Opin Pharmacol* 11, 308 (Aug, 2011).**
102. **A. G. Erlejman *et al.*, NF-kappaB Transcriptional Activity is Modulated by FK506-binding Proteins FKBP51 and FKBP52: A Role for Peptidyl-prolyl Isomerase Activity. *J Biol Chem*, (Aug 7, 2014).**

103. M. A. Callahan *et al.*, Functional interaction of human immunodeficiency virus type 1 Vpu and Gag with a novel member of the tetratricopeptide repeat protein family. *J Virol* 72, 8461 (Oct, 1998).
104. C. Cziepluch *et al.*, Identification of a novel cellular TPR-containing protein, SGT, that interacts with the nonstructural protein NS1 of parvovirus H-1. *J Virol* 72, 4149 (May, 1998).
105. H. Yin *et al.*, SGT, a Hsp90beta binding partner, is accumulated in the nucleus during cell apoptosis. *Biochem Biophys Res Commun* 343, 1153 (May 19, 2006).
106. G. Hristov *et al.*, Through its nonstructural protein NS1, parvovirus H-1 induces apoptosis via accumulation of reactive oxygen species. *J Virol* 84, 5909 (Jun, 2010).
107. C. Cziepluch *et al.*, H-1 parvovirus-associated replication bodies: a distinct virus-induced nuclear structure. *J Virol* 74, 4807 (May, 2000).
108. E. Kordes *et al.*, Isolation and characterization of human SGT and identification of homologues in Saccharomyces cerevisiae and Caenorhabditis elegans. *Genomics* 52, 90 (Aug 15, 1998).
109. R. J. Geraghty, A. T. Panganiban, Human immunodeficiency virus type 1 Vpu has a CD4- and an envelope glycoprotein-independent function. *J Virol* 67, 4190 (Jul, 1993).
110. T. Klimkait, K. Strebel, M. D. Hoggan, M. A. Martin, J. M. Orenstein, The human immunodeficiency virus type 1-specific protein vpu is required for efficient virus maturation and release. *J Virol* 64, 621 (Feb, 1990).
111. M. A. Handley, S. Paddock, A. Dall, A. T. Panganiban, Association of Vpu-binding protein with microtubules and Vpu-dependent redistribution of HIV-1 Gag protein. *Virology* 291, 198 (Dec 20, 2001).
112. B. C. Fielding *et al.*, Severe acute respiratory syndrome coronavirus protein 7a interacts with hSGT. *Biochem Biophys Res Commun* 343, 1201 (May 19, 2006).
113. K. Hanke, C. Chudak, R. Kurth, N. Bannert, The Rec protein of HERV-K(HML-2) upregulates androgen receptor activity by binding to the human small glutamine-rich tetratricopeptide repeat protein (hSGT). *Int J Cancer* 132, 556 (Feb 1, 2013).
114. F. Wang-Johanning *et al.*, Quantitation of HERV-K env gene expression and splicing in human breast cancer. *Oncogene* 22, 1528 (Mar 13, 2003).
115. L. Cegolon *et al.*, Human endogenous retroviruses and cancer prevention: evidence and prospects. *BMC Cancer* 13, 4 (2013).
116. L. Agoni, C. Guha, J. Lenz, Detection of Human Endogenous Retrovirus K (HERV-K) Transcripts in Human Prostate Cancer Cell Lines. *Front Oncol* 3, 180 (2013).
117. S. J. Wu, F. H. Liu, S. M. Hu, C. Wang, Different combinations of the heat-shock cognate protein 70 (hsc70) C-terminal functional groups are utilized to interact with distinct tetratricopeptide repeat-containing proteins. *Biochem J* 359, 419 (Oct 15, 2001).
118. F. H. Liu, S. J. Wu, S. M. Hu, C. D. Hsiao, C. Wang, Specific interaction of the 70-kDa heat shock cognate protein with the tetratricopeptide repeats. *J Biol Chem* 274, 34425 (Nov 26, 1999).
119. S. Tobaben *et al.*, A trimeric protein complex functions as a synaptic chaperone machine. *Neuron* 31, 987 (Sep 27, 2001).
120. V. Fonte *et al.*, Interaction of intracellular beta amyloid peptide with chaperone proteins. *Proc Natl Acad Sci U S A* 99, 9439 (Jul 9, 2002).

121. S. Tobaben, F. Varoqueaux, N. Brose, B. Stahl, G. Meyer, A brain-specific isoform of small glutamine-rich tetratricopeptide repeat-containing protein binds to Hsc70 and the cysteine string protein. *J Biol Chem* 278, 38376 (Oct 3, 2003).
122. H. Wang, Q. Zhang, D. Zhu, hSGT interacts with the N-terminal region of myostatin. *Biochem Biophys Res Commun* 311, 877 (Nov 28, 2003).
123. A. C. McPherron, A. M. Lawler, S. J. Lee, Regulation of skeletal muscle mass in mice by a new TGF-beta superfamily member. *Nature* 387, 83 (May 1, 1997).
124. M. Winnefeld, J. Rommelaere, C. Cziepluch, The human small glutamine-rich TPR-containing protein is required for progress through cell division. *Exp Cell Res* 293, 43 (Feb 1, 2004).
125. S. Dutta, Y. J. Tan, Structural and functional characterization of human SGT and its interaction with Vpu of the human immunodeficiency virus type 1. *Biochemistry* 47, 10123 (Sep 23, 2008).
126. A. P. Trotta *et al.*, Knockdown of the cochaperone SGTA results in the suppression of androgen and PI3K/Akt signaling and inhibition of prostate cancer cell proliferation. *Int J Cancer* 133, 2812 (Dec 15, 2013).
127. P. J. Russell, E. A. Kingsley, Human prostate cancer cell lines. *Methods Mol Med* 81, 21 (2003).
128. R. L. Bitting, A. J. Armstrong, Targeting the PI3K/Akt/mTOR pathway in castration-resistant prostate cancer. *Endocr Relat Cancer* 20, R83 (Jun, 2013).
129. J. A. Schantl, M. Roza, A. P. De Jong, G. J. Strous, Small glutamine-rich tetratricopeptide repeat-containing protein (SGT) interacts with the ubiquitin-dependent endocytosis (UbE) motif of the growth hormone receptor. *Biochem J* 373, 855 (Aug 1, 2003).
130. U. Kutay, G. Ahnert-Hilger, E. Hartmann, B. Wiedenmann, T. A. Rapoport, Transport route for synaptobrevin via a novel pathway of insertion into the endoplasmic reticulum membrane. *EMBO J* 14, 217 (Jan 16, 1995).
131. F. Wang, A. Whynot, M. Tung, V. Denic, The mechanism of tail-anchored protein insertion into the ER membrane. *Mol Cell* 43, 738 (Sep 2, 2011).
132. P. Leznicki, J. Warwicker, S. High, A biochemical analysis of the constraints of tail-anchored protein biogenesis. *Biochem J* 436, 719 (Jun 15, 2011).
133. N. Kuwabara *et al.*, Structure of a BAG6 (Bcl-2-associated athanogene 6)-Ubl4a (ubiquitin-like protein 4a) complex reveals a novel binding interface that functions in tail-anchored protein biogenesis. *J Biol Chem* 290, 9387 (Apr 10, 2015).
134. P. Leznicki, S. High, SGTA antagonizes BAG6-mediated protein triage. *Proc Natl Acad Sci U S A* 109, 19214 (Nov 20, 2012).
135. P. Leznicki *et al.*, The association of BAG6 with SGTA and tail-anchored proteins. *PLoS One* 8, e59590 (2013).
136. L. Wunderley, P. Leznicki, A. Payapilly, S. High, SGTA regulates the cytosolic quality control of hydrophobic substrates. *J Cell Sci* 127, 4728 (Nov 1, 2014).
137. P. Leznicki *et al.*, Binding of SGTA to Rpn13 selectively modulates protein quality control. *J Cell Sci* 128, 3187 (Sep 1, 2015).
138. M. Schuldiner *et al.*, The GET complex mediates insertion of tail-anchored proteins into the ER membrane. *Cell* 134, 634 (Aug 22, 2008).
139. H. B. Gristick *et al.*, Crystal structure of ATP-bound Get3-Get4-Get5 complex reveals regulation of Get3 by Get4. *Nat Struct Mol Biol* 21, 437 (May, 2014).

140. Y. W. Chang *et al.*, Crystal structure of Get4-Get5 complex and its interactions with Sgt2, Get3, and Ydj1. *J Biol Chem* 285, 9962 (Mar 26, 2010).
141. A. C. Simon *et al.*, Structure of the Sgt2/Get5 complex provides insights into GET-mediated targeting of tail-anchored membrane proteins. *Proc Natl Acad Sci U S A* 110, 1327 (Jan 22, 2013).
142. J. W. Chartron, D. G. VanderVelde, W. M. Clemons, Jr., Structures of the Sgt2/SGTA dimerization domain with the Get5/UBL4A UBL domain reveal an interaction that forms a conserved dynamic interface. *Cell Rep* 2, 1620 (Dec 27, 2012).
143. D. Nasrabadi *et al.*, Nuclear proteome analysis of monkey embryonic stem cells during differentiation. *Stem Cell Rev* 6, 50 (Mar, 2010).
144. A. Moritz *et al.*, Akt-RSK-S6 kinase signaling networks activated by oncogenic receptor tyrosine kinases. *Sci Signal* 3, ra64 (2010).
145. C. P. Walczak, M. S. Ravindran, T. Inoue, B. Tsai, A cytosolic chaperone complexes with dynamic membrane J-proteins and mobilizes a nonenveloped virus out of the endoplasmic reticulum. *PLoS Pathog* 10, e1004007 (Mar, 2014).
146. K. Ochiai *et al.*, Tumor suppressor REIC/DKK-3 and co-chaperone SGTA: Their interaction and roles in the androgen sensitivity. *Oncotarget* 7, 3283 (Jan 19, 2016).
147. J. Cheung-Flynn *et al.*, Physiological role for the cochaperone FKBP52 in androgen receptor signaling. *Mol Endocrinol* 19, 1654 (Jun, 2005).
148. D. M. Webber *et al.*, Developments in our understanding of the genetic basis of birth defects. *Birth Defects Res A Clin Mol Teratol*, (May 28, 2015).
149. A. Beleza-Meireles, M. Barbaro, A. Wedell, V. Tohonen, A. Nordenskjold, Studies of a co-chaperone of the androgen receptor, FKBP52, as candidate for hypospadias. *Reprod Biol Endocrinol* 5, 8 (2007).
150. H. Chen *et al.*, Fkbp52 regulates androgen receptor transactivation activity and male urethra morphogenesis. *J Biol Chem* 285, 27776 (Sep 3, 2010).
151. S. Tranguch *et al.*, Cochaperone immunophilin FKBP52 is critical to uterine receptivity for embryo implantation. *Proc Natl Acad Sci U S A* 102, 14326 (Oct 4, 2005).
152. Y. Hirota *et al.*, Deficiency of immunophilin FKBP52 promotes endometriosis. *Am J Pathol* 173, 1747 (Dec, 2008).
153. S. Tranguch *et al.*, FKBP52 deficiency-conferred uterine progesterone resistance is genetic background and pregnancy stage specific. *J Clin Invest* 117, 1824 (Jul, 2007).
154. Y. Hirota *et al.*, Uterine FK506-binding protein 52 (FKBP52)-peroxiredoxin-6 (PRDX6) signaling protects pregnancy from overt oxidative stress. *Proc Natl Acad Sci U S A* 107, 15577 (Aug 31, 2010).
155. J. F. Lin *et al.*, Identification of candidate prostate cancer biomarkers in prostate needle biopsy specimens using proteomic analysis. *Int J Cancer* 121, 2596 (Dec 15, 2007).
156. J. T. De Leon *et al.*, Targeting the regulation of androgen receptor signaling by the heat shock protein 90 cochaperone FKBP52 in prostate cancer cells. *Proc Natl Acad Sci U S A* 108, 11878 (Jul 19, 2011).
157. J. Hartmann *et al.*, Fkbp52 heterozygosity alters behavioral, endocrine and neurogenetic parameters under basal and chronic stress conditions in mice. *Psychoneuroendocrinology* 37, 2009 (Dec, 2012).

158. J. Giustiniani *et al.*, Decrease of the immunophilin FKBP52 accumulation in human brains of Alzheimer's disease and FTDP-17. *J Alzheimers Dis* 29, 471 (2012).
159. M. Warrier *et al.*, Susceptibility to diet-induced hepatic steatosis and glucocorticoid resistance in FK506-binding protein 52-deficient mice. *Endocrinology* 151, 3225 (Jul, 2010).
160. M. O. Goodarzi *et al.*, Small glutamine-rich tetratricopeptide repeat-containing protein alpha (SGTA), a candidate gene for polycystic ovary syndrome. *Hum Reprod* 23, 1214 (May, 2008).
161. K. G. Ewens *et al.*, Family-based analysis of candidate genes for polycystic ovary syndrome. *J Clin Endocrinol Metab* 95, 2306 (May, 2010).
162. M. S. Butler *et al.*, Small glutamine-rich tetratricopeptide repeat-containing protein alpha is present in human ovaries but may not be differentially expressed in relation to polycystic ovary syndrome. *Fertil Steril* 99, 2076 (Jun, 2013).
163. M. S. Butler, C. Ricciardelli, W. D. Tilley, T. E. Hickey, Androgen receptor protein levels are significantly reduced in serous ovarian carcinomas compared with benign or borderline disease but are not altered by cancer stage or metastatic progression. *Horm Cancer* 4, 154 (Jun, 2013).
164. Y. Wang *et al.*, Expression of small glutamine-rich TPR-containing protein A (SGTA) in Non-Hodgkin's Lymphomas promotes tumor proliferation and reverses cell adhesion-mediated drug resistance (CAM-DR). *Leuk Res* 38, 955 (Aug, 2014).
165. X. Yang *et al.*, High expression of SGTA in esophageal squamous cell carcinoma correlates with proliferation and poor prognosis. *J Cell Biochem* 115, 141 (Jan, 2014).
166. C. Lu *et al.*, Expression of SGTA correlates with prognosis and tumor cell proliferation in human hepatocellular carcinoma. *Pathol Oncol Res* 20, 51 (Jan, 2014).
167. Q. Xue *et al.*, Expression and clinical role of small glutamine-rich tetratricopeptide repeat (TPR)-containing protein alpha (SGTA) as a novel cell cycle protein in NSCLC. *J Cancer Res Clin Oncol* 139, 1539 (Sep, 2013).
168. S. P. Balk, K. E. Knudsen, AR, the cell cycle, and prostate cancer. *Nucl Recept Signal* 6, e001 (2008).
169. J. Trepel, M. Mollapour, G. Giaccone, L. Neckers, Targeting the dynamic HSP90 complex in cancer. *Nat Rev Cancer* 10, 537 (Aug, 2010).
170. Y. S. Kim *et al.*, Methoxychalcone inhibitors of androgen receptor translocation and function. *Bioorg Med Chem Lett* 22, 2105 (Mar 1, 2012).
171. A. Deeb *et al.*, A novel mutation in the human androgen receptor suggests a regulatory role for the hinge region in amino-terminal and carboxy-terminal interactions. *J Clin Endocrinol Metab* 93, 3691 (Oct, 2008).
172. G. Han *et al.*, Mutation of the androgen receptor causes oncogenic transformation of the prostate. *Proc Natl Acad Sci U S A* 102, 1151 (Jan 25, 2005).
173. J. Lu, T. Van der Steen, D. J. Tindall, Are androgen receptor variants a substitute for the full-length receptor? *Nat Rev Urol* 12, 137 (Mar, 2015).
174. S. M. Dehm, L. J. Schmidt, H. V. Heemers, R. L. Vessella, D. J. Tindall, Splicing of a novel androgen receptor exon generates a constitutively active androgen receptor that mediates prostate cancer therapy resistance. *Cancer Res* 68, 5469 (Jul 1, 2008).

175. R. Hu *et al.*, Ligand-independent androgen receptor variants derived from splicing of cryptic exons signify hormone-refractory prostate cancer. *Cancer Res* 69, 16 (Jan 1, 2009).
176. B. L. Maughan, E. S. Antonarakis, Clinical Relevance of Androgen Receptor Splice Variants in Castration-Resistant Prostate Cancer. *Curr Treat Options Oncol* 16, 57 (Dec, 2015).
177. R. Hu *et al.*, Distinct transcriptional programs mediated by the ligand-dependent full-length androgen receptor and its splice variants in castration-resistant prostate cancer. *Cancer Res* 72, 3457 (Jul 15, 2012).
178. J. Steinestel *et al.*, Detecting predictive androgen receptor modifications in circulating prostate cancer cells. *Oncotarget*, (Apr 23, 2015).
179. N. Sharifi, Steroid receptors aplenty in prostate cancer. *N Engl J Med* 370, 970 (Mar 6, 2014).
180. N. Xie *et al.*, The expression of glucocorticoid receptor is negatively regulated by active androgen receptor signaling in prostate tumors. *Int J Cancer* 136, E27 (Feb 15, 2015).
181. A. K. Miyahira, J. W. Simons, H. R. Soule, The 20th Annual Prostate Cancer Foundation Scientific Retreat report. *Prostate* 74, 811 (Jun, 2014).
182. V. A. Assimon, D. R. Southworth, J. E. Gestwicki, Specific Binding of Tetratricopeptide Repeat Proteins to Heat Shock Protein 70 (Hsp70) and Heat Shock Protein 90 (Hsp90) Is Regulated by Affinity and Phosphorylation. *Biochemistry* 54, 7120 (Dec 8, 2015).
183. C. A. Patwardhan *et al.*, Gedunin inactivates the co-chaperone p23 protein causing cancer cell death by apoptosis. *J Biol Chem* 288, 7313 (Mar 8, 2013).
184. H. A. Balsiger, R. de la Torre, W. Y. Lee, M. B. Cox, A four-hour yeast bioassay for the direct measure of estrogenic activity in wastewater without sample extraction, concentration, or sterilization. *Sci Total Environ* 408, 1422 (Feb 15, 2010).
185. H. A. Balsiger, M. B. Cox, Yeast-based reporter assays for the functional characterization of cochaperone interactions with steroid hormone receptors. *Methods Mol Biol* 505, 141 (2009).
186. J. Vilardell, J. R. Warner, Ribosomal protein L32 of Saccharomyces cerevisiae influences both the splicing of its own transcript and the processing of rRNA. *Mol Cell Biol* 17, 1959 (Apr, 1997).
187. P. C. Echeverria, D. Picard, Molecular chaperones, essential partners of steroid hormone receptors for activity and mobility. *Biochim Biophys Acta* 1803, 641 (Jun, 2010).
188. L. K. Philp *et al.*, SGTA: a new player in the molecular co-chaperone game. *Horm Cancer* 4, 343 (Dec, 2013).
189. K. R. Brandvold, R. I. Morimoto, The Chemical Biology of Molecular Chaperones--Implications for Modulation of Proteostasis. *J Mol Biol* 427, 2931 (Sep 11, 2015).
190. L. Jin, Y. Li, Structural and functional insights into nuclear receptor signaling. *Adv Drug Deliv Rev* 62, 1218 (Oct 30, 2010).
191. V. K. Arora *et al.*, Glucocorticoid receptor confers resistance to antiandrogens by bypassing androgen receptor blockade. *Cell* 155, 1309 (Dec 5, 2013).

192. Y. Imai *et al.*, CHIP is associated with Parkin, a gene responsible for familial Parkinson's disease, and enhances its ubiquitin ligase activity. *Mol Cell* 10, 55 (Jul, 2002).
193. C. Demonacos, M. Krstic-Demonacos, N. B. La Thangue, A TPR motif cofactor contributes to p300 activity in the p53 response. *Mol Cell* 8, 71 (Jul, 2001).
194. H. Wang *et al.*, Overexpression of small glutamine-rich TPR-containing protein promotes apoptosis in 7721 cells. *FEBS Lett* 579, 1279 (Feb 14, 2005).
195. M. Winnefeld *et al.*, Human SGT interacts with Bag-6/Bat-3/Scythe and cells with reduced levels of either protein display persistence of few misaligned chromosomes and mitotic arrest. *Exp Cell Res* 312, 2500 (Aug 1, 2006).
196. K. L. Meehan, M. D. Sadar, Quantitative profiling of LNCaP prostate cancer cells using isotope-coded affinity tags and mass spectrometry. *Proteomics* 4, 1116 (Apr, 2004).
197. S. Jager *et al.*, Vif hijacks CBF-beta to degrade APOBEC3G and promote HIV-1 infection. *Nature* 481, 371 (Jan 19, 2012).
198. D. Szklarczyk *et al.*, STRING v10: protein-protein interaction networks, integrated over the tree of life. *Nucleic Acids Res* 43, D447 (Jan, 2015).
199. J. D. Sander, J. K. Joung, CRISPR-Cas systems for editing, regulating and targeting genomes. *Nat Biotechnol* 32, 347 (Apr, 2014).
200. R. R. Chhipa, K. S. Lee, S. Onate, Y. Wu, C. Ip, Prx1 enhances androgen receptor function in prostate cancer cells by increasing receptor affinity to dihydrotestosterone. *Mol Cancer Res* 7, 1543 (Sep, 2009).
201. S. Y. Park *et al.*, Peroxiredoxin 1 interacts with androgen receptor and enhances its transactivation. *Cancer Res* 67, 9294 (Oct 1, 2007).
202. J. L. Sangster *et al.*, Bioavailability and fate of sediment-associated trenbolone and estradiol in aquatic systems. *Sci Total Environ* 496, 576 (Oct 15, 2014).
203. C. Kaiser *et al.*, Evaluation and validation of a novel Arxula adeninivorans estrogen screen (nAES) assay and its application in analysis of wastewater, seawater, brackish water and urine. *Sci Total Environ* 408, 6017 (Nov 1, 2010).
204. M. Faniband, C. H. Lindh, B. A. Jonsson, Human biological monitoring of suspected endocrine-disrupting compounds. *Asian J Androl* 16, 5 (Jan-Feb, 2014).
205. S. Nilsson *et al.*, Mechanisms of estrogen action. *Physiol Rev* 81, 1535 (Oct, 2001).
206. N. C. Zachos, R. B. Billiar, E. D. Albrecht, G. J. Pepe, Developmental regulation of baboon fetal ovarian maturation by estrogen. *Biol Reprod* 67, 1148 (Oct, 2002).
207. N. C. Zachos, R. B. Billiar, E. D. Albrecht, G. J. Pepe, Developmental regulation of follicle-stimulating hormone receptor messenger RNA expression in the baboon fetal ovary. *Biol Reprod* 68, 1911 (May, 2003).
208. A. Farooq, Structural and Functional Diversity of Estrogen Receptor Ligands. *Curr Top Med Chem* 15, 1372 (2015).
209. M. Levitz, B. K. Young, Estrogens in pregnancy. *Vitam Horm* 35, 109 (1977).
210. L. Milewich, P. C. MacDonald, B. R. Carr, Estrogen 16 alpha-hydroxylase activity in human fetal tissues. *J Clin Endocrinol Metab* 63, 404 (Aug, 1986).
211. N. M. Czekala, J. K. Hodges, B. L. Lasley, Pregnancy monitoring in diverse primate species by estrogen and bioactive luteinizing hormone determinations in small volumes of urine. *J Med Primatol* 10, 1 (1981).

212. M. M. McCarthy, E. D. Albrecht, Steroid regulation of sexual behavior. *Trends Endocrinol Metab* 7, 324 (Nov, 1996).
213. J. Adachi *et al.*, Indirubin and indigo are potent aryl hydrocarbon receptor ligands present in human urine. *J Biol Chem* 276, 31475 (Aug 24, 2001).
214. S. M. Powell *et al.*, Mechanisms of androgen receptor signalling via steroid receptor coactivator-1 in prostate. *Endocr Relat Cancer* 11, 117 (Mar, 2004).
215. F. Claessens *et al.*, Diverse roles of androgen receptor (AR) domains in AR-mediated signaling. *Nucl Recept Signal* 6, e008 (2008).
216. R. Gemayel *et al.*, Variable Glutamine-Rich Repeats Modulate Transcription Factor Activity. *Mol Cell* 59, 615 (Aug 20, 2015).
217. P. Lewin, *Out of reach*. (Ballantine Books, New York, ed. 1st, 2004), pp. 293 p.
218. G. B. Smejkal, Proteomics sample preparation, preservation, and fractionation. *Int J Proteomics* 2012, 701230 (2012).
219. V. R. Tenge, A. D. Zuehlke, N. Shrestha, J. L. Johnson, The Hsp90 cochaperones Cpr6, Cpr7, and Cns1 interact with the intact ribosome. *Eukaryot Cell* 14, 55 (Jan, 2015).
220. V. R. Tenge, J. Knowles, J. L. Johnson, The ribosomal biogenesis protein Utp21 interacts with Hsp90 and has differing requirements for Hsp90-associated proteins. *PLoS One* 9, e92569 (2014).

Glossary of Key Terms

AD- Alzheimer's disease

ADT- Androgen deprivation therapy

AIS- Androgen insensitivity syndrome

AF-1- Activation function 1

AF-2- Activation function 2

AR- Androgen receptor

AR-V7- AR-splice variant 7

BAG- BCL-2 athanogene

BAG-1- BCL-2 athanogene 1

BAG-6- BCL-2 athanogene 6

BF-2 Binding function 2

CHIP- COOH terminus of the Hsp70-interacting protein

Co-IP- coimmunoprecipitation

COS-1- CV-1 in origin and carrying the SV40 genetic material

CKII- Creatine kinase II

CRPC- Castration resistant prostate cancer

CRISPR- Clustered regularly-interspaced short palindromic repeats

CSP- Cysteine string protein

CT- Charcoal treated

Cyp40- Cyclophilin 40 kDa

DBD- DNA binding domain

DHT- 5α-dihydrotestosterone

DMEM- Dulbecco's modified eagle medium

DMSO- Dimethyl sulfoxide

DOC- deoxycorticosterone

EDC- Endocrine disrupting compound

EDTA- ethylenediaminetetraacetic acid

E2- 17β-Estradiol

ER- Estrogen receptor

FASP- Filter assisted sample preparation

FDR- False discovery rate

FBS- Fetal bovine serum

FKBP51- FK506 Binding Protein 51

FKBP52- FK506 Binding Protein 51

GAPDH- glyceraldehyde-3-phosphate dehydrogenase

GCUNC-45- General cell UNC45

GET- Guided Entry of TA proteins

GFP- Green fluorescence protein

GO- Geneontology

GR- Glucocorticoid receptor

GST- Glutathione-S-transferase

HDR- Hormone dose response

HERV-K (HML-2)- Human endogenous retroviruses

HIP- Hsp interacting protein

HOP- Hsp organizing protein

HPD- Histidine, proline, and aspartic acid amino acid residues

HRE- Hormone response element

HSF-1- Heat shock transcription factor 1

Hsp- Heat shock protein

Hsp40- Heat shock protein 40 kDa

Hsp70- Heat shock protein 70 kDa

Hsp90- Heat shock protein 90 kDa

IP- Immunoprecipitation

IL-6- Interleukin 6

LBD- Ligand binding domain

LC-MS/MS- Liquid chromatography- mass spectrometry/mass spectrometry

LNCaP- Lymph node derived from cancer patient

MAPK- Mitogen activated phosphokinase

MEM/EBSS- Minimal essential medium/ eagles essential salt solution

MPER- Mammalian protein extraction reagent

MR- Mineralocorticoid Receptor

NLS- Nuclear localization signal

NTD- Amino transactivation domain

NS1- Nonstructural protein 1

p23- Protein 23 kDa

PC3- AR-negative cell line

PCA- Prostate cancer

PCOS- Polycystic Ovary Syndrome

PD- Proteome Discoverer

PI3K- Phosphatidyl inositol-3-kinase

PPIase- Peptidyl prolyl cis-trans isomerase

PP5- Serine/threonine protein phosphatase 5

PR- Progesterone Receptor

PRDX1- Peroxiredoxin 1

PRDX6- Peroxiredoxin 6

PSA- Prostate specific antigen

PVDF- Polyvinylidene fluoride

RL- Reticulocyte Lysate

RLU- Relative light units

RPMI- Roswell Park Memorial Institue

SARS-CoV7a- Severe acute respiratory syndrome coronavirus

SGTA- Small Glutamine Rich TPR-Containing Protein Alpha

SGTβ- Small Glutamine Rich TPR-Containing Protein Beta

SGTAKDHeLa- SGTA knockdown Henrietta Lacks cells

SGTAKOHeLa- SGTA knockout Henrietta Lacks cells

SGTAKO22RV1- SGTA knockout 22RV1 cells

SHR- Steroid hormone receptor

STAT3- Signal transducer and activator of transcription 3

STRING- Search Tool for the Retrieval of Interacting Genes/Proteins

SUMO- Small ubiquitin like modifier

TA- Tail anchored

TPR- Tetratricopeptide repeat

TRC40- Transmembrane domain recognition complex of 40 kDa

UBP- U binding protein

UbE- Ubiquitin-dependent endocytosis

VpU- Viral protein U

WT- Wild type

Y2H- Yeast two-hybrid

Curriculum Vitae

Yenni A. Garcia earned her Bachelor of Science degree in Biological Sciences from The University of Texas at El Paso in 2010. In Fall 2010, she joined the doctoral program in Pathobiology in the Department of Biological Sciences at The University of Texas at El Paso, to study molecular endocrinology focusing on prostate cancer in Dr. Marc Cox's laboratory.

Ms. Garcia was the recipient of numerous honors and awards at UTEP. She received The University of Texas at El Paso Graduate School Dodson Research and Travel Awards. She was also a recipient of travel awards for national STEM Conferences where she communicated her work in SACNAS and the Midwest Stress Response Meeting in Evanston, IL. She participated in the Paso del Norte Venture Competition and Expo in El Paso, TX where her team was awarded second place.

While pursuing her degree, Ms. Garcia worked as a teaching assistant for General Biology and worked as a research assistant under Dr. Marc B. Cox in the Department of Biological Sciences. She is a shared first-author in *The Journal of Biological Chemistry* and has numerous co-authorships including publication in *Proceedings of the National Academy of Sciences*. She was on the organizing committee of the 1st Annual Chemical Biology and Drug Discovery Symposium held at UTEP. She has also been involved with her community where she has given talks to middle and high school students to inform them about scientific career opportunities.

Ms. Garcia's dissertation entitled, "Label-Free Quantitative Proteomics Reveals a Novel SGTA/Peroxiredoxin I Complex that Regulate Androgen Receptor Activity," was supervised by Dr. Marc B. Cox. Upon graduation, Ms. Garcia plans to pursue a postdoctoral fellowship focusing on reproductive cancers.

Permanent address: 4437 Valley Willow Way

El Paso, TX 79922

This dissertation was typed by: Yenni A. Garcia.